UNIVERSITÄTSKLINIKUM HAMBURG-EPPENDORF

Institut für Neuroimmunologie und Multiple Sklerose

Prof. Dr. Manuel A. Friese

Mechanisms of pregnancy-induced tolerance in an animal model of multiple sclerosis

Dissertation

zur Erlangung des Doktorgrades Dr. rer. biol. hum.
an der Medizinischen Fakultät der Universität Hamburg.

vorgelegt von:

Dr. Jan Broder Engler
aus Kiel

Hamburg 2014

Angenommen von der
Medizinischen Fakultät der Universität Hamburg am: **02.02.2015**

Veröffentlicht mit Genehmigung der
Medizinischen Fakultät der Universität Hamburg.

Prüfungsausschuss, der Vorsitzende: **Prof. Dr. Manuel A. Friese**

Prüfungsausschuss, zweite Gutachterin: **Priv.-Doz. Dr. Eva Tolosa**

Contents

List of Figures

List of Tables

1 Introduction

Multiple sclerosis (MS) is the most frequent inflammatory disease of the central nervous system (CNS) and affects around 2.5 million individuals worldwide[1]. Hallmark of the disease are inflammatory flares, which are associated with the infiltration of autoreactive lymphocytes into the CNS leading to inflammatory lesions with axonal demyelination and neuronal loss[2,3]. Being diagnosed in early adulthood, MS is the leading cause of neurological disability in young adults, and currently no curative treatment is available.

Intriguingly, pregnancy is well known to effectively suppress the disease activity of MS[4]. In fact, pregnancy is one of the strongest known modulators of MS disease activity with an approximately 80% reduction of relapse rates during third trimester pregnancy[5]. However, protection is limited to the gestational period and followed by a rebounding exacerbation post-partum[4-6].

It has been a longstanding dream of immunologists to learn which underlying mechanisms confer this temporal protection in order to utilize this knowledge for MS therapy. However, as pregnancy itself is a complex state with many changes in both the endocrine and the immune system, which potentially could interfere with autoimmunity, different partially redundant protective mechanisms have been proposed[7].

In recent years, evidence has accumulated that especially one cell type, namely regulatory T cells (Treg), could present a central connection point of reproductive and autoreactive immunity. Since these cells are critically involved in both controlling autoimmunity[8] and conferring tolerance to the semi-allogeneic fetus[9]. Thus, Treg-induced tolerance might be a central component of pregnancy-associated protection from MS disease activity.

In this work, the mechanisms of pregnancy-induced tolerance are investigated in an animal model of MS with a special focus on Treg. For the introduction, the structure and function of the immune system, the clinical presentation and pathogenesis of MS and the immunological prerequisites of reproduction are outlined in the following.

1.1 The immune system

During the course of evolution, species have always been confronted with potentially harmful pathogens including bacteria, viruses, fungi, protists and helminths. Central function of the immune system is the recognition and effective control of those pathogens, while minimizing collateral damage to affected tissues. However, threats for the organism

are not always introduced from the outside, but also arise from uncontrolled proliferation of cancer cells, which need to be efficiently tackled. At the same time, environmental antigens that do not possess pathogenic potential such as allergens should be tolerated. Thus, the discrimination between 'dangerous' and 'non-dangerous' is a critical challenge for the immune system[10], especially since incorrect decisions can lead to uncontrolled infections or tumours on the one hand and autoimmune or allergic tissue damage on the other hand.

This ambitious task is addressed by a plethora of specialized work-sharing immune cell subsets. These are classically assigned to the phylogenetically older 'innate immunity', which is present at birth, and the phylogenetically younger 'adaptive immunity', which is built up after birth and further educated throughout the lifetime of an organism.

1.1.1 Innate and adaptive immunity

The innate immune system recognises evolutionarily conserved pathogen-associated molecular patterns (PAMP) through a limited repertoire of germ-line encoded pattern-recognition receptors (PRR)[11]. Innate immune cells include phagocytes, such as neutrophils, macrophages and dendritic cells (DC), as well as mast cells, eosinophils, basophils, and natural killer (NK) cells. Often, they are the first to make contact with potential pathogens and consecutively recruit other immune cells by secretion of soluble messenger molecules such as interleukins and chemokines[12]. Furthermore, they can directly attack pathogens, neoplastic or infected cells by phagocytosis, secretion of anti-viral interferons and anti-microbial defensins, activation of the cell-lysing complement system or induction of apoptosis[11].

However, during co-evolution with their hosts, pathogens have continuously evolved strategies to escape recognition, most obviously by introducing variations into the motives bound by PRR. This sparked an evolutionary arms race of PAMP and PRR diversity with a clear advantage for pathogens, as they usually possess a considerably shorter generation time and thereby higher genetic flexibility than their hosts. To keep pace with this variability, adaptive immunity evolved in jawed vertebrates, introducing somatic recombination and hypermutation into specialized immune cells[13]. These mechanisms enable the generation of a diverse repertoire of antigen receptors on so-called lymphocytes. Upon recognition of their antigen, these cells can clonally expand, affinity-maturate their receptors and even persist as long-living memory cells that can be quickly reactivated upon a secondary antigenic challenge[14].

Of note, the classical dichotomy of innate and adaptive immunity as two autonomously operating branches is continuously softened. In fact, co-stimulatory molecules, cytokines

and chemokines provided by innate immune cells are essential to induce T and B cell responses[15]. Hence, only a functioning interplay between both systems ensures adequate host defence[11,15].

1.1.2 Lymphocytes

Lymphocytes are the effector cells of the adaptive immune system and can be subdivided into T cells and B cells, representing cell-mediated and humoral immunity, respectively.

Cell-mediated immunity

T cells recognize small antigen fragments, which are presented via major histocompatibility complex (MHC) molecules on the surface of other cells, with their highly diverse T cell receptor (TCR). While $CD8^+$ killer T cells are restricted to MHC class I molecules, which are present on all nucleated cells, $CD4^+$ T helper cells depend on presentation of antigen via MHC class II by antigen-presenting cells (APC) like macrophages, dendritic cells (DC) and B cells[14].

$CD8^+$ killer T cells patrol the body in search for virus-infected or otherwise damaged or dysfunctional cells. Killer T cells are activated by TCR-mediated recognition of pathology-associated antigens presented via MHC class I, which stimulates them to release membrane-perforating and apoptosis-inducing molecules, such as perforin, granzymes and granulysin[16].

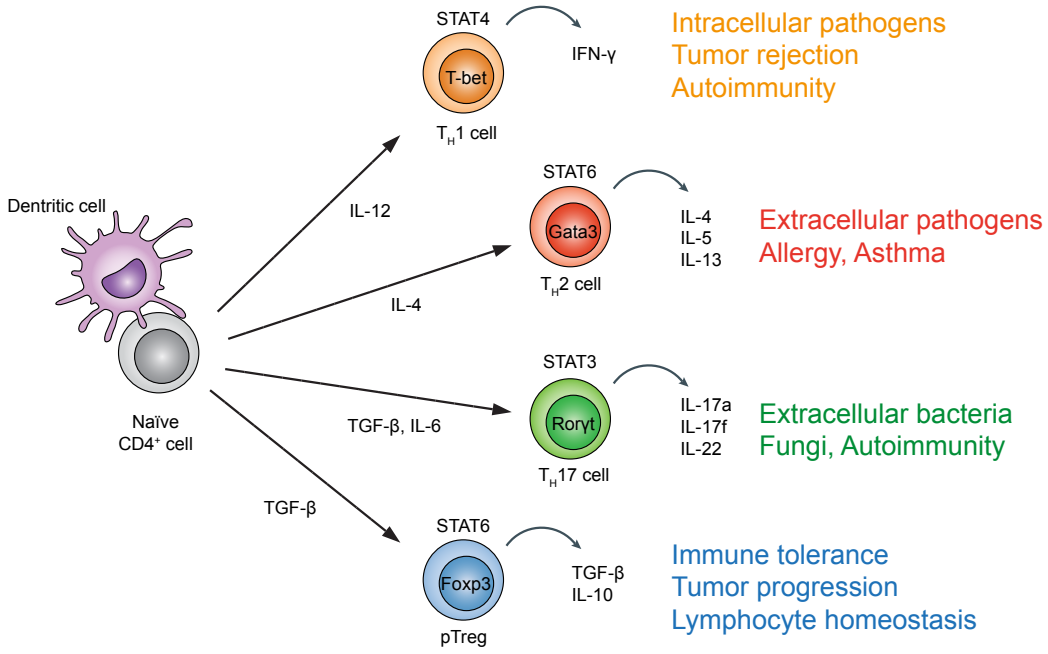

Figure 1.1 Differentiation of $CD4^+$ cells

Depending on the co-stimulatory surrounding, naïve $CD4^+$ T cells can differentiate into indicated subtypes, each characterized by specific transcription factors, secretory profiles and functions. Modified from[17].

$CD4^+$ T helper cells are activated by TCR-mediated recognition of antigen that is presented via MHC class II on APC. Depending on the co-stimulatory environment present at the inflammatory site they can differentiate into different specialized effector subsets (**Fig. 1.1**).

T_H1 cells, for example, are induced by IL-12, express the transcription factor T-bet, secrete IFN-γ, activate macrophages and are involved in the defence against intracellular pathogens and tumours. At the same time, they are held responsible for autoreactive tissue damage in autoimmune diseases like MS, rheumatoid arthritis and type I diabetes[18]. T_H2 cells are induced by IL-4, express the transcription factor Gata3, secrete IL-4, IL-5 and IL-13 and are involved in the recruitment of B cells and eosinophils. T_H2 responses are effective in controlling extracellular pathogens and helminths, yet also play a pathogenic role in allergy and asthma[14]. T_H17 cells were initially discovered in the early 2000s by their ability to produce the cytokine IL-17[19,20]. They can be induced by TGF-β in combination with IL-6, express the transcription factor Rorγt[21], produce IL-17a, IL-17 and IL-22 and play a prominent role in defence against fungi and extracellular bacteria but also in autoimmunity[22].

Humoral immunity

The highly diverse antigen receptors of B cells are surface-bound antibodies. Upon receptor engagement, antigen-antibody complexes are internalized, antigens are digested it into smaller peptides and presented via MHC class II to $CD4^+$ T helper cells. After receiving co-stimulatory signals from $CD4^+$ cells, B cells can differentiate into plasma cells and secrete millions of copies of their soluble antibody. These antibodies can directly interact with pathogens impeding their attachment or locomotion. Furthermore, antibodies can trigger secondary pathways of pathogen destruction by activating the complement system or marking pathogens for uptake and degradation by phagocytes[14,23].

1.1.3 Immunological tolerance

During the development of T cells and B cells, somatic recombination generates a highly diverse repertoire of antigen receptors to keep pace with pathogen variability. Since this is a non-supervised, chance-driven process, it naturally gives rise to autoreactive cell clones that recognise self-antigens. As these autoreactive cells would mount immune responses against the own body's tissue, they need to be eliminated by mechanisms that ensure immunological tolerance to 'self'.

Thymic selection

T cell precursors originate from the bone marrow and translocate to the thymus to undergo TCR re-arrangement as double-negative ($CD4^-CD8^-$) thymocytes. After acquisition of a functional TCRαβ dimer, thymocytes develop into double-positive ($CD4^+CD8^+$) cells and are subjected to a two-step thymic selection process. In step one, only thymocytes that recognise self-peptide–MHC complexes on cortical thymic epithelial cells (cTEC) with a sufficiently strong affinity receive a survival signal while others die by neglect[24]. This positive selection ensures, that all future T cells are able to interact with peptide–MHC, which is essential for antigen recognition. After positive selection, thymocytes commit to either the CD4 or CD8 lineage[25] – thereby becoming single positive – and migrate to the thymic medulla. In step two, potentially autoreactive single-positive cells that show very high affinity to self-peptide–MHC on medullary thymic epithelial cells (mTEC) are depleted from the T cell repertoire by induction of apoptosis[26]. This negative selection ensures that mainly self-tolerant mature single-positive cells leave the thymus as naïve T cells.

Even though thymic selection is quite efficient in shaping the T cell repertoire – of 50 million thymocytes entering selection every day, more than 90% are deleted[27] – escape of a single autoreactive clone could potentially lead to devastating autoaggression. Thus, additional mechanisms have evolved to ensure immunological tolerance in the periphery.

Regulatory T cells

Although the existence of 'suppressor T cells' has already been postulated in the early 1970s[28], it took more than 25 years for this concept to be successfully re-introduced by Sakaguchi *et al.* claiming a substantial role for regulatory T cells (Treg) in maintaining immune tolerance by down-regulating effector T cells responses[29]. Defects of the key transcription factor of Treg, forkhead box P3 (Foxp3), results in generalised autoimmune inflammation, known as scurfy phenotype in mice[30] and immunodysregulation polyendocrinopathy enteropathy X-linked syndrome (IPEX) in humans[31]. Meanwhile, Treg function and development has been intensively studied and quantitative or functional Treg impairment could be linked to a number of autoimmune diseases[8,32-35]

Based on their ontogeny, there are two subsets of $CD4^+Foxp3^+$ Treg: thymus-derived tTreg and peripherally induced pTreg[36,37]. Foxp3 expression of tTreg is acquired during thymic selection and stabilized by complete demethylation of the Treg-specific demethylated region (TSDR) inside the Foxp3 locus[38-40]. Data from TCR transgenic mouse lines indicate that single-positive thymocytes that show increased affinity to self-peptide–MHC during negative selection, yet do not reach the threshold for induction of apoptosis, are turned into tTreg. This leads to a tTreg population with border-line affinity to autoantigens that would be capable to efficiently suppress autoantigen-specific T cell

responses in the periphery[27,41]. In contrast, pTreg are peripherally induced from naïve $CD4^+$ T cells in the presence of TGF-β (**Fig. 1.1.**), a process that depends on the conserved non-coding DNA sequence 1 (CNS1) in the Foxp3 locus[42,43]. Foxp3 expression in pTreg is less stable in comparison to tTreg, which is also reflected in incomplete TSDR demethylation[39]. However, both $Foxp3^+$ Treg subtypes are characterized by a strong capacity to suppress $CD4^+Foxp3^-$ conventional effector T cells (Tcon).

To exert their suppressive control of Tcon, Treg possess a number of different effector mechanisms (**Fig. 1.2**). These mechanisms include high expression of cytotoxic T lymphocyte antigen 4 (Ctla4), which interacts with CD80/86 on DC inducing the enzyme indoleamine 2,3-dioxygenase (IDO) that in turn catabolizes tryptophan and thereby depletes this essential building block for T cell proliferation[44]. Furthermore IDO expression interferes with DC maturation, thus rendering DC unable to provide co-stimulatory signals to Tcon. Another surface protein, lymphocyte-activation gene 3 (Lag3) on Treg, competes with Tcon for MHC class II binding and thereby impedes Tcon priming[45]. Apart from these cell-cell contact dependent mechanisms, Treg also can suppress Tcon by altering the local cytokine milieu. Through high expression of the IL-2 receptor alpha chain CD25 Treg function as a sink for IL-2, thus, depleting an agent essential for autocrine self-stimulation of Tcon[32,34]. Finally, Treg produce IL-10, which has direct anti-inflammatory functions[46].

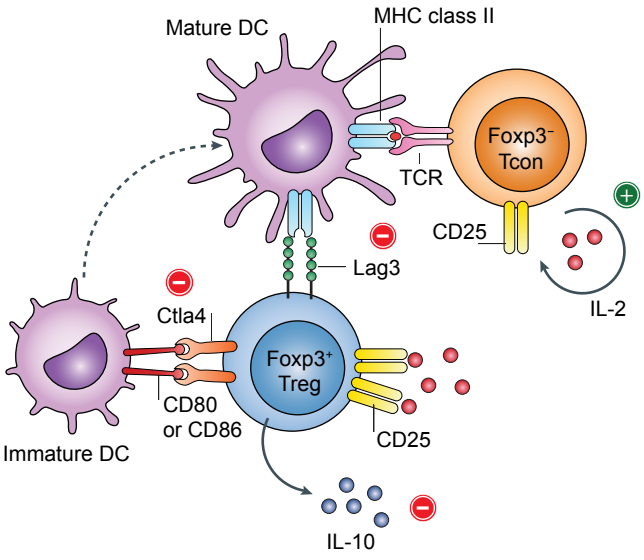

Figure 1.2 Suppressive mechanisms of Treg
$CD4^+Foxp3^+$ regulatory T cells (Treg) possess different mechanisms to suppress $CD4^+Foxp3^-$ conventional effector T cells (Tcon). Treg produce directly suppressive cytokines like IL-10, bind co-stimulatory molecules like CD80/86 on dendritic cells (DC) via Ctla4 arresting them in an immature state, interfere with MHC class II via Lag3 and deplete IL-2 by high expression of the IL-2 receptor alpha chain CD25. Modified from[32,34].

1.2 Multiple sclerosis

It was in 1868 when Jean-Martin Charcot for the first time systematically described the histological examination of brain lesions from patients that had been suffering from vision loss, clumsiness, poor balance and cognitive impairments[47]. In this work, entitled 'Histologie de la sclérose en plaques', he established a disease entity that is characterized by sclerotic CNS lesions and since then known as multiple sclerosis (MS)[47,48]

Today, around 2.5 million individuals are affected by MS worldwide[1] while autoreactive T cell responses seem to play a key role in MS pathology. Data from animal models and human studies indicate that both T_H1 and T_H17 cells contribute to CNS inflammation resulting in destruction of myelin sheaths, axonal and neuronal damage and ultimately progressive neurological disability[3]. Depending on the disease activity, patients require a walking aid after 10–20 years and are restricted to bed after 20–30 years of disease duration[49,50]. Being diagnosed in young adults, MS has a severe socioeconomic impact with an annual cost per MS patient of €35,000 in Australia in 2010 – the largest component being indirect costs due to loss of productivity[51]. However, currently no curative treatment is available.

1.2.1 Clinical presentation

On the basis of the disease course, two forms of MS can be distinguished: 80% of the patients present with relapsing-remitting MS (RRMS) characterised by isolated attacks of disease activity with complete or incomplete remission between attacks, a disease onset between 20 and 40 years of age and a female predominance of approximately 2:1. The other 20% of the patients present with primary progressive MS (PPMS) characterised by a gradually progressive clinical course, a disease onset between 30 and 50 years of age and a similar incidence among men and women[48,49,52]. Notably, about two-thirds of RRMS patients switch from a relapsing-remitting disease course to secondary progressive MS (SPMS) after an average disease duration of 15 years[49] – a phenomenon referred to as conversion.

Depending on the localisation of CNS lesions, MS patients can suffer from almost any neurological symptom, with some of them being more common than others. While RRMS typically starts with sensory disturbances, unilateral optic neuritis, diplopia, trunk and limb paresthesias, limb weakness, clumsiness, gait ataxia, and neurogenic bladder and bowel symptoms; PPMS rather manifests with a slowly evolving upper-motor-neuron syndrome of the legs, cognitive decline, visual loss, brain-stem syndromes and vegetative symptoms including bowel, bladder, and sexual dysfunction[2,48].

Active inflammatory attacks are usually treated with intravenous corticosteroids, although this therapy appears to be only effective in limiting acute symptoms without significant impact on long-term outcome. Severe relapses that do not respond to corticosteroids can be treated by plasmapheresis[48].

Outside acute relapses, a number of disease-modifying drugs have been licensed for prophylactic treatment[53]. These first line drugs for RRMS include interferon beta[54], glatiramer acetate[55], teriflunomide[56] and dimethyl fumarate[57]. While the exact mechanisms are enigmatic, it has been shown that interferon beta down-modulates MHC class II expression on monocytes, macrophages and their brain-specific equivalent, the microglia, and might thereby prevent re-stimulation of autoreactive T cells[58]. The amino acid copolymer glatiramer acetate has multiple effects in the innate as well as in the adaptive immune system, unitedly shifting the balance from pro-inflammatory to anti-inflammatory signalling pathways[59]. Teriflunomide reversibly inhibits dihydroorotate dehydrogenase, a key enzyme involved in pyrimidine synthesis, which is essential for DNA replication. Consequently, the drug reduces activation and proliferation of B and T cells[56,60]. Lastly, dimethyl fumarate has been shown to inhibit secretion of pro-inflammatory cytokines by splenocytes and protect neuronal cell cultures from oxidative stress[61]. In case of refractory disease, natalizumab[62], fingolimod[63], mitoxantrone[64] and cyclophosphamide[65] are approved as second-line therapeutics. The humanized monoclonal antibody natalizumab is directed against very late antigen-4 (VLA-4) on immune cells, which mediates binding to vascular cell adhesion molecule-1 (VCAM-1) on endothelial cells. Upon blockade of this interaction, activated T cells cannot adhere to CNS endothelium to cross the blood–brain barrier and cause inflammatory lesions[66]. Similarly, fingolimod – a sphingosine 1-phosphate receptor modulator – also interferes with lymphocyte migration by impeding their egression and holding them trapped in the secondary lymphoid organs[67]. Finally, mitoxantrone and cyclophosphamide are anti-neoplastic agents also utilized in cancer therapy that impede lymphocyte proliferation. However, none of the currently available treatments can cure MS and extensive effort is undertaken to discover new therapeutic strategies and translate them into the clinical setting[53].

1.2.2 Aetiology

MS is characterized by a complex aetiology that results from the interplay of genetic and environmental risk factors.

A genetic component of MS risk is indicated by an increased disease concordance in monozygotic twins, however this component might have been historically overestimated since recent studies report a 20% concordance rate[68] compared to up to 30% in older studies[69]. Interestingly however, in a monozygotic twin pair with only one individual

affected by MS no evidence for genetic, epigenetic or transcriptome differences that explained disease discordance was found[70]. Nevertheless, the lifetime risk for relatives of MS index patients is 1.5–3.5% for children and 3–4% for siblings, while adopted children share the background risk of approximately 0.1%[71,72].

A more recent method that enabled the un-biased assessment of genetic variation in case versus control cohorts are genome-wide association studies (GWAS) emerging in the early 2000s. In this study type, individuals are genotyped for single nucleotide positions in the genome that are known to show substantial variability in the human population. Over 60 million so-called single nucleotide polymorphisms (SNP) are currently listed (NCBI dbSNP as of 07/2014), while over 900,000 can be assessed in parallel by a current human SNP array. Those data give a good measure of genetic variability and can be compared between MS patients and healthy controls. In the biggest so far conducted MS GWAS study 9,772 cases and 17,376 controls were compared for 465,434 autosomal SNP[73]. Most of the differentially represented SNP were located in genes associated with T cell activation (CD40, CD80, CD86, MHC class II variant DRB1*15:01), differentiation (IFNγR, IL12, IL12R, STAT3) or homeostasis (IL7, IL7R, IL2, IL2RA), underlining the current understanding of MS as an autoimmune disease[73,74].

Apart from genetic factors that convey MS susceptibility, a diverse set of environmental risk factors has been reported[75-77]. One striking observation is the uneven geographical distribution of MS with high prevalence in North America, Europe and Australia and low prevalence in equatorial regions. This distribution has motivated researchers to conduct migration studies in order to dissect the genetic risk present at birth from the environmental risk present at the place of residence[78-80]. Markedly, the MS risk seems to assimilate to the local prevalence up to early adulthood[81], indicating an environmental risk factor that exerts its function in this susceptible period. Accordingly, different infectious agents including Epstein–Barr virus (EBV)[82,83] and humane herpes virus 6 (HHV6)[84] have been suspected to confer MS risk by molecular mimicry to CNS autoantigens, although the relevance of such a mechanism is still under debate[85]. Other environmental risk factors include smoking of cigarettes[86] and vitamin D deficits, caused by restriction of either dietary intake or sun light exposure[77].

1.2.3 Immunopathology

The hallmark of MS brain pathology are focal demyelinated plaques in the white matter. However, gradually progressive disease courses – like PPMS and SPMS – are rather characterized by diffuse injury of the normal appearing white matter, cortical demyelination and widespread microglia activation[87,88]. Both axonal injury and

neurodegeneration show an association with inflammation, which is represented by cellular infiltrates in histologic sections[89].

Indeed, there is substantial evidence that autoreactive T cell responses are critically involved in MS pathogenesis[3]. However, tracking down autoreactivity to one causal target autoantigen turned out to be difficult. Nevertheless, many studies provided evidence that myelin basic protein (MBP)-reactive T cells are enriched in sera and cerebrospinal fluid of MS patients[90-92]. Furthermore, a therapeutic tolerisation approach using sequence modified human $MBP_{83–99}$ in MS patients accidentally triggered relapses, supporting a role of MBP as a relevant autoantigen[93]. Another study concentrated on the TCR repertoire in MS lesions and found an overrepresentation of TCR β sequences previously described in MS lesion-derived MBP-specific T cell clones [94]. Finally, an antibody raised against MBP–MHC class II complexes successfully stained APC in MS brain lesions, suggesting active presentation of MBP in CNS inflammatory plaques[95].

Complementing human studies, a whole area of MS research has focussed on animal models of MS. Since these models allow to introduce genetic modifications, their usage for the first time enabled in-depth analysis of underlying molecular mechanisms. However, every animal model comes with limitations, especially regarding translatability of results to humans[96]. Some of them are discussed below.

1.2.4 Animal models

In 1885 Louis Pasteur successfully established a vaccination against rabies by immunising patients with spinal cord homogenates of infected rabbits. Spinal cord preparation included a drying step of several days, which was introduced to reduce the virulence of the active immunisation[97]. However, as vaccine efficiency decreased, drying times were reduced and simultaneously cases of ascending paralysis eventually leading to death by respiratory failure were reported[98]. These observations finally lead to the discovery that immunisation with CNS derived antigens can give rise to an experimental autoimmune encephalomyelitis (EAE), which was consecutively utilized as an animal model for CNS inflammation[97,99].

Different components of the myelin sheath that isolates neuronal axons and enables saltatory conduction can be used for immunisation. These include myelin basic protein (MBP), myelin oligodendrocyte glycoprotein (MOG) and proteolipid protein (PLP). In rodents, immunisation of C57BL/6 mice with $MOG_{35–55}$ peptide results in a monophasic EAE course while immunisation of SJL mice with $PLP_{139–151}$ peptide resembles a rather relapsing-remitting phenotype[97]. EAE symptoms usually start with weakness of the tail and proceed to a progressive paralysis of the hind limbs. Importantly, EAE can also be

induced by adoptive transfer of MOG or PLP-specific encephalitogenic $CD4^+$ T cells[100-102], highlighting the relevance of $CD4^+$ T cells in EAE pathogenesis. Additionally, introducing transgenic expression of MHC class II-restricted, MOG-specific TCR into $CD4^+$ T cells results in spontaneous EAE[103,104]. Likewise, transgenic animals expressing a combination of MBP-specific humanized TCR and corresponding human MHC develop spontaneous disease[102]. While this was initially shown for $CD4^+$ T cells[105,106], more recently the same strategy was successfully applied to $CD8^+$ T cells, highlighting the potential contribution of $CD8^+$ T cell to CNS autoimmunity[107,108].

Currently, it is assumed that MS pathology starts with CNS autoantigen-specific $CD4^+$ T cells, which have escaped negative selection in the thymus. This appears to be a common phenomenon as myelin-reactive T cells can be detected in the blood of MS patients but also healthy controls[109,110]. Thus, the exclusive presence of these cells is not sufficient to cause MS. However, when these cells are primed by APC presenting myelin or myelin cross-reactive epitopes, they get licensed to enter the subarachnoid space[111] and can be reactivated by perivascular macrophages or DC[3]. Then, T cells enter the CNS parenchyma, activate microglia and endothelial cells and together with local macrophages establish an inflammatory cytokine milieu that attracts additional immune cells and drives demyelination and neuronal injury[3].

However, the triggering mechanisms of this cascade remain incompletely understood. Since myelin-reactive T cells are also present in healthy individuals, additional peripheral tolerance mechanisms need to fail in order to unleash autoimmune CNS inflammation. One central guarantor of peripheral tolerance being Treg, numerous studies in both human and mice indicate Treg failure to be a critical component of MS pathology[112,113].

1.2.5 Regulatory T cells

Quantitative or functional Treg impairment could be linked to a number of autoimmune diseases, including systemic lupus erythematosus[114,115], rheumatoid arthritis[116,117], autoimmune polyglandular syndrome[118] and type I diabetes[119]. Similarly, Treg in MS were reported to have a diminished suppressive potential to control Tcon proliferation and IFN-γ production[120,121]. Additionally, the impairment of Treg function in MS patients was correlated with a decrease in Foxp3 and Ctla4 expression[122-124]. However, Treg frequencies in the peripheral blood are not found to be consistently altered[112].

Since Treg assessment in humans is limited due to methodological restrictions, deeper insights have been obtained in EAE models. Early reports indicated that the absence of αβTreg in RAG-1-deficient mice crossed to MBP-TCR transgenic mice resulted in spontaneous EAE development, while Treg/RAG-1-competent MBP-TCR transgenic mice

remained healthy[125]. Additionally, adoptive transfer of both whole splenocytes and $CD4^+CD25^+$ Treg was able to rescue RAG-1-deficient transgenic MBP-TCR mice from EAE development[126]. However, aforementioned genetic models introduce severe alterations into the adaptive immune system, thus implications might be somewhat limited. Nevertheless, in more recent studies a protective effect of adoptive Treg transfer on EAE could also be shown in wildtype mice[127-129], while Treg depletion aggravated the disease[130]. Interestingly, IL-10 seems to be an important effector mechanism of adoptively transferred Treg since $IL\text{-}10^{-/-}$ Treg failed to confer EAE protection[131]. Taken together, there is quite a substantial body of evidence indicating a protective role of Treg in both MS and EAE[112].

1.3 Pregnancy

Reproduction is fundamental to the maintenance and evolution of species. However, to ensure successful pregnancy the mother's immune system has to efficiently establish tolerance towards the semiallogeneic conceptus providing a secure niche for fetal development. This need was particularly introduced in the development of placental mammals that realize fetal nutrition via an extensive fetomaternal interface – the placenta. In contrast, egg-laying animals equip their fetuses with a nutrition storage represented by the yolk sac and surround them with a protective eggshell, thus, lacking a direct fetomaternal interface (**Fig. 1.3**).

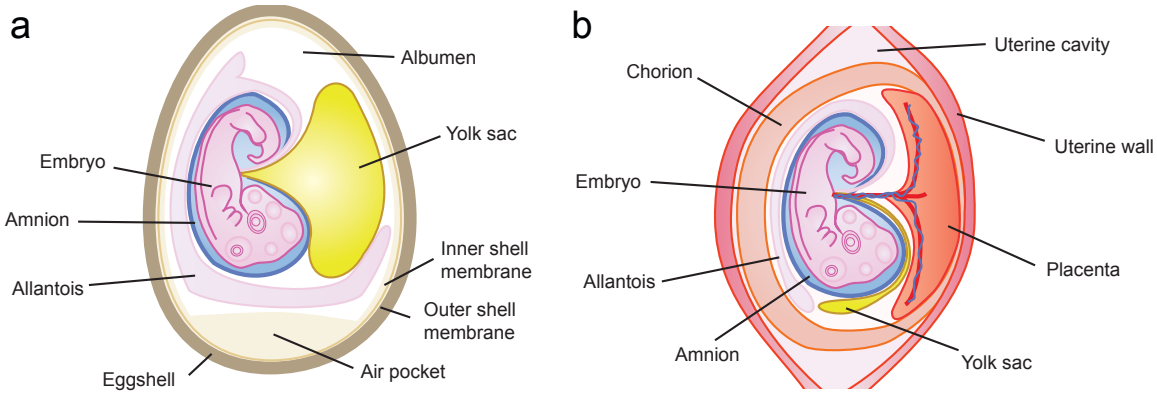

Figure 1.3 Fetomaternal interface in egg-laying and placental animals
Schematized cross-section of the fetal situation inside the fertilized egg (**a**) and the pregnant uterus (**b**).

1.3.1 Reproductive immunology

Multiple mechanisms have evolved to prevent fetus-directed immune responses and alloreactive infiltration of the fetomaternal interface[9,132]. Among these, decidual $CD56^{bright}$ NK cells (dNK) are recruited to and locally expanded in the decidua and serve important functions partly by secretion of macrophage inhibitory cytokine-1 (MIC-1) and TGF-β1 –

both inducing tolerogenic DC (tDC) – and by promoting local generation of Treg[132]. Likewise, galectine-1 produced by dNK and decidual stromal cells (DSC) induces tDC and promotes apoptosis of activated T cells thereby preventing fetal demise[133,134]. Another mechanism is the effective entrapment of DC in the decidua, thus preventing them from egressing to the lymph nodes to prime T cells with fetal antigen[135]. Even in the case effector T cells are generated in the periphery, their infiltration into the decidua is abrogated by epigenetic silencing of CXCL9, CXCL10, CXCL11 and CCL5 in DSC, resembling those chemokines that are critical for T cell attraction[136].

More recently, researchers have also more closely focussed on the function of Treg in fetomaternal tolerance. Markedly, peripheral CNS1-dependend induction of pTreg was shown to be an evolutionary achievement of placental mammals, while CNS1-deficiency provoked increased fetal loss[43]. Hence, for the first time evolution of Treg and the Foxp3 locus could be linked to the increased requirements in regards to fetomaternal tolerance, introduced by placentation[43,137].

Nevertheless, already earlier studies in both mice and humans have reported a decisive role of Treg in fetomaternal tolerance[9,132,138]. In mice, Treg were observed to expand during pregnancy while their depletion resulted in fetal loss[139]. Conversely, adoptive transfer of Treg into abortion-prone mice prevented fetal rejection[140]. In humans, Treg expansion in the peripheral blood of pregnant individuals was also repeatedly reported[141-143], however, also converse findings have been obtained[9,144]. Nevertheless, ample evidence has been provided that links Treg failure with various pregnancy complications, including recurrent pregnancy loss[145-149].

To investigate fetal-specific T cells responses, a number of animal studies made use of Act-mOVA transgenic animals ubiquitously expressing membrane-bound ovalbumin (mOVA) under the actin promoter. When mating these animals to wildtype females, OVA is expressed in 50% of the fetuses but is unknown to the mother's immune system, thus resembling a fetal-restricted neoantigen. In those models, it could be established that especially 'fetal-specific' Treg are expanding during pregnancy, persist for long time periods post-partum and readily assemble to ensure fetomaternal tolerance in consecutive matings[150]. Although Treg expansion is mainly fetal antigen-specific in the first place, another group showed that these cells are also able to suppress T cell responses to unrelated antigens in the from of a bystander suppression[151]. This has functional consequences as Treg expansion leaves pregnant individuals more prone to infections with certain pathogens including *Listeria* and *Salmonella* species, while Treg depletion was able to restore host defence[152]. Thus, pregnancy-induced Treg represent a promising cell population when studying tolerogenic off-target effects, as it might be the case in pregnancy-induced reduction of CNS autoimmunity[7].

1.3.2 Pregnancy and autoimmunity

Pregnancy is well known to suppress the inflammatory activity of many cell-mediated autoimmune diseases including rheumatoid arthritis[153,154], autoimmune hepatitis[155] and MS[4-6], usually followed by a disease rebound post-partum.

In MS, this temporal pregnancy-mediated protection was initially described in a French seminal cohort[4] and has now been replicated in many prospective clinical studies[6]. Similarly, pregnancy was reported to protect rodents from EAE in both SJL/J and C57BL/6 mice[156-158], thus providing a useful tool for studying the effect of pregnancy on CNS autoimmunity.

Hormonal effects

In early pregnancy, the steroid hormones estradiol (E2) and progesterone (P4) drive the differentiation of endometrial stromal cells into large glycogen-filled DSC[159]. This process called decidualisation ensures proper nutrition of the invading blastocyst and prepares the uterus for housing the developing fetus. However, also at later stages increasing progesterone levels sustain pregnancy, while administration of the unspecific progesterone receptor antagonist mifepristone (RU486) induces abortion in the first months of pregnancy.

In C57BL/6 mice pregnancy duration is around 21 days, while the day after successful mating is considered gestational/embryonic day 0.5 (E0.5). P4 serum levels show a first peak on gestational day E6.5, increasing from 10 to 30 ng/ml followed by massive rise to around 100 ng/ml from E10.5 to E17.5[160]. E2 serum levels exhibit a moderate increase from 40 to 60 pg/ml until E17.5 and then sharply increase shortly before parturition to 200 pg/ml[161]. Both treatment with E2 and P4 have been reported to ameliorate EAE[162-164] and to expand Treg[165,166]. However, the protective effect of E2 in EAE was independent of Treg presence[167], and a number of other target cells and cellular mechanisms have been proposed including tolerogenic B cells[167,168] and the induction of tolerogenic DC[169]. Importantly, although the administration of different pregnancy hormones can interfere with EAE development, the exact mechanism by which pregnancy protects from autoimmunity still remains elusive.

1.4 Aims

MS is the most frequent inflammatory disease affecting the CNS and is associated with the infiltration of autoreactive immune cells. During pregnancy, MS patients show ameliorated disease activity resulting in decreased relapse rates, while post-partum disease activity is increased before returning to the individual pre-pregnancy rate. $Foxp3^+$ Treg, which are expanding during pregnancy and are crucial for establishing tolerance to the fetus, are hypothesized to play a pivotal role in mediating this pregnancy-associated control of autoimmunity. However, the precise mechanism by which this occurs is currently unknown.

In order to study this phenomenon, the following specific aims were addressed:

1. Establishment of an EAE mouse model that mimics the protective effect of pregnancy in order to enable more detailed analysis of the underlying mechanisms
2. Characterisation of CNS-infiltrating cells in this model to generate hypotheses about cell types involved in pregnancy protection
3. Characterisation of Treg frequency and phenotype by flow cytometry in different lymphoid organs throughout pregnancy and at post-partum time points
4. Investigation of the impact of pregnancy-related steroid hormones on the immunological balance of regulatory and conventional T cells
5. Assessment of gene expression dynamics in regulatory and conventional T cells in pregnancy and at a post-partum time point
6. Identification of potential molecular pathways involved in conferring pregnancy-associated protection or shifting the immunological balance

By investigating the role of Treg in pregnancy-associated CNS tolerance and revealing pathways that lead to their increased frequency and functionality, this work ultimately aims to identify new therapeutic strategies to re-establish tolerance in MS and other autoimmune diseases.

2 Material and Methods

2.1 Material

2.1.1 Reagents

All reagents and chemicals were purchased from Sigma Aldrich and Carl Roth, unless otherwise indicated.

Table 2.1 Reagents for animal experiments

Reagent	Company
Freund's adjuvant, incomplete	Difco laboratories
Mouse/rat $MOG_{35–55}$ peptide, MEVGWYRSPFSRVVHLYRNGK-NH_2	Schafer-N
Mycobacterium tuberculosis H37	Difco laboratories
Pertussis toxin, from Bordetella pertussis	Calbiochem

Table 2.2 Reagents for cell isolation and cell culture

Reagent	Company
[methyl-^{3}H]-Thymidine	Amersham
2-Mercaptoethanol	Gibco
Anti-PE MicroBeads	Miltenyi Biotec
$CD4^+CD25^+$ Regulatory T Cell Isolation Kit, mouse	Miltenyi Biotec
$CD4^+$ T Cell Isolation Kit II, mouse	Miltenyi Biotec
Collagenase A, from Clostridium histolyticum	Roche
DNaseI, from bovine pancreas	Roche
Dulbecco's Phosphate Buffered Saline (PBS), 1X and 10X	PAA
Ethanol, absolute	Th. Geyer
Ethylenediaminetetraacetic acid (EDTA), 0.5 M solution	Fluka
Fetal calf serum (FCS)	PAA
Hamster anti-mouse CD3 (clone 145-2C11)	BioLegend
HBSS	PAA
LowTox Rabbit Complement M	Cedarlane
Mouse/rat $MOG_{35–55}$ peptide, MEVGWYRSPFSRVVHLYRNGK-NH2	Schafer-N

Penicillin/Streptomycin, 10,000 units/ml	Invitrogen
Percoll	GE Healthcare
Rat anti-mouse CD90.2 (clone30-H12)	BioLegend
Recombinant murine IL-2	eBioscience
RPMI 1640 with stable L-Glutamine	PAA
Scintillation solution	Perkin-Elmer
Trypan blue solution, 0.4%	Sigma Aldrich
Tuerk's solution	Merck

Table 2.3 Hormones and compounds

Reagent	Company
Progesterone	Sigma
Mifepristone (RU486)	Sigma
Dexamethasone	Sigma
D(–)Norgestrel	Sigma

Table 2.4 Reagents for flow cytometry

Reagent	Company
BD Cytometer Setup & Tracking Beads	BD Biosciences
BD TrueCount tubes	BD Biosciences
FACS Clean Solution	BD Biosciences
FACS Flow, 20l	BD Biosciences
FACS Lysing Solution	BD Biosciences
FACS Rinse Solution	BD Biosciences
Foxp3 Staining Buffer Set	eBioscience
LIVE/DEAD Fixable Aqua Dead Cell Stain Kit	Life Technologies
LIVE/DEAD Fixable Near-IR Dead Cell Stain Kit	Life Technologies
Propidium iodide staining solution	BioLegend
Sodium azide	Roth
TruStain FcX, anti-mouse CD16/32	BioLegend

Table 2.5 Reagents for DNA extraction and genotyping PCR

Reagent	Company
Agarose Ultra Pure	Life Technologies
dNTP Mix	Fermentas
Hot Start DNA polymerase and buffer	Fermentas
GeneRuler 1kb Plus DNA Ladder	Fermentas
QuickExtract	Epicentre
RotiSafe	Roth

Table 2.6 Reagents for RNA extraction, cDNA synthesis and real-time PCR

Reagent	Company
2-Mercaptoethanol	Gibco
Ethanol, absolute	Th. Geyer
RevertAid H Minus first Strand Synthesis Kit	Thermo Scientific
RNA isolation columns, RNeasy Mini Kit	Quiagen
TaqMan Gene Expression Master Mix	Life Technologies

Table 2.7 Reagents for western blot

Reagent	Company
Antioxidant	Life Technologies
BCA Protein Assay	Thermo Scientific
Chemiluminescent Substrate, WesternSure Premium	LI-COR
Dry milk, blotting grade	Roth
LDS sample buffer, 4X	Life Technologies
Methanol	Roth
MOPS SDS running buffer, 20X	Life Technologies
Precast gels, 4–12% Bis-Tris	Life Technologies
Prestain marker, SeeBlue Plus2	Life Technologies
Protease inhibitor cocktail	Roche
Reducing Agent, 10X	Life Technologies
Transfer buffer, 20X	Life Technologies

2.1.2 Antibodies

Table 2.8 Antibodies for flow cytometry

Antigen	Clone	Staining	Dilution	Fluorochrome	Company
CD3e	145-2C11	Surface	1:100	PerCP-Cy5.5	BioLegend
CD4	GK1.5	Surface	1:1,000	PE-Cy7	eBioscience
CD8a	53-6.7	Surface	1:300	Pacific blue	BioLegend
CD11b	M1/70	Surface	1:300	FITC	BioLegend
CD11c	N418	Surface	1:300	PE-Cy7	eBioscience
CD25	PC61.5	Surface	1:100	Alexa 488, APC	eBioscience
CD45	30-F11	Surface	1:100	APC-Cy7	BioLegend
B220	RA3-6B2	Surface	1:250	V500	BD Horizon
CD103	2E7	Surface	1:100	Alexa 647	BioLegend
Ctla4	UC10-4B9	Intracellular	1:100	APC	eBioscience
Foxp3	FJK-16s	Intracellular	1:300	PE, eFluor 450	eBioscience
Ki67	B56	Intracellular	1:20	PE	BD Biosciences
Ly6G	1A8	Surface	1:300	V450	BD Biosciences
NK1.1	PK136	Surface	1:150	PE	eBioscience

Table 2.9 Antibodies for western blot

Antigen	Clone	Host	Label	Company
Beta-actin	4967	rabbit	none	Cell Signaling
GR	ab3580	rabbit	none	Abcam
rabbit IgG		goat	HRP	LI-COR

2.1.3 Primers and real-time PCR assays

Table 2.10 Primers for genotyping PCR

Genotyping Primer	Sequence 5'-3'
Actin-fwd	AGA GGG AAA TCG TGC GTG AC
Actin-rev	CAA TAG TGA TGA CCT GGC CGT
Cre-fwd	TAA CAT TCT CCC ACC GCT AGT ACG
Cre-rev	AAA CGT TGA TGC CGG TGA ACG TGC
GRflox1-forw	GCG GTC TGG CAG TAA AAA CTA TC
GRflox2-rev	GTG AAA CAG CAT TGC TGT CAC TT
GRflox3-rev	GGC ATG CAC ATT ACT GGC CTT CT
Egfp-fwd	CCT ACG GCG TGC AGT GCT TCA GC
Egfp-rev	CGG CGA GCT GCA CGC TGC CGT CCT C

Table 2.11 Real-time PCR assays

Gene name	Taqman Assay ID	Company
Esr1	Mm00433149_m1	Life Technologies
Hsd11b1	Mm00476182_m1	Life Technologies
Hsd11b2	Mm01251104_m1	Life Technologies
Nr3c1	Mm00433832_m1	Life Technologies
Pgr	Mm00435628_m1	Life Technologies
Tbp	Mm00446971_m1	Life Technologies
Tsc22d3	Mm01306210_g1	Life Technologies

2.1.4 Buffers, solutions and media

Table 2.12 Buffers, solutions and media

CNS digestion solution	1 mg/ml Collagenase A 0.1 mg/ml DNaseI in RPMI 1640
FASC buffer	0.1% BSA 0.02% NaN_3 in 1X PBS
MACS buffer	0.5% BSA 2 mM EDTA in 1X PBS
Mouse complete medium	10% FCS 50 µM 2-Mercaptoethanol 100 U/ml Penicillin/Streptomycin in RPMI 1640
Red Blood Cell (RBC) Lysis Buffer	0.15 M NH_4Cl 10 mM $KHCO_3$ 0.1 mM Na_2EDTA in ddH_2O pH = 7.4
Tris-buffered saline (TBS), 10X	200 mM Tris 1.5 M NaCl pH = 7.4–7.6

TBS-T	0.1% Tween 20 in 1X TBS
RIPA buffer	50 mM Tris 180 mM NaCl 1 mM Sodium pyrophosphate 1% NP-40 in ddH2O pH = 7.4
TAE buffer, 50X	2 M Tris 0.05 M EDTA 5.7% Acetic Acid in ddH2O

2.1.5 Equipment

Table 2.13 Equipment

Equipment	Company
ABI Prism 7900 HT Fast Real-Time PCR System	Applied Biosystems
BD FACS Aria Cell Sorter	Perkin-Elmer
BD FACS LSR II FACS analyser	BD Biosciences
Beta counter, 1450 Microbeta	Perkin-Elmer
Centrifuges	Eppendorf, Heraeus
Fridges (4°C) and freezers (−20°C and −80°C)	Liebherr, Sanyo
Gamma irradiator, Biobeam 2000 (Cs-137, 49.2 TBq)	Eckert & Ziegler
Harvester 96 MACH III M	Tomtec
Incubator, Hera Cell 240	Thermo Scientific
Incubator, INC153	Memmert
Luminescence imaging system, LAS 4000 mini	GE Healthcare
MACS magnets	Miltenyi Biotec
Nanodrop Nd-1000	Peqlab
PCR cycler, FlexCycle	Analytik Jena
PCR tanks and power supply	Peqlab, Biometra
Pipets and pipette controllers	Gilson, Eppendorf, Brand
Power Supply, BluePower 500	Serva
Rotators, shakers and waterbath	GLW, IKA, GFL
Sterile bank, Safe2020	Thermo Scientific

Thermomixer	Eppendorf
Western blot system (Gel tank, blot module)	Life Technologies

2.1.6 Consumables

Table 2.14 Consumables

Consumable	Company
Cell culture plates	Greiner
Cell strainer, 40 µm	BD Biosciences
Columns for magnetic cell isolation, MS, LS and LD	Miltenyi Biotec
Eppendorf tubes	Sarstedt
FACS tubes, 5 ml	Sarstedt
Falcon tubes, 15 and 50 ml	Greiner
Filtermat A	Perkin-Elmer
Filtermat bag	Perkin-Elmer
Liquid reservoir for multichannel pipettes	Roth
Nitrocellulose transfer membrane, Protran, 0.45 µm	Schleicher Schuell
PCR plate, 96 well and PCR plate sealing tape	Sarstedt
Pipette tips	Sarstedt
Serological pipettes, 5, 10 and 25 ml	Greiner
Syringes and needles	Braun

2.1.7 Software

Table 2.15 Software

Software	Company
FACS Diva analysis software	BD Biosciences
FlowJo vX for Mac FACS analysis software	TreeStar
NanoDrop ND-1000 V3.5.2	Thermo Scientific
Papers2 reference manager for Mac	Mekentosj
Prism 6 for Mac	GraphPad Software
RQ Manager	Applied Biosystems
SDS v2.4	Applied Biosystems

2.1.8 Laboratory animals

C57BL/6 wildtype mice were initially obtained from The Jackson Laboratory, USA, and were housed and bred in the Central Animal Facility at the University Medical Center Hamburg-Eppendorf (UKE). These animals are hereinafter referred to as wildtype mice.

DEREG mice[170], Tg(Foxp3-DTR/EGFP)23.2Spar, were generated by Tim Sparwasser, TWINCORE, Hannover, Germany, and kindly provided by Prof. Dr. Ulf Panzer, III. Department of Internal Medicine, UKE.

$GR^{fl/fl}$ mice[171], $Nr3c1^{tm2Gsc}$, were generated by Günther Schütz, German Cancer Research Center, Heidelberg. These animals were crossed to *Lck*-Cre mice[172] and kindly provided by Prof. Dr. Holger Reichardt, Göttingen University Medical School.

All mice were kept under specific pathogen-free conditions in the Central Animal Facility and at the Center for Molecular Neurobiology Hamburg (ZMNH). All animal experiments were approved by the local ethics committee (Behörde für Soziales, Familie, Gesundheit und Verbraucherschutz in Hamburg; G12/012).

2.2 Methods

2.2.1 Genotyping

Genetically modified mice were genotyped by polymerase chain reaction (PCR). For this purpose, tail biopsies were taken from new-born mice, genomic DNA was extracted using QuickExtract reagent and used as template for the following PCR reactions.

In the presence of the DEREG transgene, usage of the primers Egfp-fwd and Egfp-rev (see **Tab 2.10**) resulted in a 350 bp amplicon. A PCR for *Actin* was performed in the same well using the primers Actin-fwd and Actin-rev and served as a positive control with a 150 bp amplicon. For the PCR reaction 2.0 µl of template was added to a master mix containing 14.25 µl ddH_2O, 2.5 µl 10X Hot Start Buffer, 1.5 µl $MgCl_2$ (25 mM), 0.5 µl dNTPs (10 mM), 0.25 µl Hot Start polymerase and 1.0 µl of each primer (10 µM). The amplification was done in a PCR cycler as follows: 95°C for 10 min, 32 cycles of 94°C, 63°C and 72°C steps for 30 seconds each, 72°C for 5 min.

$GR^{fl/fl}$ mice were genotyped using the primers GRflox1-forw, GRflox2-rev and GRflox3-rev. In this PCR the wildtype allele, the floxed allele and the deleted allele are represented by 225 bp, 275 bp and 390 bp amplicon, respectively. For details, see also **Fig 3.12**. For the PCR reaction 2.0 µl of template was added to a master mix containing 14.75 µl ddH_2O, 2.5 µl 10X Hot Start Buffer, 2.0 µl $MgCl_2$ (25 mM), 0.5 µl dNTPs (10 mM), 0.25 µl Hot Start polymerase and 1.0 µl of each primer (10 µM). The amplification was done in a PCR

cycler as follows: 95°C for 5 min, 35 cycles of 94°C, 63°C and 72°C steps for 30, 60, 60 seconds, respectively, 72°C for 10 min.

Presence of the *Lck*-Cre transgene was confirmed by using the primers Cre-fwd and Cre-rev, which resulted in a 215 bp amplicon. *Actin* positive control was included as described above. For the PCR reaction 2.0 µl of template was added to a master mix containing 13.75 µl ddH_2O, 2.5 µl 10X Hot Start Buffer, 2.0 µl $MgCl_2$ (25 mM), 0.5 µl dNTPs (10 mM), 0.25 µl Hot Start polymerase and 1.0 µl of each primer (10 µM). The amplification was done in a PCR cycler as follows: 94°C for 5 min, 35 cycles of 94°C, 55°C and 72°C steps for 30, 30, 45 seconds, respectively, 72°C for 7 min.

All PCR products were resolved by electrophoresis on a 2% (DEREG, *Lck*-Cre) or 3% ($GR^{fl/fl}$) agarose gel, stained with RotiSafe and visualized on a UV transilluminator.

2.2.2 Allogeneic mating

Age-matched (10–20 weeks) female mice where primed with housing material from fertile males for one week. Then females were introduced to the cages of single BALB/c males in a ratio of two to one and mated for three consecutive nights. Successfully mated females where identified every morning by the presence of a vaginal plug. Plugged animals were separated and weighted daily to confirm pregnancy. The day of plug was considered gestational day 0.5 (E0.5).

2.2.3 EAE induction

Mice were immunized subcutaneously with 200 µg $MOG_{35–55}$ peptide in complete Freund's adjuvant containing 4 mg/ml *Mycobacterium tuberculosis*. In addition 200 ng pertussis toxin was injected intravenously on the day of immunisation and 48 h later. Animals were scored daily for clinical signs by the following system: 0, no clinical deficits; 1, tail weakness; 2, hind limb paresis; 3, partial hind limb paralysis; 3.5, full hind limb paralysis; 4, full hind limb paralysis and forelimb paresis; 5, premorbid or dead. Animals reaching a clinical score ≥ 4 had to be sacrificed according to the regulations of the Animal Welfare Act. In these animals the last observed score was carried forward for statistical analysis.

2.2.4 Cell isolation

Immune cell isolation from lymph nodes and spleen

For preparation of immune cells from lymphatic tissue, mice were anesthetized with a gas mixture of 80% CO_2 and 20% O_2 and consecutively sacrificed by inhalation of 100% CO_2. Inguinal, axillary, brachial, para-aortal lymph nodes (LN) and spleens were harvested with sterile instruments and collected into ice cold PBS. Single cell suspension was prepared

by homogenization through a 40 µm cell strainer. Cells were pelleted by centrifugation (300 g, 10 min, 4°C) and treated with Red Blood Cell (RBC) Lysis Buffer for 5 min at 4°C. Lysis was stopped by adding an excess of ice cold PBS, cells were pelleted and washed in PBS. Then, cells were resuspended in PBS or Mouse complete medium depending on the follow-up application.

Isolation of CNS-infiltrating leukocytes

For the isolation of CNS-infiltrating cells, mice were anesthetized and sacrificed as above and immediately intracardially perfused with ice cold PBS to remove leukocytes from intracranial blood vessels. Brain and spinal cord were prepared with sterile instruments, minced with a scalpel and incubated with agitation in CNS digestion solution containing collagenase A and DNAseI for 60 min at 37°C. Tissue was triturated through a 40 µm cell strainer and washed with PBS (300 g, 10 min, 4°C). Homogenized tissue was resuspended in 30% isotonic Percoll and 78% isotonic Percoll was carefully layered underneath. After gradient centrifugation (1,500 g, 30 min, 4°C), CNS-infiltrating immune cells including microglia were recovered from the gradient interphase. Recovered cells were washed twice and resuspended in ice cold PBS.

2.2.5 Magnetic-activated cell sorting (MACS)

Magnetic isolation of $CD4^+$ T cells

$CD4^+$ T cells were isolated from single cell suspensions of leukocytes using $CD4^+$ T cell isolation kit II according to the manufacturer's instructions. Briefly, cell suspension was incubated in MACS buffer with a biotinylated antibody cocktail that binds multiple immune cell subsets but at the same time exclusively spares $CD4^+$ T cells. Then, antibody-bound non-$CD4^+$ T cells were targeted by anti-biotin-microbeads and depleted from the suspension by a MACS LD column, which was placed in a strong magnetic field. Non-labeled $CD4^+$ T cells were recovered from the flow through and utilized for down-stream applications.

Magnetic isolation of $CD4^+CD25^+$ Treg

Treg were isolated from single cell suspensions of leukocytes using $CD4^+CD25^+$ Regulatory T Cell Isolation Kit according to the manufacturer's instructions. Briefly, $CD4^+$ cells were isolated as described above, followed by a consecutive separation of CD25-PE labeled cells by anti-PE-microbeads. Purity of resulting $CD4^+CD25^-$ Tcon and $CD4^+CD25^+$ Treg populations was routinely above 90% (**Fig. 2.1**).

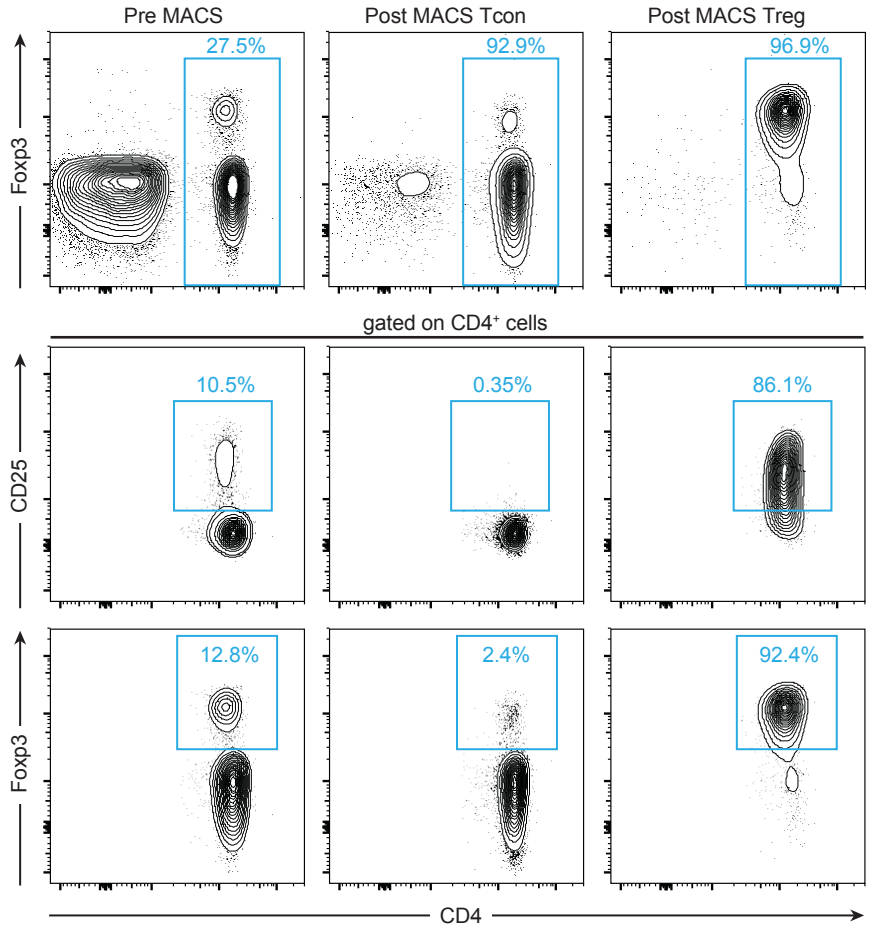

Figure 2.1 Magnetic-activated cell sorting of $CD4^+CD25^+$ Treg
Single cell suspension was prepared from inguinal, axillary, brachial, para-aortic lymph nodes and spleen (left panel) and $CD4^+CD25^-$ Tcon (middle panel) and $CD4^+CD25^+$ Treg (right panel) were separated by magnetic-activated cell sorting. Purity of resulting populations is determined by flow cytometric analysis of CD4, CD25 and Foxp3 expression.

2.2.6 Cell culture experiments

Steroid assay of splenocytes

Isolated splenocytes were cultured in Mouse complete medium at a cell density of 0.5×10^6 cells per well in a 96 well round bottom plate for a period of 48 h. Cells were either treated with the vehicle control ethanol (EtOH), progesterone (P4), dexamethasone (DEX), norgestrel (NOR) or with a combination of steroid and 1 µg/ml of the steroid receptor inhibitor mifepristone (RU486). Each experimental condition was set up in four to six replicate wells, which were pooled before flow cytometric analysis of viable cells.

Generation of feeder cells

For the generation of accessory feeder cells 30×10^6 naïve wildtype splenocytes were resuspended in 900 µl HBSS medium and 100 µl LowTox Rabbit Complement M and 5 µl of Rat anti-mouse CD90.2 were added. Cells were then incubated with mild agitation for 30 min at 37°C to deplete T cells. The reaction was stopped by adding an excess of ice

cold HBSS. Then, cells were washed twice with ice cold HBSS (300 g, 10 min, 4°C), resuspended in 5 ml HBSS, irradiated with 35 Gy in a Biobeam 2000 gamma irradiator, washed twice with ice cold HBSS (300 g, 10 min, 4°C) and utilized as non-proliferative, T cell-depleted feeder cells.

Treg suppression assay

Treg and Tcon were isolated by MACS and used as suppressors and responders, respectively. Feeder cells were generated as described above. All cells were resuspended in Mouse complete medium at 1×10^6 cells/ml. Then 5×10^4 Tcon and 5×10^4 feeder cells were plated per well in a 96 well round bottom plate. Treg were added to achieve the following final Treg:Tcon ratios 1:1, 1:2, 1:4, 1:8, 1:16 and 0:1. Tcon responder cells were stimulated for proliferation with 1 µg/ml anti-CD3 antibody. Unstimulated wells were used as negative control. All experimental conditions were plated in triplicate and adjusted to a final volume of 200 µl/well. Cells were cultured for 72 h and proliferation per well was assessed by [^{3}H]-Thymidine incorporation assay.

[^{3}H]-Thymidine incorporation assay

After 48 h or 72 h of culture, cells were pulsed with 1 µCi radioactively labeled [^{3}H]-Thymidine, which is inserted into the DNA only by proliferating cells and can be detected by a Beta counter. After pulsing, cells were incubated another 16 h and then harvested and spotted on filtermats according to the manufacturer's instructions. Spotted filtermats were dried at 60°C, transferred into plastic bags containing 5 ml β-Scintillation solution and sealed with a plastic sealer. Incorporated activity per well was assessed in counts per minute (cpm) by a Beta counter. Relative proliferation was calculated relative to the positive control without addition of Treg or steroid.

Steroid dose response assay

Treg and Tcon were isolated by MACS, feeder cells were generated as described above. Treg and Tcon were cultured separately in Mouse complete medium at 5×10^4 cells/well in the presence of 5×10^4 irradiated feeder cells in 96 well round bottom plates. Cells were stimulated for proliferation with 1 µg/ml anti-CD3 antibody and 50 U/ml recombinant murine IL-2 and treated with increasing concentrations of dexamethasone (DEX). Conditions lacking responder cells, feeder, stimulation or DEX treatment were included as controls. All experimental conditions were plated in triplicate and adjusted to a final volume of 200 µl/well. After a 48 h culture period, proliferation per well was assessed by [^{3}H]-Thymidine incorporation assay. Curve fit and curve characteristics were computed using Prism software.

Cell death assay

Treg and Tcon were isolated by MACS and cultured separately in Mouse complete medium at 1 × 10^5 cells/well in 96 well round bottom plates. Cells were treated either with the vehicle control ethanol (EtOH), dexamethasone (DEX) or with a combination of DEX and 1 µg/ml of the steroid receptor inhibitor mifepristone (RU486). Dead cells were identified by propidium iodide positivity after 4 h and 6 h culture time. Cell death was calculated as fold change relative to vehicle control.

2.2.7 Flow cytometry

Identification of dead cells

Dead cells were identified using the LIVE/DEAD Fixable Dead Cell Stain Kit according to manufacturer's instructions. Briefly, before surface staining, cells were washed twice with ice cold PBS (350 g, 5 min, 4°C) to remove soluble protein that interferes with the staining procedure. Cells were resuspended in 100 µl PBS containing the diluted staining reagent (1/1,000) and incubated for 30 min at 4°C. Then, cells were washed twice with ice cold PBS (350 g, 5 min, 4°C) and subjected to surface staining.

Surface staining

Per staining reaction 1 × 10^6 isolated leukocytes were transferred to 5 ml tubes, pelleted and resuspended in 100 µl FACS buffer containing TruStain Fc receptor block (final dilution 1/1,000) and a cocktail of indicated directly labeled antibodies. Cells were stained for 30 min at 4°C, washed with ice cold FACS buffer (350 g, 5 min, 4°C) and then either resuspended in 200 µl FACS buffer for acquisition or further proceeded to intracellular staining.

Cell quantification using TruCount tubes

Every TruCount tube contains a defined number of fluorescent beads, which can be identified and counted by the flow cytometer. By adding a defined volume of a cell suspension of unknown concentration the ratio of cell events and bead events can be used to calculate the absolute cell number in the original sample. To determine the absolute numbers of CNS-infiltrating leukocytes, isolated cells were resuspended in 1 ml FACS buffer, 100 µl of the resulting cell suspension was transferred to a TruCount tube and incubated with TruStain Fc receptor block (1:1,000) and anti-CD45-APC-Cy7 (1:1,000) antibody for 20 min at 4°C. The stained sample was diluted with 300 µl FACS buffer and immediately analysed. The total number of CNS-infiltrating $CD45^+$ immune cells was calculated by the following formula: #$CD45^+$ cells = (#Total beads per tube/ #Acquired beads) × #Acquired $CD45^+$ cells × dilution (see also **Fig. 2.2a**). By initially

gating on CD45$^+$ cells in all additional panels, this number could be used to also calculate the absolute numbers of all consecutively analysed immune cell subsets.

Intracellular staining

Staining of intracellular proteins such as the nuclear transcription factor Foxp3 or the cell cycle protein Ki67 requires fixation and permeabilisation and was performed using Foxp3 Staining Buffer Set according to manufacturer's instructions. Briefly, after surface staining cells were pelleted (350 g, 5 min, 4°C), resuspended in 500 µl freshly prepared Fix/Perm solution and incubated for 30 min at 4°C. Cells were washed twice with permeabilisation buffer (350 g, 5 min, 4°C) and subsequently stained with intracellular antibody cocktail in 100 µl permeabilisation buffer containing TruStain Fc receptor block (1/1,000). After an incubation period of 30 min at 4°C cells were washed twice with permeabilisation buffer (350 g, 5 min, 4°C) and resuspended in 200 µl FACS buffer for acquisition.

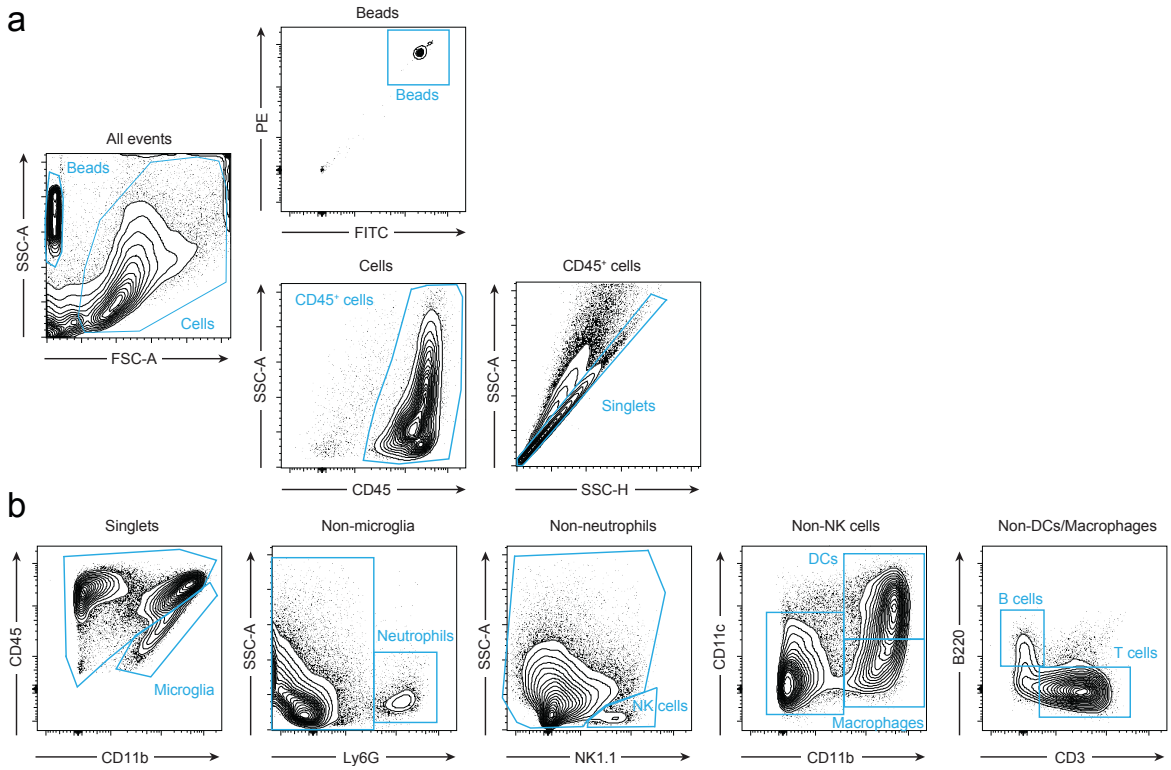

Figure 2.2 Gating strategy for immune cell phenotyping

(**a**) In a first step, cell and TruCount bead populations were identified by forward/sideward scatter (FSC/SSC). Beads were additionally gated to be highly fluorescent in both the PE and FITC channel. Cells were gated to be CD45$^+$, duplets were excluded by gating on Singlets in SSC height/area. (**b**) In CNS samples microglia were identified as CD45^{int}CD11b$^+$, remaining cells were used to identify stepwise neutrophils (Ly6G$^+$), NK cells (NK1.1$^+$), DCs (CD11b$^+$CD11c$^+$) and macrophages (CD11b$^+$CD11c$^-$) and finally, B cells (B220$^+$) and T cells (CD3$^+$).

Immune cell phenotyping

For immune cell phenotyping, leukocytes from spleen, lymph nodes or infiltrated CNS tissue were isolated and stained for flow cytometric analysis as described above. Immune

cell subsets were identified by the following gating strategy (see **Fig. 2.2**). In additional staining panels, T cells were further divided into cytotoxic T cells ($CD8^+$), T helper cells ($CD4^+$) and Treg ($CD4^+Foxp3^+$). Antibodies were generally diluted according to **Tab. 2.8**. Only in CNS analysis, CD4-PE-Cy7 was used at a higher concentration of 1:100.

Data acquisition and analysis

For data acquisition a BD FACS LSR II FACS analyser running FACS Diva software was utilized. Data analysis was performed using FlowJo vX for Mac analysis software.

2.2.8 Fluorescence-activated cell sorting (FACS)

For isolation of Foxp3-GFP^+ Treg from DEREG mice, leukocytes from inguinal, axillary, brachial, para-aortal lymph nodes (LN) and spleen were isolated as described above. Pooled cells (around 5–10 × 10^7) were resuspended and stained in 1 ml MACS buffer containing TruStain Fc receptor block (1/1,000) and CD4-PB antibody (1:300). Cells were incubated for 30 min at 4°C and then washed with ice cold PBS (300 g, 10 min, 4°C), resuspended in ice cold PBS and flushed through a 40 µm cell strainer to remove debris that could occlude the cell sorter nozzle. Cell sorting was performed on a BD FACS Aria Cell Sorter at the FACS Sorting Core Unit at the UKE using the sorting strategy shown below (**Fig. 2.3**). Cells were collected into cooled FCS-coated 5 ml tubes containing Mouse complete medium with increased FCS fraction of 20%.

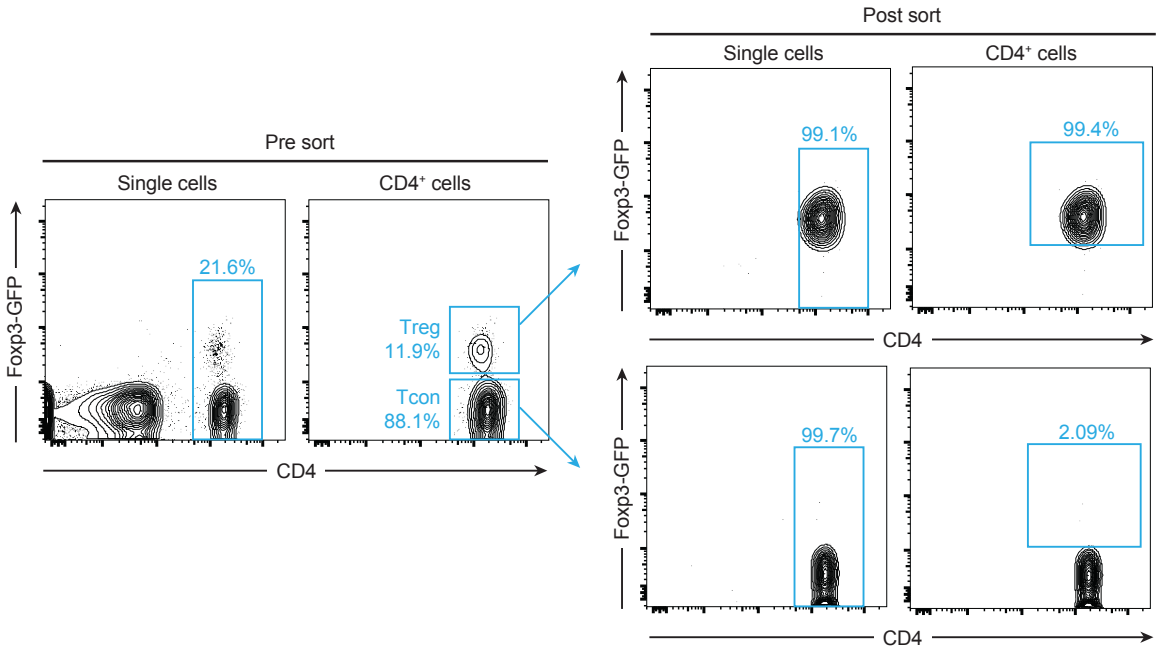

Figure 2.3 Fluorescence-activated cell sorting of Foxp3-GFP^+ Treg

Stained leukocytes from DEREG mice were gated on $CD4^+$ singlets. Inside $CD4^+$ cells Foxp3-GFP^+ Treg and Foxp3-GFP^- Tcon were identified and sorted into two different 5 ml tubes (**left panel**). Reanalysis of sorted cells revealed population purities above 98% (**right panel**).

Purity of sorted $CD4^+Foxp3\text{-}GFP^+$ Treg and $CD4^+Foxp3\text{-}GFP^-$ Tcon was routinely above 98%. For consecutive gene expression analysis, cells were washed with ice cold PBS (300 g, 10 min, 4°C), pelleted, snap frozen in liquid nitrogen and stored at −80°C.

2.2.9 RNA isolation, cDNA synthesis and real-time PCR

RNA isolation

RNA was isolated using RNeasy Mini Kit according to manufacturer's instructions. Briefly, samples of around 2×10^6 cells were washed in ice cold PBS (300 g, 10 min, 4°C), pelleted, snap frozen in liquid nitrogen and stored at −80°C until further processing. At the time of RNA isolation, cell pellet was resuspended in 350 µl RLT buffer containing 2-Mercaptoethanol (1:100) and actively disrupted by repetitive passage through a 30G needle. Cell debris was removed by centrifugation (>8,000 g, 3 min, RT) and supernatant was transferred to a new RNase-free vial. Then, an equal volume of 70% ethanol was added and the whole sample was transferred onto a RNA isolation column. After centrifugation (>8,000 g, 15 sec, RT), column-bound RNA was consecutively washed with 700 µl RW1 buffer (>8,000 g, 15 sec, RT), 500 µl RPE buffer (>8,000 g, 15 sec, RT) and 500 µl RPE buffer (>8,000 g, 2 min, RT) and finally eluted with 30 µl RNase-free water into a fresh RNase-free 1.5 ml vial. Isolated RNA was immediately kept on ice and concentration was determined photometrically by Nanodrop. Samples were stored at −80°C until further processing.

cDNA synthesis

For cDNA synthesis, 500 ng of isolated RNA was added to 1 µl random hexamer primers and adjusted to a final volume of 12 µl per reaction with RNase-free water. Samples were denatured at 65°C for 5 min, then 4 µl 5X Reaction buffer, 1 µl Ribolock RNase inhibitor, 2 µl 10 mM dNTPmix and 1 µl RevertAid H Minus reverse transcriptase were added. Samples were mixed well and reaction was incubated for 5 min at 25°C. Then, reverse transcription was performed at 42°C for 60 min and terminated by inactivation at 70°C for 5 min. Transcribed cDNA was stored at −20°C.

Real-time PCR

Gene expression was analysed by real-time PCR performed in an ABI Prism 7900 HT Fast Real-Time PCR System. The TaqMan assays used, containing a set of primers and a reporter probe, are listed in **Tab. 2.11**. All cDNA samples were diluted 1:10 in RNase-free water and run in triplicate according to the manufacturer's instructions with minor modifications. Briefly, per single reaction, 0.5 µl TaqMan assay, 5.0 µl 2X Gene Expression Master Mix, 2.5 µl RNase-free water and 2.0 µl cDNA sample were mixed and run in a 96 well plate. Reaction was initialized by holding 50°C for 2 min and 95°C for

10 min, followed by 40 cycles with 95°C for 15 sec and 60°C for 1 min. In all assays, the housekeeping gene *Tbp*, encoding TATA-binding protein was used as endogenous control. Gene expression of genes of interest was calculated as $2^{-\Delta CT}$ relative to *Tbp* expression. For analysis SDS v2.4 and RQ Manager software was used.

2.2.10 Microarray analysis

Gene expression array analysis of Treg sorted from virgin and E18.5 pregnant DEREG mice (*n* = 4 per group) was done by the Transkriptomanalyselabor at the University Medical Center Göttingen (Head: Dr. Gabriela Salinas-Riester) according to locally established protocols. Differentially expressed candidate genes were identified by a fold change ≥ 1.5 and a false discovery rate-corrected *P*-value < 0.05.

2.2.11 Western blot

Cell Lysis

Thymocytes were isolated from mouse thymus analogously to isolation of leukocytes from spleen described above. Isolated cells were washed with ice cold PBS (300 g, 10 min, 4°C), pelleted, snap frozen in liquid nitrogen and stored at −80°C until further processing. At the time of cell lysis, cell pellet was resuspended in 100 µl RIPA buffer containing protease inhibitor cocktail and actively disrupted by repetitive passage through a 30G needle. Samples were then incubated with agitation for 30 min at 4°C. Cell debris was removed by centrifugation (1,000 g, 10 min, 4°C) and protein-containing supernatant was transferred to a new vial.

Determination of protein concentration

Protein concentration was determined by BCA Protein Assay according to the manufacturer's instruction. Briefly, 10 µl of sample or protein standard was added in triplicate to flat bottom 96 well plates, then 200 µl freshly prepared BCA solution was added to each well. After incubation for 30 min at 37°C, absorbance at 562 nm was assessed by a spectrophotometer and protein concentration was calculated according to the protein standard curve.

Protein electrophoresis

Protein electrophoresis was performed according to the manufacturer's instruction. Briefly, protein samples were mixed with 4X LDS sample buffer, 10X Reducing Agent and adjusted to a concentration of 2 µg/µl with RIPA buffer. Samples were denatured for 5 min at 95°C and 15 µl (30 µg) per lane were loaded onto 4–12% Bis-Tris precast gels. Electrophoresis was performed using MOPS SDS running buffer at constant 180 V for 60 min.

Protein transfer and detection

Proteins were transferred onto a nitrocellulose membrane by wet-blot electrophoresis (30 V, 60 min). The blotted membrane was blocked for 1 h at RT in 5% dry milk resolved in TBST. Membrane was incubated with the first antibody in TBST over night at 4°C, thoroughly washed with TBST and incubated for 1 h with the secondary antibody in TBST at RT. After thorough washing with TBST the blot was developed with chemiluminescent HRP substrate and documented with a Luminescence imaging system.

2.2.12 Statistical analysis

All data are presented as mean values ± s.e.m. Mean differences between two experimental groups were determined by unpaired, two-tailed Student's *t*-test. Comparison of three or more groups was performed by one-way analysis of variance (ANOVA) with Bonferroni's *post hoc* test. Statistical analysis comparing two groups under multiple conditions or over time was performed by two-way ANOVA with Bonferroni's *post hoc* test. Differences in disease incidence and survival were assessed by Fisher's exact test and Chi square test, respectively. All statistical analyses were performed using Prism 6 for Mac. Significant results are indicated by asterisks: $*P < 0.05$; $**P < 0.01$.

3 Results

3.1 Protective effect of pregnancy

3.1.1 Establishment of an animal model

In order to study the impact of pregnancy on CNS autoimmunity, experimental autoimmune encephalomyelitis (EAE) was utilized as animal model. Before EAE induction, allogeneic mating of two unrelated mouse lines – C57BL/6 and BALB/c – was performed to achieve a setting in which the mother's immune system has to establish tolerance towards genetically different fetuses. This would not be the case in a mating of C57BL/6 with C57BL/6 since all individuals of an inbred line are supposed to be genetically identical. At gestational day E7.5 ± 1, EAE was induced by subcutaneous injection of the $MOG_{35–55}$ peptide in complete Freund's adjuvant. In addition, pertussis toxin (PTX) was administered intravenously on the day of immunisation and 48 h later. Onset of disease and delivery of the pups were expected around day 7 and day 12 after immunisation, respectively. Non-pregnant females served as a control group (**Fig. 3.1a**).

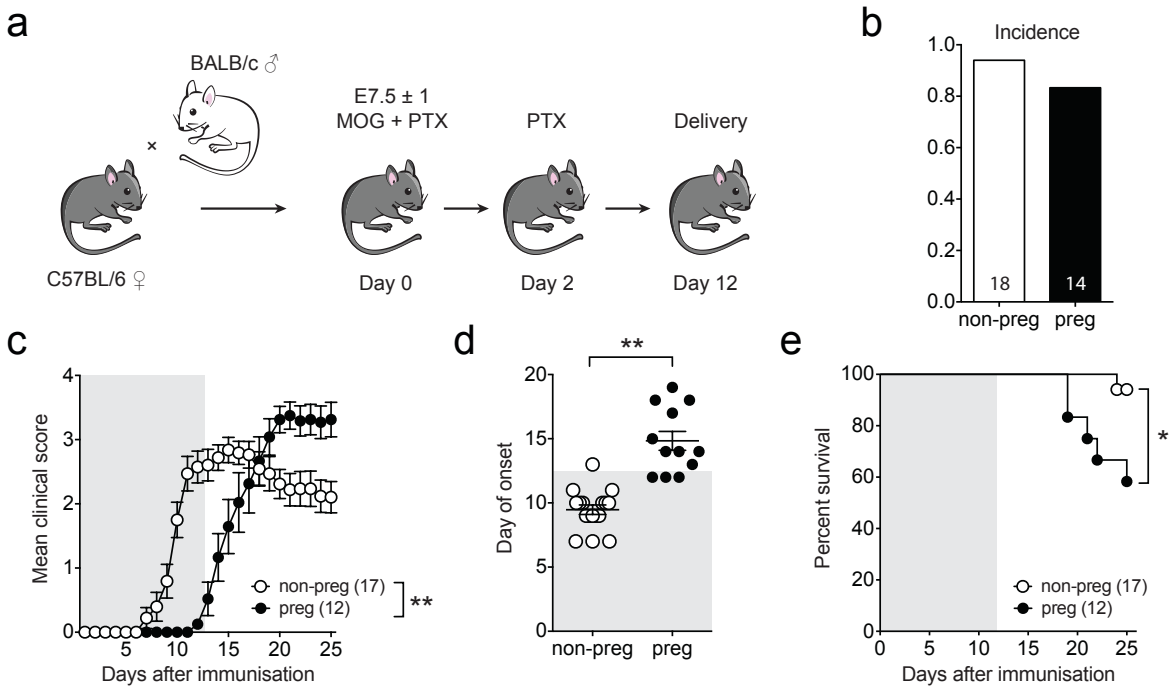

Figure 3.1 Pregnancy protects from CNS autoimmunity

(**a**) Experimental setup of pregnancy EAE. Non-pregnant age-matched females served as controls. Disease incidence (**b**), clinical course (**c**), day of onset (**d**) and survival (**e**) is shown for non-pregnant (n = 17; white) and pregnant (n = 12; black) animals. Grey shaded areas represent pregnancy. Data are pooled from four independent experiments. Statistical analyses were performed by Fisher's exact test in **b**, two-way ANOVA with Bonferroni's *post hoc* test in **c**, Student's *t*-test in **d** and Chi square test in **e**. *P < 0.05; **P < 0.01

In both experimental groups the disease incidence was observed to be above 80% with no significant difference between the groups (Fisher's exact test; $P = 0.5681$; **Fig. 3.1b**). In further analysis EAE non-responders were excluded. The disease activity of non-pregnant controls showed a typical course, beginning at day 7, reaching a peak around day 15 and then gradually declining to a chronic plateau around day 20. However, pregnant animals started to develop disease around the day of delivery (day 12), then progressed to high disease scores around day 20 and showed no clear remission phase until the end of the observed period at day 25. Disease courses (interaction of group and time) were significantly different in two-way ANOVA ($P < 0.0001$). Additionally, Bonferroni's *post hoc* test detected group differences on day 10–15 and 20–25 (**Fig. 3.1c**). As suggested by the disease course, the day of onset was delayed in pregnant animals (Student's *t*-test; $P < 0.0001$; **Fig. 3.1d**) while a higher disease burden apart from day 20 was also reflected by decreased survival of pregnant animals (Chi square test; $P = 0.0165$; **Fig. 3.1e**).

Taken together, pregnant animals showed a temporal protection from EAE with increased post-partum disease activity as observed in clinical studies in humans. Thus, the established model closely mimics the effects of pregnancy in human MS patients and might therefore deliver valuable insights into the mechanistic underpinning of this phenomenon.

3.1.2 Analysis of CNS-infiltrating immune cells

Since motor function defects assessed by the clinical score are a consequence of inflammatory injury of responsible neurons and their projections, the infiltration of immune cells into the CNS was assessed by flow cytometry. For this analysis, animals of both groups were sacrificed at day 10 during the disease course – a time point when pregnant animals were still protected while non-pregnant animals already presented clinical symptoms (Student's *t*-test; $P = 0.0278$; **Fig. 3.2a**). After isolation of CNS-infiltrating leukocytes, these cells were counted with TruCount technology and subsequently phenotyped by flow cytometry. Indeed, the total number of infiltrating leukocytes was decreased in pregnant animals (Student's *t*-test; $P = 0.0089$; **Fig. 3.2b**) and this was mainly reflected in reduced numbers of infiltrating DCs and T cells (**Fig. 3.2c**). Within T cells, all studied subsets showed a homogenous reduction in the CNS from pregnant animals. Thus, reduction of CNS-infiltrating T cells was not driven by a single subset, but rather represents a sum effect of all infiltrating T cell subsets (**Fig 3.2d**). In summary, autoreactive T cell priming, expansion, infiltration or a combination of these processes appears to be inhibited during pregnancy and results in reduced CNS infiltration.

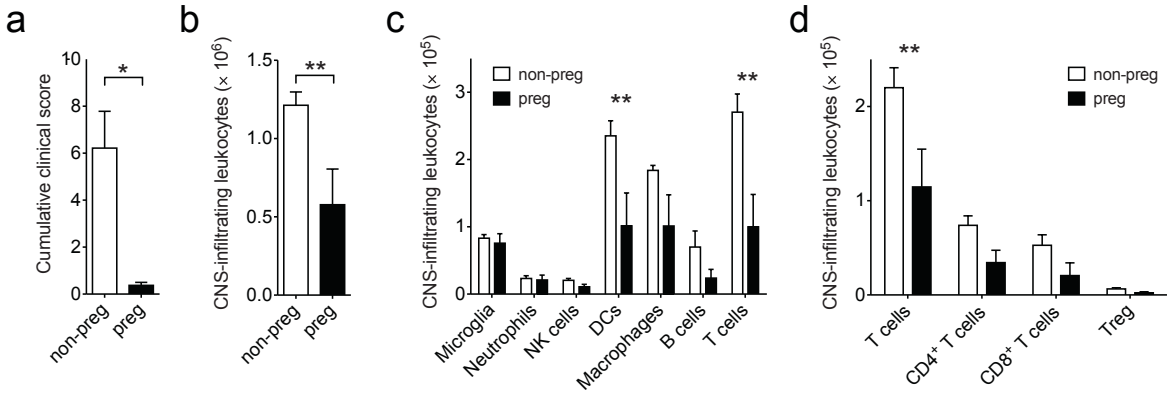

Figure 3.2 Pregnancy reduces the number of CNS-infiltrating leukocytes
(**a**) Non-pregnant ($n = 4$; white) and pregnant ($n = 8$; black) animals were sacrificed 10 days after EAE induction. Cumulative clinical score up to day 10 was calculated. (**b–c**) CNS-infiltrating leukocytes were isolated and absolute numbers of infiltrating immune cell populations were assessed by flow cytometry. Data are shown for one representative experiment out of two. Statistical analyses were performed by Student's *t*-test in **a** and **b**, and two-way ANOVA with Bonferroni's *post hoc* test in **c** and **d**. *$P < 0.05$; **$P < 0.01$

3.2 Treg during pregnancy

3.2.1 Treg frequency and phenotype

Since Treg are known to play a crucial role in both establishing tolerance towards the developing fetus and preventing autoimmune diseases, Treg frequency and phenotype were assessed in different lymphoid organs during allogeneic pregnancy in healthy female mice. $CD4^+Foxp3^+$ Treg preferentially accumulated in para-aortal lymph nodes, which are directly draining the uterus. However, elevated frequencies could also be detected in inguinal lymph nodes and spleen (**Fig. 3.3**). Of note, Treg frequencies were beginning to increase in middle to late pregnancy (E10.5–E18.5) and stayed at elevated levels as long as post-partum day 30 (PP30).

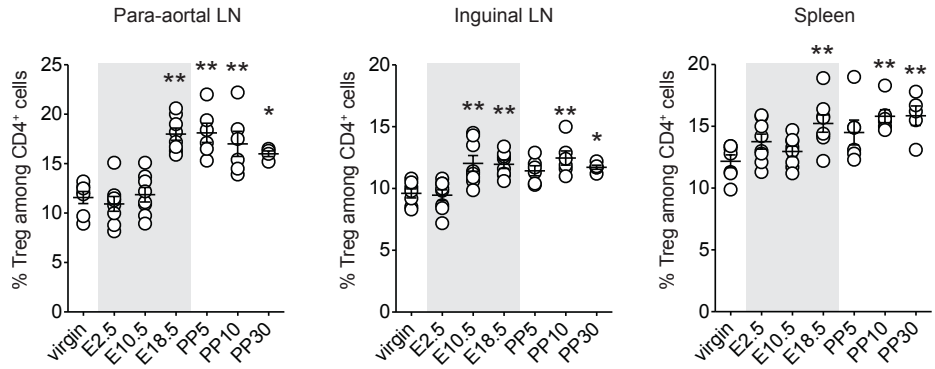

Figure 3.3 Treg expansion during pregnancy
Female mice were sacrificed on indicated pregnancy (E2.5–E18.5) and post-partum (PP5–PP30) time points. Immune cells were prepared from para-aortal lymph nodes (LN), inguinal LN and spleen and $CD4^+Foxp3^+$ Treg were analysed by flow cytometry. Grey shaded areas represent pregnancy. Data are representative of one experiment with four to eight animals per group. Statistical analyses were performed by one-way ANOVA with Bonferroni's *post hoc* test in comparison to virgin control mice. *$P < 0.05$; **$P < 0.01$

In order to get insights into phenotype and proliferative activity of $CD4^+Foxp3^+$ Treg and $CD4^+Foxp3^-$ Tcon during allogeneic pregnancy, additional markers were analysed on both cell types. The protein Ki67 is a cellular marker for proliferation[173,174] and can be readily assessed by flow cytometry. In Treg, two proliferative bursts could be identified, one in early (E2.5) and one in late (E18.5) pregnancy. These bursts are coinciding with (i) the first contact to paternal sperm antigen before implantation and (ii) the late high rate increase of fetal antigenic mass, respectively, and were most pronounced in para-aortal LN (**Fig. 3.4a**).

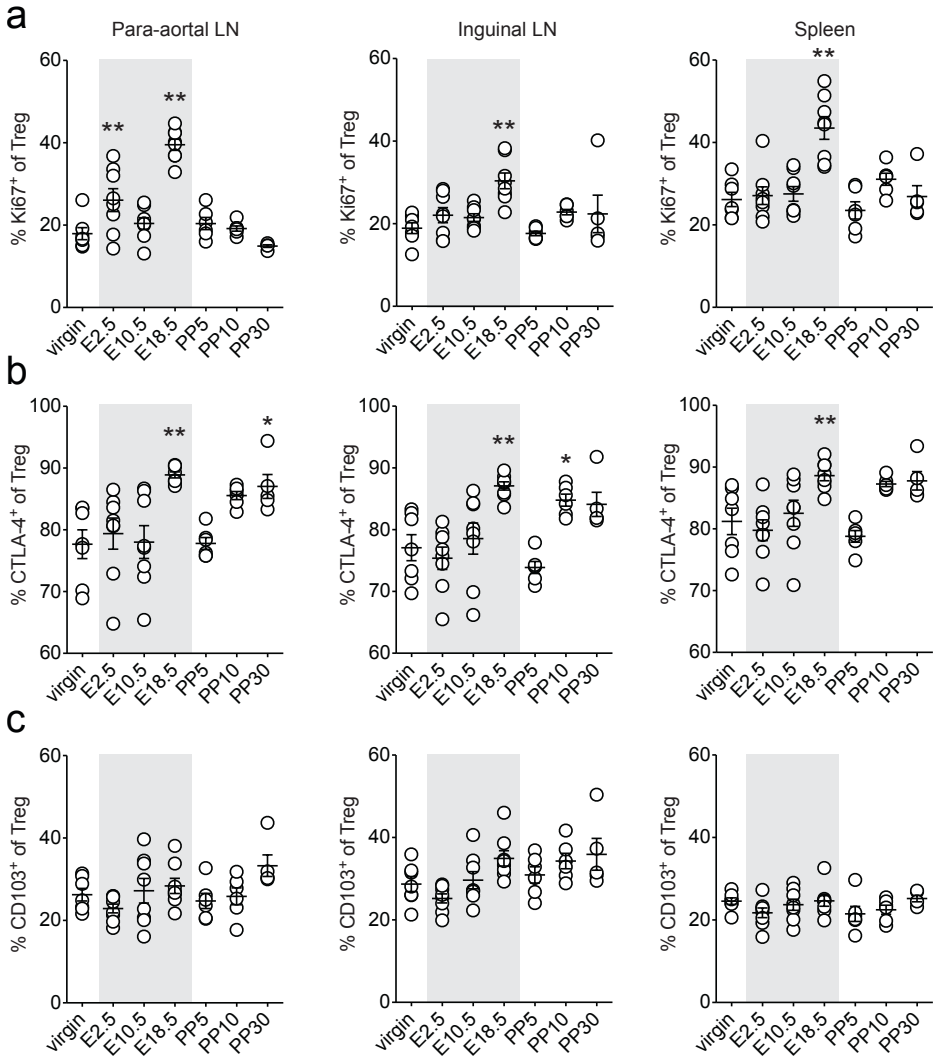

Figure 3.4 Treg phenotype during pregnancy

Female mice were sacrificed on indicated pregnancy (E2.5–E18.5) and post-partum (PP5–PP30) time points. Immune cells were prepared from para-aortal lymph nodes (LN), inguinal LN and spleen and $CD4^+Foxp3^+$ Treg were analysed by flow cytometry. Grey shaded areas represent pregnancy. Data are representative of one experiment with four to eight animals per group. Statistical analyses were performed by one-way ANOVA with Bonferroni's *post hoc* test in comparison to virgin control mice. $^*P < 0.05$; $^{**}P < 0.01$

Ctla4 is an immunosuppressive molecule present on Treg that interacts with CD80/86 on antigen-presenting cells and can thereby induce indoleamine 2,3-dioxygenase (IDO), an

enzyme that degrades the essential amino acid L-tryptophan, thus depleting a substrate essential for T cell proliferation[44,175]. Notably, Ctla4 expression on Treg peaked in late gestation (E18.5) followed by a sharp decline after delivery (**Fig. 3.4b**). The integrin αE (CD103) has been shown to be essential for Treg homing into inflamed tissue – especially skin – and CD103$^+$ Treg resemble a population with increased suppressive capacity in antigen-induced arthritis[176,177]. However, the frequency of CD103$^+$ Treg did not significantly differ in the assessed lymphoid organs throughout pregnancy (**Fig. 3.4c**).

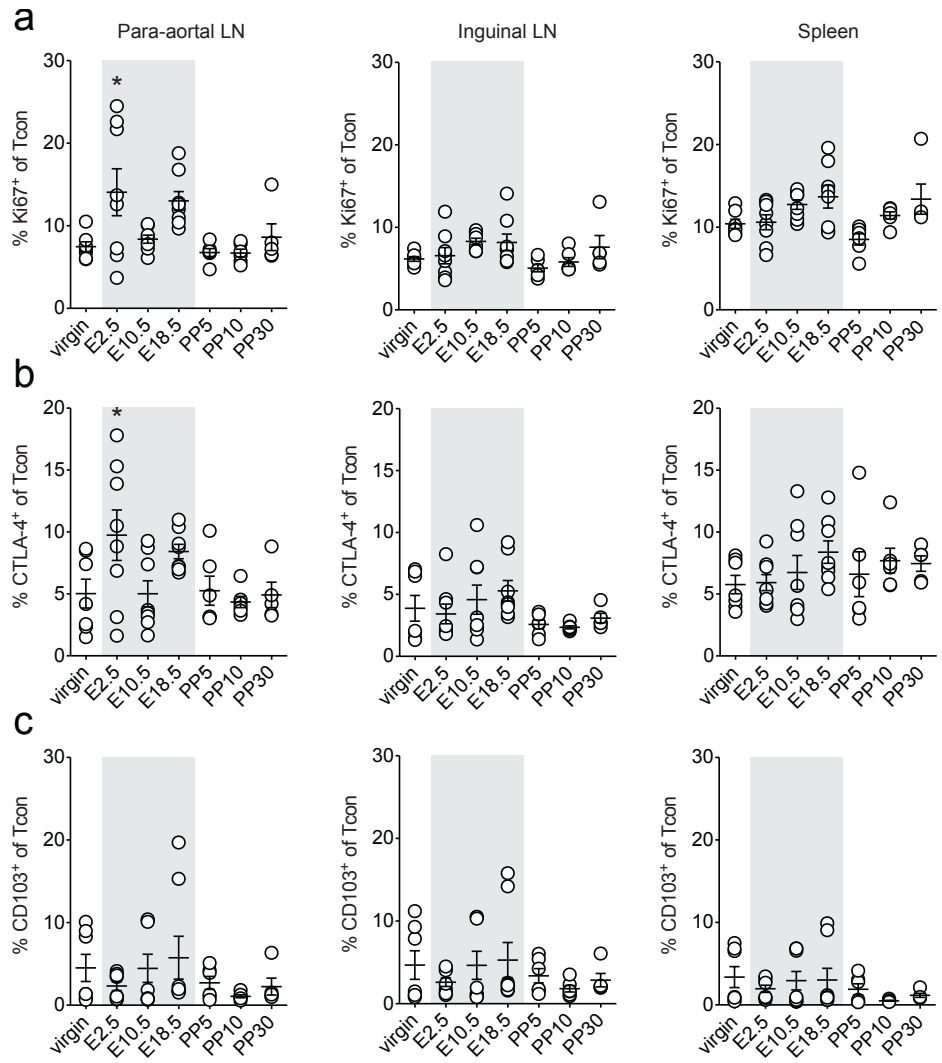

Figure 3.5 Tcon phenotype during pregnancy

Female mice were sacrificed on indicated pregnancy (E2.5–E18.5) and post-partum (PP5–PP30) time points. Immune cells were prepared from para-aortal lymph nodes (LN), inguinal LN and spleen and CD4$^+$Foxp3$^-$ Tcon were analysed by flow cytometry. Grey shaded areas represent pregnancy. Data are representative of one experiment with four to eight animals per group. Statistical analyses were performed by one-way ANOVA with Bonferroni's *post hoc* test in comparison to virgin control mice. *P < 0.05; **P < 0.01

Since CD4$^+$Foxp3$^-$ Tcon resemble the effector cells responsible for mounting anti-fetal responses, next, proliferation and phenotype of these cells was assessed throughout allogeneic pregnancy. The expression of Ki67, Ctla4 and CD103 were generally lower on

Tcon as compared to Treg (compare *y*-axes of **Fig. 3.4** and **Fig. 3.5**). Only one significant proliferative burst was observed in para-aortal LN directly after sperm contact (E2.5), while proliferation appeared tightly controlled at later time points (**Fig. 3.5a**). Similarly, the frequency of Ctla4$^+$ Tcon peaks in early pregnancy – which indicates initial Tcon activation – but did not reach statistical significance at later time points. The frequency on CD103$^+$ Tcon showed no significant changes throughout pregnancy (**Fig. 3.5b,c**).

3.2.2 Treg function

Since Treg presented with higher proliferative activity and increased Ctl4 expression in late pregnancy, suppressive activity of E18.5 Treg was compared to those of virgin mice. This was achieved by setting up cultures of virgin Tcon responder cells, stimulating these cells for proliferation and adding suppressive Treg in varying ratios.

Indeed, E18.5 Treg showed a subtle but significant increase in suppressive capacity as compared to Treg from virgin mice (two-way ANOVA; $P = 0.0226$; **Fig. 3.6**).

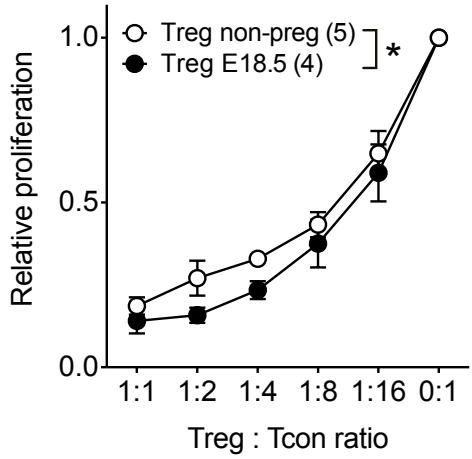

Figure 3.6 Suppressive capacity of Treg from pregnant individuals
Treg isolated from non-pregnant ($n = 5$; white) and pregnant (E18.5; $n = 4$; black) mice were added to stimulated Tcon responder cells at different ratios. Tcon proliferation was assessed by [^{3}H]-Thymidine incorporation and normalized to maximal proliferation in the absence of Treg. Data are representative of one experiment. Statistical analysis was performed by two-way ANOVA with Bonferroni's *post hoc* test. *$P < 0.05$; **$P < 0.01$

Taken together, pregnancy led to a strong increase in Treg frequencies, shifting the Treg-Tcon balance in favour of potentially protective Treg. At the same time, Treg presented with high proliferation and increased expression of suppressive Ctla4 especially in late gestation – a time point when also their suppressive capacity was increased.

3.3 Treg enrichment by steroids

Pregnancy is a state with increased levels of different steroid hormones including progesterone, estradiol, estriol and cortisol, most of which are essential to successful pregnancy outcome and peak in late gestation. Progesterone (P4), for instance, has been shown to have beneficial effects in EAE[164] and to favour Treg expansion *in vivo*[166]. Therefore, P4 effects on the splenocytes were tested *in vitro* as a possible mechanism for Treg expansion during pregnancy.

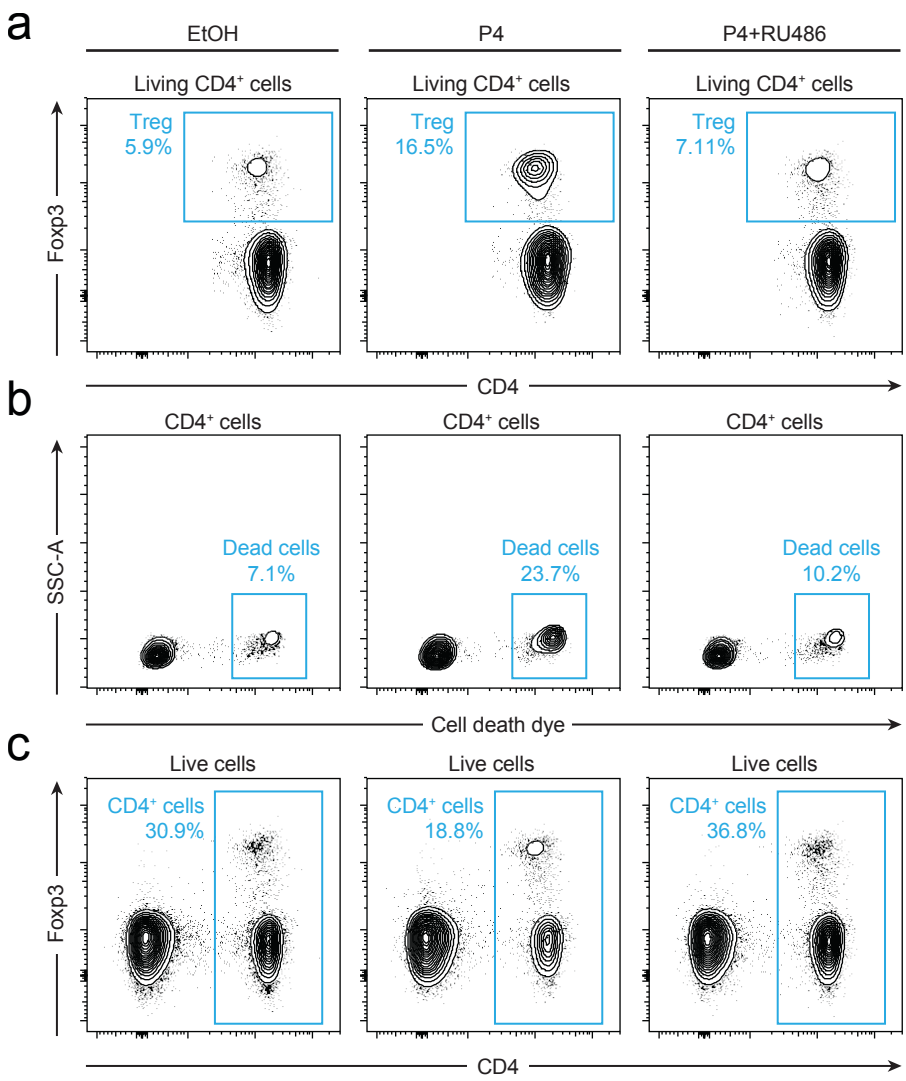

Figure 3.7 Progesterone enriches Treg
Isolated splenocytes were cultured for 48 h in the presence of either the vehicle control ethanol (EtOH), 300 ng/ml progesterone (P4) or progesterone in addition with 1 µg/ml mifepristone (P4+RU486). Cells were analysed by flow cytometry. Dot plots are representative of at least three independently analysed animals.

Indeed, 300 ng P4 – approximately 100 ng are present in sera of pregnant mice – caused increased Treg frequencies after 48 h of incubation. While treatment with the vehicle control ethanol (EtOH) resulted in Treg frequencies around 5% of viable $CD4^+$ cells, P4 increased this frequency about 3-fold to around 15%. To ensure a receptor-mediated

rather than an unspecific effect, the steroid receptor antagonist mifepristone (RU486) was administered in addition with P4. Notably, RU486 was able to abrogate the P4 effect, resulting in Treg frequencies near EtOH baseline (**Fig. 3.7a**).

However, the relative increase of Treg could be caused by active expansion or a passive enrichment. To address this question, proliferation of Treg was assessed by Ki67 and cell death was measured. Importantly, P4 treatment resulted in increased cell death and decreased $CD4^+$ cell frequencies (**Fig. 3.7b,c**), while Ki67 expression on Treg was not altered (data not shown). Also these effects could be fully antagonized by RU486. Hence, P4 seems to induce cell death of the CD4 compartment preferentially in Tcon and thereby passively enriches Treg. This hypothesis, claiming a differential steroid sensitivity of Treg and Tcon, will be further evaluated in **Section 3.5**.

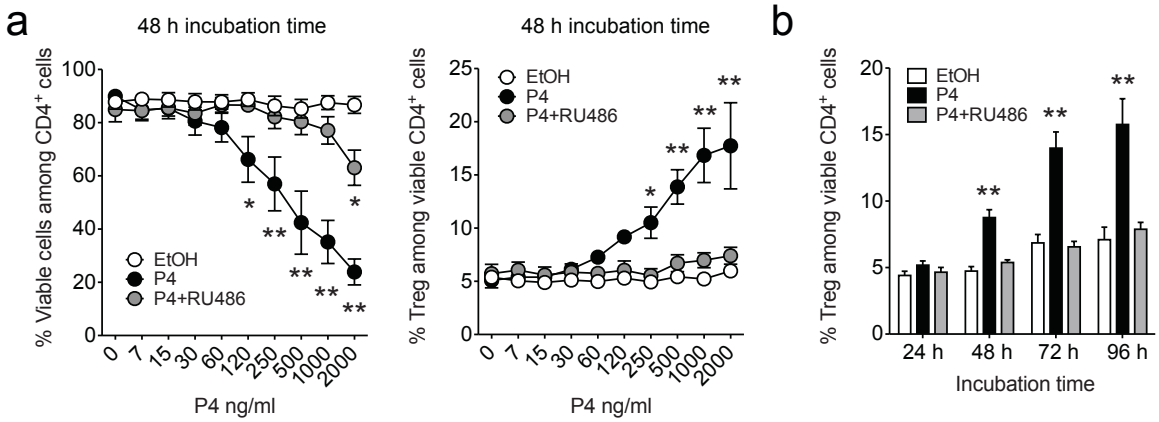

Figure 3.8 Treg enrichment is dose and time dependent

Isolated splenocytes were cultured in the presence of either the vehicle control ethanol (EtOH), progesterone (P4) or progesterone in addition with 1 µg/ml mifepristone (P4+RU486). Dose (**a**) and time (**b**) dependency of cell death and Treg enrichment was measured. Data are representative of five pooled experiments with one mouse per experiment in **a** and one experiment with five animals in **b**. Statistical analysis was performed by two-way ANOVA with Bonferroni's *post hoc* test in comparison to vehicle control (EtOH). **P* < 0.05; ***P* < 0.01

To get an impression of the kinetics of Treg enrichment, different doses and incubation times were tested. A significant reduction of viable $CD4^+$ cells was already observable with 120 ng/ml P4. However, Treg enrichment was significant beginning from 250 ng/ml. RU486 (1 µg/ml) was, at most P4 doses, sufficient to abolish the effect, only 2,000 ng/ml were not fully antagonized, as the frequency of viable $CD4^+$ cells could not be completely restored (**Fig. 3.8a**). Furthermore, the Treg enrichment showed a clear time dependency (**Fig. 3.8b**). These observations are compatible with a receptor-mediated dose- and time-dependent Treg enrichment effect of P4.

3.3.1 Steroid target cells and receptors

In a splenocyte culture many different immune cell types are present including but not restricted to B cells, T cells, DCs, macrophages and NK cells. In principal, all of these cell types are potentially involved in sensing P4 and mediating the observed *in vitro* effect. Hence, the question whether P4 directly acts on $CD4^+$ T cells or indirectly via another accessory cell type was addressed. In order to do so, $CD4^+$ cells were enriched by MACS (**Fig. 3.9a**) and cultured in the presence of P4. Importantly, a significant Treg enrichment could also be observed in these $CD4^+$ cultures (**Fig. 3.9b**). Although the purity of $CD4^+$ cells were around 80–90% and still allowed some influence of accessory cells, these results were indicative for a direct action of P4 on $CD4^+$ T cells.

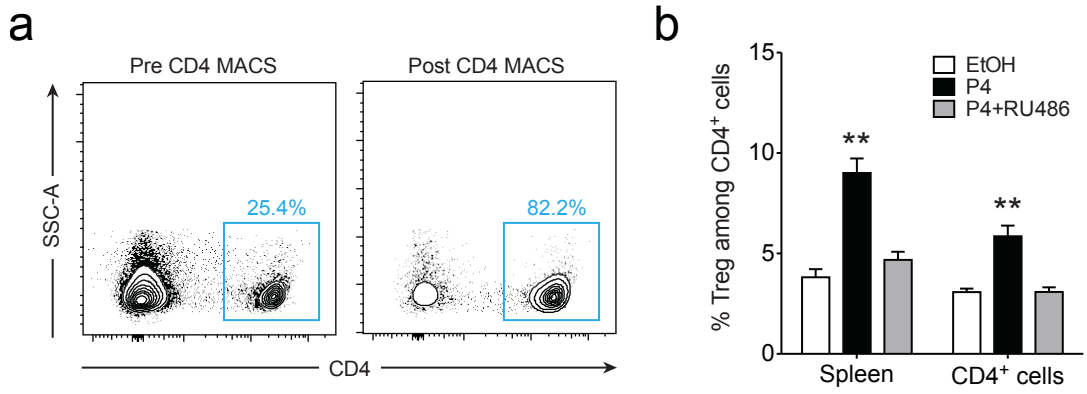

Figure 3.9 Progesterone effect is T cell intrinsic

$CD4^+$ cells were isolated by MACS (a) and cultured in the presence of either the vehicle control ethanol (EtOH), 300 ng/ml progesterone (P4) or progesterone in addition with 1 µg/ml mifepristone (P4+RU486). Dot plots in **a** is representative of four MACS enrichments. Data are representative of one experiment with four mice. Statistical analysis was performed by two-way ANOVA with Bonferroni's *post hoc* test in comparison to vehicle control (EtOH). $*P < 0.05$; $**P < 0.01$

Since P4 seemed to be directly sensed by $CD4^+$ T cells, their expression of potentially P4-binding steroid receptors was analysed. Additionally, the questions whether expression of steroid receptors might (i) be different in Tcon versus Treg or (ii) show a dynamic change throughout pregnancy was addressed. After establishing allogeneic pregnancy, female C57BL/6 mice were sacrificed in late gestation (E18.5) and 5 days post-partum (PP5) and were compared to age-matched virgin female mice (non-preg). Tcon and Treg were isolated by MACS and gene expression was analysed by real-time PCR.

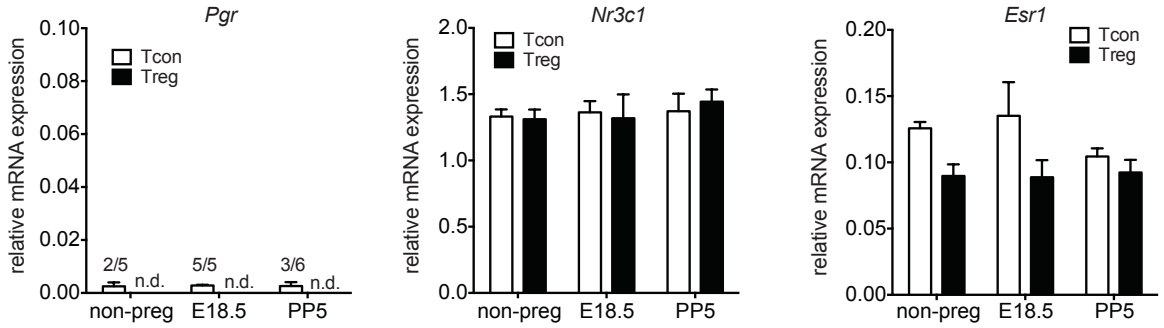

Figure 3.10 Steroid receptor expression of T cells

Tcon (white) and Treg (black) were isolated by MACS from non-pregnant (non-preg; *n* = 5), pregnant (E18.5; *n* = 5) and post-partum (PP5; n = 6) mice and analysed for mRNA expression of progesterone receptor (*Pgr*), glucocorticoid receptor (*Nr3c1*) and estrogen receptor α (*Esr1*). Expression was normalized to the housekeeping gene *Tbp*. Data are representative of one experiment. Statistical analysis was performed by two-way ANOVA with Bonferroni's *post hoc* test. **P* < 0.05; ***P* < 0.01; n.d. = Not detected; x/y = Number of samples with signal.

Strikingly, expression of the progesterone receptor (PR) gene *Pgr* was hardly detectable (**Fig. 3.10**). These results are in line with data from the Immunological Genome Project (Immgen) that collects whole genome expression profiles from a wide spectrum of immune cell subsets[178]. In this data – accessible at www.immgen.org – *Pgr* expression is below the baseline threshold in all of the analysed key populations including T cells. Notably, in the present data, *Pgr* expression was also not up-regulated during pregnancy, as observed in other tissues. At the same time, expression of the glucocorticoid receptor (GR) gene *Nr3c1* and the estrogen receptor α gene *Esr1* was readily detectable but showed no significant differences between Tcon and Treg or throughout pregnancy (**Fig. 3.10**).

Taken together, evidence suggested that P4 is directly sensed by $CD4^+$ T cells thereby mediating Treg enrichment. However, progesterone receptor (PR) was not found to be expressed on $CD4^+$ T cells. Remarkably, glucocorticoid receptor (GR) was present at high levels in both Treg and Tcon but likewise lacked a pregnancy-related dynamic. Nevertheless, GR appeared to be a potential target for P4, especially since steroid receptors are known to be promiscuous and bind to several steroid derivatives with different affinity[179].

Taking into account a possible cross talk of P4 to other steroid receptors, different steroid receptor agonists were tested in parallel. Notably, the compound with the highest affinity to the GR, namely dexamethasone (DEX), showed the strongest Treg enrichment, while the PR-specific norgestrel (NOR) failed to enrich Treg and P4 exhibited an intermediate effect (**Fig. 3.11**). Thus, both P4 and DEX might act via the GR to mediate Treg enrichment.

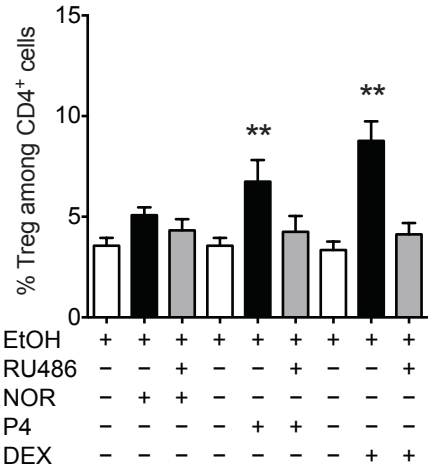

Figure 3.11 Treg enrichment by GR agonists
Isolated splenocytes were cultured for 48 h in the presence of either vehicle control (EtOH), 300 ng/ml norgestrel (NOR), 300 ng/ml progesterone (P4), 500 pg/ml dexamethasone (DEX) or steroid in addition with 1 µg/ml mifepristone (RU486). Living cells were analysed by flow cytometry. Data are representative of one experiment with four mice. Statistical analysis was performed by one-way ANOVA with Bonferroni's *post hoc* test in comparison to vehicle control (EtOH). **P* < 0.05; ***P* < 0.01

3.4 Glucocorticoid receptor in T cells

3.4.1 T cell specific GR knockout

To definitely pinpoint a possible contribution of the GR in the observed Treg enrichment, a T cell-specific GR knockout mouse was used. In $GR^{fl/fl}$ mice, exon 3 of the GR locus *Nr3c1* is flanked by *LoxP* sites and thereby 'floxed'. *LoxP* sites are 34 bp recognition sites, which can be targeted by the enzyme Cre recombinase. In the presence of Cre, exon 3 gets excised from the floxed GR^{fl} locus resulting in a non-functional GR^{Δ} locus (**Fig. 3.12a**). Accordingly, by crossing $GR^{fl/fl}$ mice to *Lck*-Cre mice, which transgenically express Cre recombinase under the T cell-specific *Lck* promoter, a T cell-specific GR knockout mouse ($GR^{fl/fl}$*Lck*-Cre) can be generated. To prove the functionality of this previously described knockout[180,181] (generous gift of Prof. Reichardt), the wildtype, floxed and deleted *GR* alleles were detected by PCR in different cell preparations from $GR^{fl/fl}$*Lck*-Cre mice and $GR^{fl/fl}$ controls (**Fig. 3.12b**). Deleted *GR* was detected in the majority of thymocytes and $CD4^+$ splenocytes from $GR^{fl/fl}$*Lck*-Cre mice, while whole splenocytes containing T cells but also other immune cells showed an incomplete deletion. No deletion was observed in tail biopsies of $GR^{fl/fl}$*Lck*-Cre mice, which do not contain relevant T cell numbers. $GR^{fl/fl}$ control mice and wildtype animals exclusively presented with the floxed and wildtype locus, respectively.

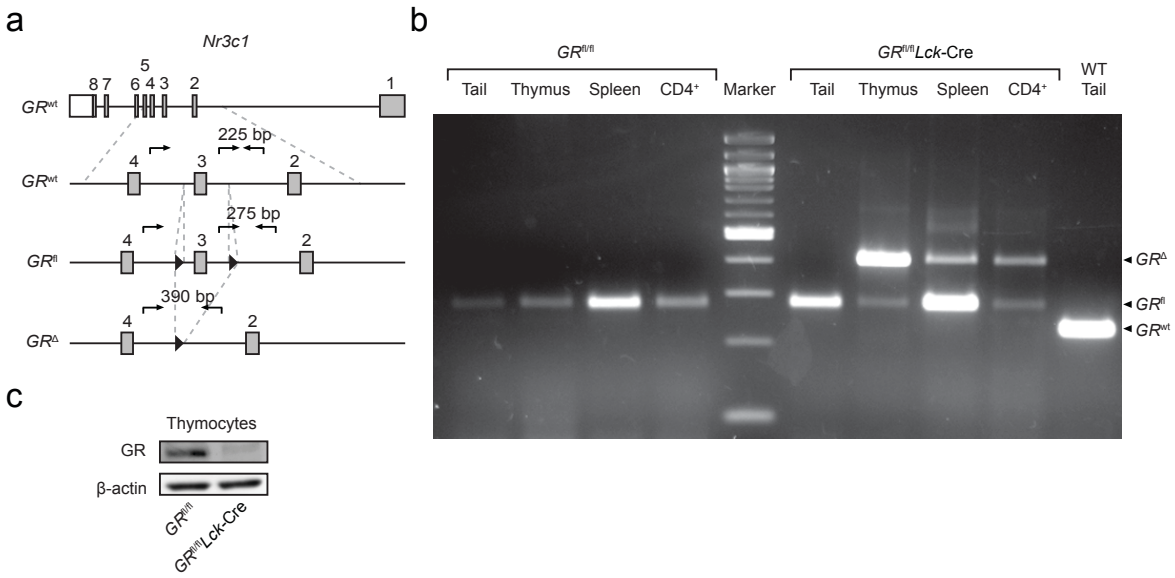

Figure 3.12 Validation of T cell-specific GR knockout mice
(**a**) Gene locus of the glucocorticoid receptor (GR; locus: *Nr3c1*). Wildtype (GR^{wt}), floxed (GR^{fl}) and deleted (GR^{Δ}) alleles are shown. Arrows indicate binding sites of genotyping primers. PCR product length is indicated. (**b**) PCR analysis of different cell types from indicated genotypes. Primers and products as indicated in **a**. (**c**) Immunoblot analysis of whole cell lysates from isolated thymocytes. β-actin is shown as loading control.

To additionally prove that deletion of exon 3 results in the absence of GR protein, immunoblot analysis of isolated thymocytes were performed. Expectedly, the GR protein band was readily detected in $GR^{fl/fl}$ control mice but was absent in $GR^{fl/fl}$*Lck*-Cre mice (**Fig. 3.12c**). In summary, the T cell-specific deletion of the GR could be successfully validated.

3.4.2 Immune cell composition in $GR^{fl/fl}$*Lck*-Cre mice

As GR is also known to play a role in thymic T cell development[182], harvested splenocytes from both, $GR^{fl/fl}$*Lck*-Cre mice and $GR^{fl/fl}$ controls, were analysed to rule out *a priori* differences in their immune cell composition. However, neither the frequencies of B cells, NK cells, neutrophils, macrophages and dendritic cells, nor the frequencies of T cells and T cell subsets including Treg showed a significant difference between groups (**Fig. 3.13**).

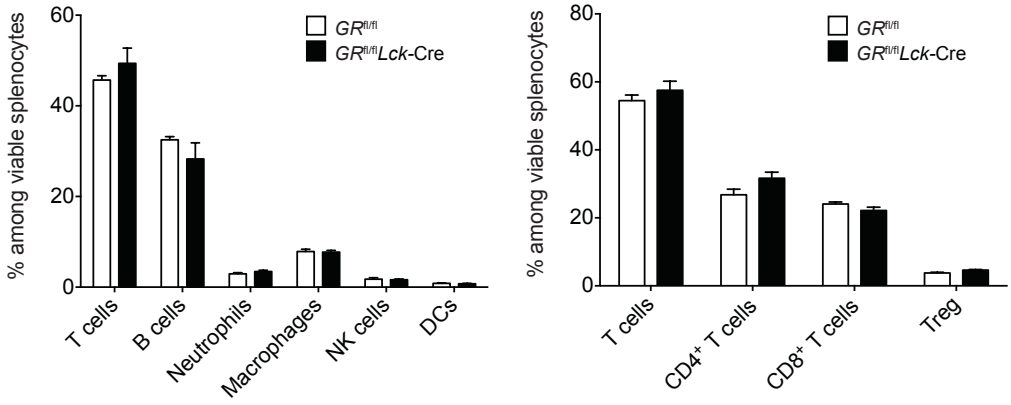

Figure 3.13 Immune cell composition in T cell-specific GR knockout mice
Splenocytes were isolated from *GR*$^{fl/fl}$*Lck*-Cre mice (n = 4; black) and *GR*$^{fl/fl}$ controls (n = 4; white) and immune cell composition was analysed by flow cytometry. Data are shown for one representative experiment out of two. Statistical analyses were performed by two-way ANOVA with Bonferroni's *post hoc* test. *P < 0.05; **P < 0.01

3.4.3 Treg enrichment in in *GR*$^{fl/fl}$*Lck*-Cre mice

Coming back to the hypothesis that both P4 and DEX might act via the GR on T cells to mediate Treg enrichment, the T cell-specific GR knockout mouse appeared to be a suitable tool to address this question.

Splenocytes were isolated from both *GR*$^{fl/fl}$*Lck*-Cre mice and *GR*$^{fl/fl}$ controls and cultured for 48 h in the presence of P4 or DEX. As expected, Treg enrichment was readily detected in the *GR*$^{fl/fl}$ control mice, however, in *GR*$^{fl/fl}$*Lck*-Cre mice this effect was completely abolished (**Fig. 3.14**). This experiment provided proof that both P4 and DEX are sensed by T cells via the GR. A prominent role for the PR in this system could be thereby excluded, since PR is present in *GR*$^{fl/fl}$*Lck*-Cre but fails to mediate Treg enrichment.

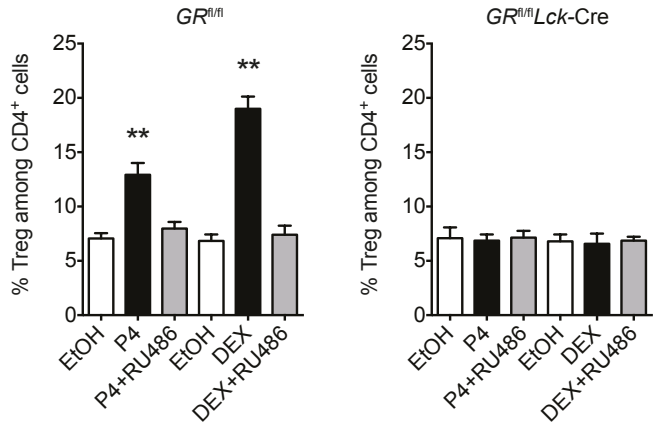

Figure 3.14 Treg enrichment in T cell-specific GR knockout mice
Splenocytes were isolated from *GR*$^{fl/fl}$ controls (n = 4) and *GR*$^{fl/fl}$*Lck*-Cre mice (n = 4) and cultured for 48 h in the presence of either vehicle control (EtOH), 300 ng/ml progesterone (P4), 500 pg/ml dexamethasone (DEX) or steroid in addition with 1 µg/ml mifepristone (RU486). Living cells were analysed by flow cytometry. Data are shown for one representative experiment out of two. Statistical analyses were performed by two-way ANOVA with Bonferroni's *post hoc* test in comparison to vehicle control (EtOH). *P < 0.05; **P < 0.01

3.5 Glucocorticoid receptor and tolerance induction during pregnancy

Taken together, present data indicate a potential role of GR in T cells for shifting the balance between regulatory and conventional T cells after being engaged by pregnancy-related steroid hormones. As this mechanism might be contributing to the establishment of tolerance to both fetal antigens and CNS autoantigens during pregnancy, its biological relevance was further investigated *in vivo*.

3.5.1 Reproductive phenotype of *GR*$^{fl/fl}$*Lck*-Cre mice

To address the question whether GR on T cells is involved in fetomaternal tolerance in allogeneic pregnancy, the reproductive phenotype of *GR*$^{fl/fl}$*Lck*-Cre and *GR*$^{fl/fl}$ females was analysed.

Females from both experimental groups were mated to BALB/c males and pregnant animals were sacrificed at gestational day E13.5, as this is the optimal time point to macroscopically assess the fetal loss rate[134]. However, regarding number of implantations, number of viable fetuses, number of abortions and fetal loss rate, no significant differences were observed (**Fig. 3.15**)

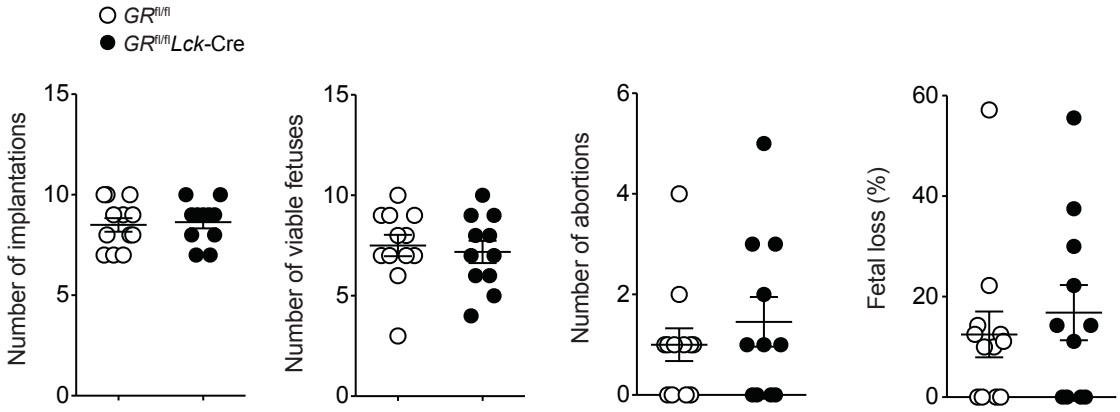

Figure 3.15 Reproductive phenotype of T cell-specific GR knockout mice
Allogeneic pregnancy was established in female *GR*$^{fl/fl}$ controls (n = 12) and *GR*$^{fl/fl}$*Lck*-Cre mice (n = 11) and fetal loss was assessed at gestational day E13.5. Data are pooled from two independent experiments. Statistical analyses were performed by Student's t-test. *P < 0.05; **P < 0.01

3.5.2 Pregnancy EAE in *GR*$^{fl/fl}$*Lck*-Cre mice

Next, the question whether GR on T cells is involved in mediating the tolerance induction towards CNS autoantigens during pregnancy was assessed.

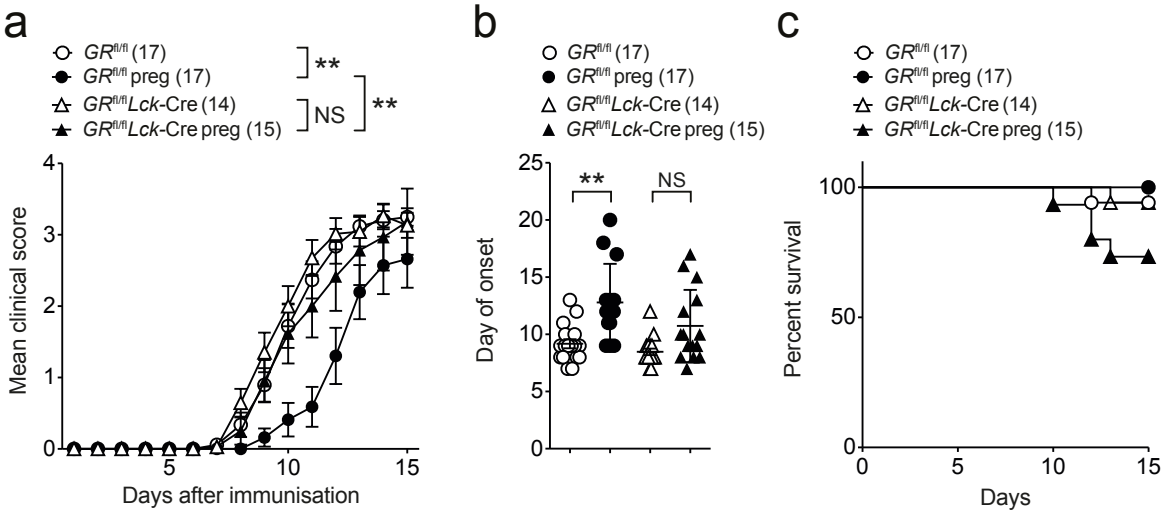

Figure 3.16 Loss of EAE protection in pregnant T cell-specific GR knockout mice
EAE was induced in non-pregnant and pregnant *GR*$^{fl/fl}$*Lck*-Cre (*n* = 14 and *n* = 15, respectively) and non-pregnant and pregnant *GR*$^{fl/fl}$ females (*n* = 17 per group). Clinical course (**a**), day of onset (**b**) and survival (**c**) is shown. Data are pooled from two independent experiments. Statistical analyses were performed by two-way ANOVA with Bonferroni's *post hoc* test in **a**, one-way ANOVA with Bonferroni's *post hoc* in **b** and Chi-square test in **c**. **P* < 0.05; ***P* < 0.01

To this end, EAE was induced in non-pregnant and pregnant *GR*$^{fl/fl}$*Lck*-Cre (*n* = 14 and *n* = 15, respectively) and non-pregnant and pregnant *GR*$^{fl/fl}$ females (*n* = 17 per group). As expected from the initial EAE experiments, pregnancy resulted in a protection from EAE in *GR*$^{fl/fl}$ control mice. This protection was reflected in the clinical disease course (Two-way ANOVA, group × time interaction; *GR*$^{fl/fl}$ vs. *GR*$^{fl/fl}$ preg; *P* < 0.0001) as well as in the day of onset (One-way ANOVA with Bonferroni's *post hoc* test; *P* = 0.0008). However, pregnant *GR*$^{fl/fl}$*Lck*-Cre mice were not protected during pregnancy. Neither the disease course (*P* = 0.6651), nor the day of onset (*P* = 0.0678) was significantly different in comparison to non-pregnant *GR*$^{fl/fl}$*Lck*-Cre mice (**Fig. 3.16a,b**). Importantly, also the direct comparison of the disease course of pregnant *GR*$^{fl/fl}$*Lck*-Cre and pregnant *GR*$^{fl/fl}$ mice showed a significant difference (*P* = 0.0026). At the same time, differences in survival were not observed, although the *P* value was very close to statistical significance (Chi-square test; *P* = 0.0580; **Fig. 3.16c**).

Taken together, although GR on T cells appears to be dispensable for fetal protection, it is indispensable for controlling CNS autoimmunity during pregnancy.

3.6 Differential steroid sensitivity in T cells

Since Treg enrichment by steroid treatment *in vitro* was not due to Treg proliferation but closely linked to increased cell death in $CD4^+$ cells, this effect could be explained by an increased steroid sensitivity of Tcon in comparison to Treg. Consequently, Tcon would be more effectively depleted by steroid challenge, while steroid resistant Treg are positively selected and hence accumulate.

To address this hypothesis, MACS-isolated Treg and Tcon were cultured separately and challenged with increasing doses of DEX. In a first experiment, cell cultures were stimulated for proliferation with anti-CD3 antibody in the presence of feeder cells and recombinant murine IL-2 and proliferative response was measured by [^{3}H]-Thymidine incorporation. After normalizing proliferation to untreated controls, a dose response curve was computed using Prism6 software. Notably, especially at higher DEX concentrations (10^{-8} M and more) better proliferative responses were observed in Treg as compared to Tcon. This was also reflected in a significantly higher curve bottom value, as inferred from the dose-response curves. (Student's *t*-test; P = 0.0069; **Fig. 3.17a**).

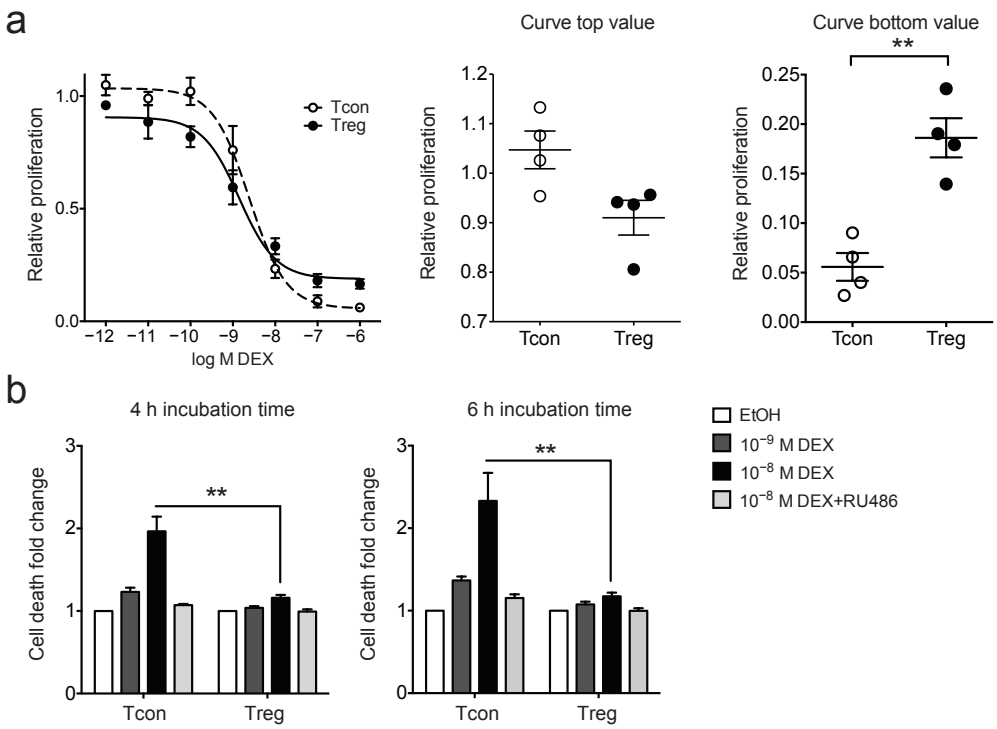

Figure 3.17 Treg are more resistant to steroids

(**a**) MACS-isolated Treg and Tcon were cultured separately for 48 h in the presence of irradiated feeder cells, 1 µg/ml anti-CD3 antibody, 50 U/ml recombinant murine IL-2 and the indicated DEX concentrations. Proliferation was assessed by [^{3}H]-Thymidine incorporation. Curve fit and curve characteristics were computed. (**b**) MACS-isolated Treg and Tcon were cultured separately for 4 h and 6 h in the presence of indicated DEX concentrations. Dead cells were identified by propidium iodide positivity and cell death was calculated as fold change relative to vehicle control (EtOH). Data are representative of four and three samples in **a** and **b**, respectively, each pooled from two to three animals. Statistical analyses were performed by Student's *t*-test in **a** and two-way ANOVA with Bonferroni's *post hoc* test in **b**. **P* < 0.05; ***P* < 0.01

In a second experiment, Treg and Tcon were challenged with DEX under non-stimulatory conditions and induced cell death was measured by propidium iodide staining. Markedly, DEX-induced cell death was significantly more pronounced in Tcon than in Treg. At a concentration of 10^{-8} M DEX cell death fold change was nearly twice as high in Treg as it was in Treg (Two-way ANOVA with Bonferroni's *post hoc* test; $P < 0.0001$; **Fig. 3.17b**).

To summarize, Treg appeared to be more resistant to steroid challenges than Tcon under both proliferative and non-proliferative conditions. Differential sensitivity of Treg and Tcon might therefore be the mechanism underlying the enrichment of Treg *in vitro* but also the need for GR expression in T cells to establish protection from CNS autoimmunity during pregnancy *in vivo*.

3.7 Mechanisms of Treg resistance

To further investigate the molecular mechanism underlying steroid sensitivity of Treg and Tcon during pregnancy, the expression of different key molecules of glucocorticoid action was studied by real-time PCR.

The enzyme 11-beta hydroxysteroid dehydrogenase (11β-HSD) regulates the intracellular availability of glucocorticoids to activate their receptors and thereby modulates target gene transcription[183]. Two isozyms of 11β-HSD with antagonistic functions have been identified. While type 1 (11β-HSD-1) converts inactive 11-ketosteroids (11-dehydrocorticosterone in rodents and cortisone in humans) into active glucocorticoids (corticosterone in rodents and cortisol in humans), type 2 (11β-HSD-2) does the opposite – namely inactivating glucocorticoids to their respective 11-ketosteroids[183,184]. Hence, low expression of the activating 11β-HSD-1 and high expression of inactivating 11β-HSD-2 can protect cells from glucocorticoid-mediated apoptosis. Additionally, glucocorticoid-induced leucine zipper (Gilz), a glucocorticoid-induced inhibitor of proliferation that also plays a role in apoptotic pathways[185], was studied as a readout for GR target gene induction.

In non-pregnant and post-partum animals, Tcon presented with higher expression of the 11β-HSD-1 gene *Hsd11b1* in comparison to Treg, rendering them potentially more sensitive to glucocorticoid-induced apoptosis. However, during pregnancy Tcon showed adaptive down-regulation of *Hsd11b1* and up-regulation of the 11β-HSD-2 gene *Hsd11b2*, both rendering them more steroid resistant at this late gestational time point. Yet, despite these adaptive mechanisms, Tcon still showed constantly higher GR signalling activity in comparison to Treg as assessed by expression of the Gilz gene *Tsc22d3* (**Fig. 3.18a**).

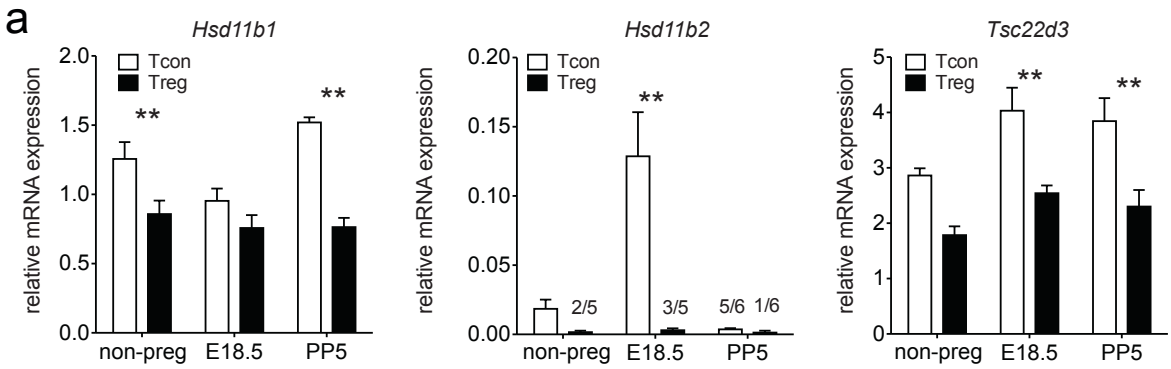

Figure 3.18 GR pathway components

(**a,b**) Tcon (white) and Treg (black) were isolated by MACS from non-pregnant (non-preg; *n* = 5), pregnant (E18.5; *n* = 5) and post-partum (PP5; *n* = 6) mice and analysed for mRNA expression of 11-beta hydroxysteroid dehydrogenase type 1 and 2 (*Hsd11b1* and *Hsd11b1*) and glucocorticoid-induced leucine zipper (Gilz, locus: *Tsc22d3*). Expression was normalized to the housekeeping gene *Tbp*. Data are representative of one experiment. Statistical analysis was performed by two-way ANOVA with Bonferroni's *post hoc* test. **P* < 0.05; ***P* < 0.01; x/y = Number of samples with signal.

In summary, E18.5 Tcon showed some changes that are indicating an increased steroid resistance at late gestation. However, *Tsc22d3* expression – as a net effect of GR signalling activity – and expression of glucocorticoid-activating 11β-HSD-1 was constantly lower in Treg giving a possible mechanistic explanation of Treg steroid resistance.

3.7.1 Pregnancy-regulated genes in Treg

Surprisingly, gene expression of all so far studied genes showed some dynamics throughout pregnancy in the Tcon but not in the Treg compartment (**Fig. 3.10, Fig. 3.18**). Hence, to identify genes that might render Treg more potent to compete with Tcon-driven feto- and autoreactive responses during pregnancy, a non-biased whole genome expression analysis was performed. To this end, Treg from pregnant and non-pregnant female mice were sorted to high purity (> 98%) by fluorescence-activated cell sorting. Since staining of intranuclear Foxp3 requires fixation and permeabilisation, living Foxp3$^+$ Treg are usually not accessible by sorting. To overcome this obstacle, DEREG mice[170], expressing a green fluorescent protein (GFP) under the Foxp3 promoter were used. In these mice, living Treg can be identified as CD4$^+$Foxp3-GFP$^+$ cells (compare **Fig. 2.3**). After isolation, gene expression of Treg from pregnant and non-pregnant mice was assessed in quadruplicate by microarray analysis.

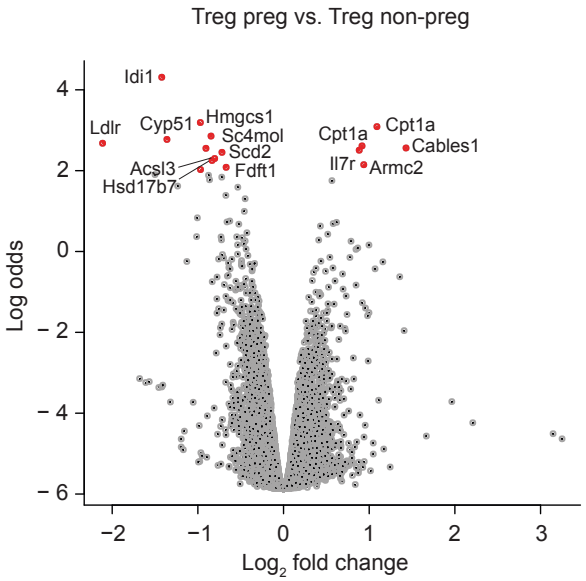

Figure 3.19 Pregnancy-regulated genes in Treg

Treg from pregnant (n = 4) and non-pregnant (n = 4) female DEREG mice were sorted to high purity (> 98%) by fluorescence-activated cell sorting and gene expression was assessed by microarray analysis. Volcano plot of microarray data shows gene expression $\log_2$ fold change (x-axis) against log odds as measure for statistical significance (y-axis). Differentially expressed candidate genes, identified by a fold change ≥ 1.5 and false discovery rate-corrected P-value < 0.05 are marked in red.

By plotting microarray data as so-called 'volcano plot', gene fold change between groups (x-axis) and gene significance (y-axis) can be assessed in parallel. Thus, significantly up- and down-regulated genes can be identified by their localisation in the upper right and upper left quadrant, respectively (**Fig. 3.19**).

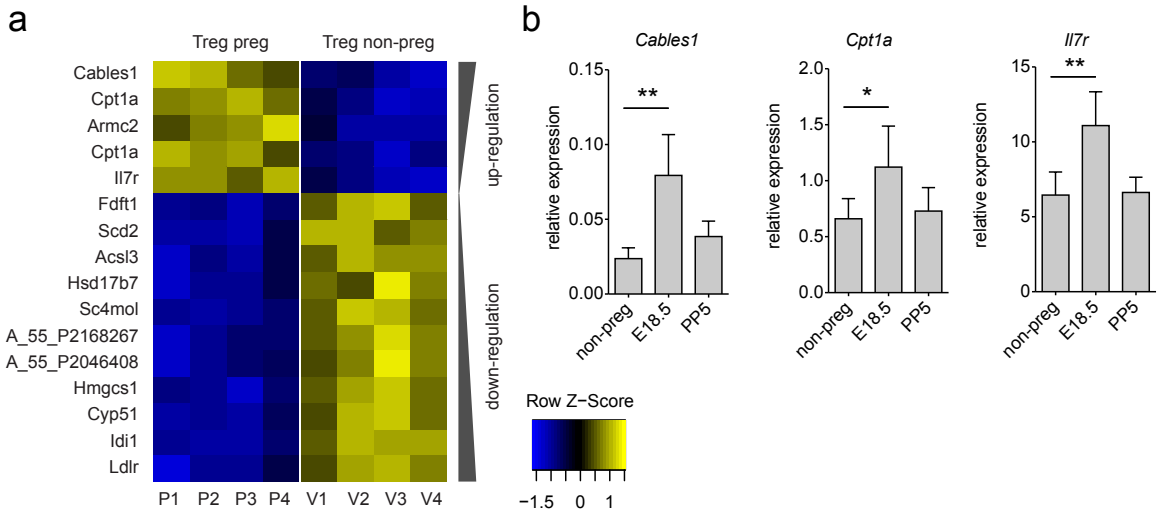

Figure 3.20 Validation of candidate genes

(**a**) Identified candidate genes are shown as heat map. Treg samples from pregnant (*n* = 4; P1–P4) and non-pregnant (*n* = 4; V1–V4) female DEREG mice are shown. (**b**) Validation of selected candidate genes in independent MACS-isolated Treg samples from non-pregnant (non-preg; *n* = 5), pregnant (E18.5; *n* = 5) and post-partum (PP5; *n* = 6) mice by real-time PCR. Expression was normalized to the housekeeping gene *Tbp*. Data are representative of one experiment. Statistical analysis in **b** was performed by one-way ANOVA with Bonferroni's *post hoc* test. **P* < 0.05; ***P* < 0.01.

Using a fold change ≥ 1.5 and a false discovery rate-corrected *P*-value < 0.05 as criteria for differentially expressed genes, four up- and eleven down-regulated candidates were identified (**Fig. 3.20a**). To assess the accuracy of the microarray analysis, three of the up-regulated candidate genes were additionally validated by real-time PCR from independent Treg samples (**Fig. 3.20b**).

To summarize, non-biased whole genome expression analysis revealed a limited number of differentially regulated candidate genes, whose explicit functions will be investigated in future research projects.

4 Discussion

Although attending neurologists and gynaecologists have been suspecting for decades that pregnancy has a protective effect on MS[186-188], Confavreux and colleagues were the first to systematically address this clinical observation in a large seminal cohort study in the late 1990s following 254 MS patients from one year before pregnancy to one year post-partum[4]. Markedly, the mean annual relapse rate of 0.7 before pregnancy gradually declined throughout gestation, reaching 0.2 in the third trimester. However, in the first three months post-partum the relapse rate rebounded to 1.2 before returning to the pre-pregnancy rate[4]. Meanwhile, these results have been confirmed in many prospective clinical studies[5,6] indicating a substantial benefit especially of third trimester pregnancy for MS disease activity.

The goal of this thesis was to translate the pregnancy-associated protection from CNS autoimmunity into an animal model of MS and to investigate the cellular and molecular underpinnings with a special focus on regulatory T cells.

4.1 Protective effect of pregnancy

To investigate the impact of pregnancy on CNS autoimmunity, C57BL/6 females were mated to BALB/c males in order to establish allogeneic pregnancy. This setting was chosen since in syngeneic matings of inbred mice, the mother and fetuses are genetically identical – except for the Y chromosome in approximately 50% of the fetuses. In this artificial situation, the fetuses do not comprise 'foreign antigens' for the mother's immune system, thus annulling the need for effective tolerance induction. In fact, Treg expansion is more pronounced in allogeneic pregnancy[139,189] and depletion of pTreg by CNS1-deficiency results in increased abortion rates in allogeneic but not in syngeneic pregnancy[43]. Likewise, a Treg-mediated impairment of host defence was observed only in allogeneic pregnancy[152]. Thus, allogeneic pregnancy better suits the situation in the 'outbred' human population and ensures a need for the establishment of proper fetomaternal tolerance.

Since the strongest protective effect was observed during third trimester pregnancy in humans[6], pregnant animals were immunised for EAE on gestational day E7.5 ± 1. Thus the onset of disease was expected around E14.5 when the third trimester of mouse pregnancy begins. Indeed, pregnant animals were temporarily protected from developing EAE and showed a significant delay of onset to the post-partum period. However, once

post-partum animals developed EAE the disease activity was overshooting in a rebounding fashion, which was reflected in the clinical course as well as in reduced animal survival. At the same time, the disease incidence was not significantly different between pregnant and non-pregnant animals. These results are in agreement with previous studies reporting reduced EAE activity in both pregnant SJL and C57BL/6 mice[156-158]. However, different experimental setups have been used. While in one study C57BL/6 animals with already established disease were mated at the first signs of remission[157], in another study mice were immunised for EAE in late gestation (E17.5)[158]. In contrast to the results of this work, both groups reported a rather stable diminishment of disease activity in pregnant mice without a prominent rebound of disease activity post-partum.

To further investigate whether the preservation of motor function in pregnant EAE mice is accompanied by reduced infiltration of immune cells into the CNS, a detailed flow cytometry analysis of infiltrating leukocytes was performed. By utilising TruCount technology the relative abundance of invading immune cell subsets could be further assessed in absolute numbers, thus enabling a meaningful representation of the infiltrate. For analysis, a time point in the middle of the protective period (day 10 post immunisation) was chosen, when non-pregnant animals already presented substantial EAE symptoms. Indeed, while non-pregnant control animals presented with around 1.2 million infiltrating leukocytes, this number was halved in pregnant animals. This difference was most prominently driven by a lack of DC and T cells in the infiltrate of pregnant mice. Thus, pregnancy hindered T cells, which are the prominent drivers of autoreactive inflammation in EAE[3], to enter the CNS parenchyma resulting in reduced clinical disease activity. Hence, autoreactive T cell priming, expansion, infiltration or a combination of these processes appears to be more tightly controlled during pregnancy.

The established model of pregnancy-associated CNS tolerance closely mimics the effects of pregnancy in MS patients including a strong post-partum rebound phenomenon that was so far not reported in C57BL/6 mice[157,158]. It appears to be a valuable model to further investigate the influence of pregnancy on CNS autoimmunity.

4.2 Treg dynamics during pregnancy

Since Treg are prominently involved in both preventing autoimmune disorders[29] and conferring fetomaternal tolerance[9], their frequency, phenotype and function was analysed during the course of pregnancy in order to identify changes relevant to CNS tolerance induction. To assess local as well as more systemic Treg changes, para-aortal lymph nodes (LN) were compared to subcutaneous inguinal LN and spleen as an organ that reflects systemic changes in the circulation. As previously described, para-aortal LN

directly drain the uterus and resemble the place were fetal-specific T cell priming primarily takes place[135,190]. Accordingly, most pronounced Treg expansion was observed in para-aortal LN starting from 10% Treg in $CD4^+$ cells in virgin animals and increasing to above 18% in late gestation. Surprisingly however, expansion of Treg was observed relatively late in gestation with the first significant increase in para-aortal LN being detected at E18.5. In contrast, other studies reported Treg expansion already in the first days of gestation[139,190]. However, the authors partly used different mating systems (CBA males) and generally defined $CD4^+CD25^+$ cells as Treg, a population that in principle can be contaminated by activated fetus-reactive T cells that also express CD25. The Treg dynamics observed in this work more closely resemble the results obtained by another study analysing fetal antigen-specific Treg in a mating system with a known paternal-antigen[150]. Here, the authors report a slow increase of fetal antigen-specific Treg reaching a peak in late pregnancy followed by slow decline towards post-partum time points. Interestingly, fetal antigen-specific Treg persisted as long as post-partum day 100 (PP100) resembling a fetal antigen-specific memory Treg population that readily re-assembled upon subsequent pregnancies[150]. Similarly, in this work elevated Treg levels were observed as long as PP30, which was the latest time-point assessed.

Analysing the Treg phenotype, two proliferative bursts were identified by intracellular Ki67 staining[173,174]. The first burst was observed at E2.5, a time point even before the implantation of the blastocyst, which takes place at E4.5[9]. Strikingly, a study focussing on the role of male seminal fluid in tolerance induction also reported a first paternal antigen-specific Treg response as early as E3.5[190]. By making use of a paternal tumour cell engraftment model, the authors showed that exposure to paternal seminal fluid antigens lead to paternal antigen-specific tolerance that impeded tumour rejection. This effect was independent of fertilization and embryo development, as mating of uterine-ligated females, in which implantation is abolished, also failed to reject paternal tumours[190]. Thus, Treg proliferation at E2.5, as observed in this work, is likely to reflect a first paternal antigen-specific priming event caused by contact to BALB/c seminal fluid. This rationale is supported by the observation that also in Tcon a proliferative burst can be detected at E2.5, thus possibly representing the paternal antigen-specific effector response that is consecutively intercepted by expanding Treg. Furthermore, this early proliferative burst was only detected in uterus-draining para-aortal LN but not in inguinal LN or spleen, indicating a locally limited exposure to paternal sperm antigens, probably drained via uterus-derived lymphatic vessels. The second proliferative burst of Treg was observed in late gestation when the fetus is growing at the highest rate resulting in rapid enlargement of the fetomaternal interface and increased antigenic load[9]. This second burst was also detectable in inguinal LN and in the spleen, which argues for a more systemic antigen exposure. In fact, Act-mOVA models suggested a systemic release of fetal antigens into

the maternal circulation, coinciding with the onset of placental perfusion in mid-gestation[191,192].

Since a number of molecules expressed by Treg have been linked to their suppressive potential[34], the phenotypic analysis was further expanded to assess Ctla4 and CD103 on Treg and Tcon during pregnancy. While CD103 expression endows Treg with higher suppressive capacity, it also licenses Tcon to access inflamed tissues[176,177]. However, CD103 expression was not significantly changed on Treg or Tcon. Notably, Ctla4 expression on Treg peaked in late gestation at E18.5 followed by a sharp decline after delivery. As Ctla4 is an immunosuppressive molecule that interacts with CD80/86 on APC and leads to IDO-mediated suppression of Tcon proliferation[44,175], this increase of Ctla4 expression might lead to higher suppressive capacity of late pregnancy Treg. To address this question, Treg were isolated from non-pregnant and E18.5 pregnant C57BL/6 animals and analysed for their capacity to suppress proliferative Tcon responses. Indeed, E18.5 Treg presented a subtle but significant suppressive superiority in comparison to Treg from non-pregnant mice.

Thus, pregnancy does not only lead to a strong increase in Treg frequencies, driven by a first local and later systemic exposure to fetal antigen. This work could also show increased expression of suppressive Ctla4 on Treg in late gestation, an adaptation that might be involved in rendering these cells better suppressors, as observed in *in vitro* suppression assays.

4.3 Effects of pregnancy hormones

To further investigate whether the Treg pool might be supported during pregnancy by increasing levels of pregnancy-associated steroid hormones, the effects of selected hormones were assessed in splenocyte cultures. In doing so, progesterone (P4) appeared to be a promising candidate, as P4 serum levels prominently increase in the second half of gestation[160], a period when also Treg frequency and CNS protection are most pronounced. Indeed, treatment of full splenocytes with 300 ng/ml P4 resulted in a near 3-fold increase in Treg frequency. Importantly, this effect was fully reversible by the steroid receptor antagonist mifepristone (RU486), indicating a receptor-mediated rather than an unspecific P4 effect. Looking more closely into P4-treated cultures, Treg augmentation was accompanied by a decrease in viable $CD4^+$ cells. This observation raised the possibility that increased Treg frequencies were due to passive enrichment rather than active expansion, hypothesising a better survival of $CD4^+$ Treg in comparison to $CD4^+$ Tcon. In fact, dose and time kinetics suggested a positive correlation of $CD4^+$ cell depletion and Treg enrichment.

However, the precise target cells of P4 action still needed to be identified, especially since splenocyte cultures consist a whole repertoire of immune cells including B cells, T cells, DCs, granulocytes, macrophages and NK cells, among others. Thus, P4 could be either directly acting on $CD4^+$ T cells or indirectly via another secondary cell type. To address this question, $CD4^+$ T cells were enriched my magnetic isolation and subjected to P4 treatment, while whole splenocytes served as control condition. Although the limited purity of $CD4^+$ T cell preparations does not completely rule out an involvement of accessory cells, over 80%-pure CD4+ T cells still presented with a robust P4-driven Treg enrichment, thus indicating a direct action of P4 on $CD4^+$ T cells. In order to unveil a possible differential expression of the progesterone receptor (PR) in Treg and Tcon or a modulation throughout pregnancy – both of which would have implications for P4-driven Treg enrichment – expression of the PR gene *Pgr* was analysed by real-time PCR. Surprisingly, *Pgr* expression was hardly observable and showed no induction during pregnancy in Treg or Tcon. Importantly, the *Pgr* real-time PCR gave strong signals in ovary and uterus samples, thus indicating that the assay itself worked properly. Yet, the obtained results are still in agreement with data from The Immunological Genome Project (Immgen) that collects whole genome expression profiles from a wide spectrum of immune cell subsets[178]. In all accessible key immune cell populations, including T cells, that are listed in the Immgen database, *Pgr* expression is below the baseline threshold (ImmgenDB as of 07/2014, accessible at www.immgen.org).

These results raised the possibility that P4 might not signal via the PR, which appeared to be absent in T cells, but rather via another promiscuous steroid receptor. In fact, the glucocorticoid receptor (GR) and the estrogen receptor α (ER) were readily detected on mRNA level. Furthermore, the relative binding affinity (RBA) of P4 to the GR is around 40 when considering its affinity to the PR 100, thus leaving a relevant potential for cross-signalling activity[179]. To further substantiate this hypothesis, three different steroids were assessed in parallel for their capacity to enrich Treg. Norgestrel (NOR) possessing a RBA < 2 for the GR and > 260 for the PR, dexamethasone (DEX), possessing a RBA = 100 for the GR and < 0.2 for the PR, and P4 taking an intermediate position between NOR and DEX[179,193]. Notably, the compound with the highest affinity to the GR, namely DEX, showed the strongest Treg enrichment, followed by P4, which also possesses some GR affinity. Yet, PR-specific NOR showed no significant Treg enrichment.

These data indicate that P4, which is present at high levels in the serum, especially in the second half of pregnancy, is effective in shifting the immunological balance in favour of tolerogenic Treg, at least in the addressed *in vitro* conditions. In this context, P4 appears to directly act on $CD4^+$ T cells and some evidence indicates that possibly the GR and not

the PR might be the target steroid receptor mediating this effect. Importantly, the P4 dose used in these experiments was 300 ng/ml while around 100 ng/ml is readily measured in the serum of mice in late gestation[160]. Thus, experimental concentrations are still close to the physiological serum range and local P4 concentrations near to the site of P4 synthesis in the reproductive tract might be considerably higher. Additionally, lower doses of 100 ng/ml still showed some Treg enrichment after 48 h of culture time.

In a broader perspective, also other pregnancy-related hormones have been studied for their capacity to influence both Treg and autoimmunity. For instance, estradiol (E2) treatment of ovariectomised and prepubertal mice was reported to expand functional Treg and increase their Foxp3 expression[165,194]. In addition, E2 treatment also ameliorates the course of EAE, while this protective effect required the presence of estrogen receptor alpha (*Esr1*) but not beta (*Esr2*)[162]. The same group of investigators showed that E2 protection was Treg independent and proposed a role for regulatory B cells[167,168]. However, shortly after, they claimed induction of PD-1 on Treg to be a central mechanism of regulatory B cell-mediated E2-driven protection[195]. Another group focussing on the closely related estriol (E3) also reported treatment-related EAE protection[196-198] while this effect was later attributed to the generation of tolerogenic DC, which also upon adoptive transfer were able to control EAE disease activity[169].

Since E3 is characterized by fewer side effects and increased safety in comparison to E2[199], E3 was also assessed in a therapeutic setting in female human MS patients[200]. Indeed, a pilot study in RRMS demonstrated a decrease in number and volume of gadolinium enhancing MRI lesions in comparison to the pretreatment baseline[201]. Accompanying analyses additionally revealed a decreased peripheral T cell to B cell ratio, increased IL-10 production[202] and decreased matrix metalloproteinase 9 expression[203] by peripheral blood mononuclear cells of E3 treated patients. However, further placebo-controlled studies are needed to establish a therapeutic effect of E3 in MS, some of which are currently under way[200].

With respect to P4, treatment with subcutaneous P4-releasing implants at the onset of disease has also been shown to ameliorate the course of EAE in C57BL/6 mice[164]. However, in this study P4 had no effect on the systemic frequency of Treg[164]. In contrast, another study reported a substantial increase of uterine and systemic Treg frequencies when treating ovariectomised female mice with subcutaneous injection of P4 resolved in sesame oil[166]. Additionally, P4 was shown to drive naïve human cord blood cells but not adult peripheral T cells into suppressive Treg while impeding their differentiation into T_H17 cells[204]. However, the data regarding P4 effects on Treg induction still remain controversial[138].

Nevertheless, in the present work P4 treatment had a reproducible and pronounced *in vitro* effect in shifting the balance between Treg and Tcon in favour of potentially CNS-protective Treg.

4.4 Glucocorticoid receptor knockout in T cells

Since only indirect evidence has suggested a signalling of P4 via the GR to enrich Treg *in vitro*, a GR knockout system was considered to be the best model to definitely pinpoint this hypothesis. Since complete GR-deficiency in $GR^{-/-}$ mice results in death of the pups within a few hours after birth due to respiratory failure[205], we made use of $GR^{fl/fl}$ mice, which were generated to specifically deliver GR-deficiency to a defined cell type using Cre-Lox recombination[171]. This model was initially applied to study the role of GR in neuronal cells by crossing $GR^{fl/fl}$ to *Nestin*-Cre mice. Since activity of the *Nestin* promoter is restricted to neuronal cells, transgenic expression of Cre recombinase under the *Nestin* promoter results in Cre-mediated disruption of the floxed *GR* locus specifically in Neurons[171]. In consecutive studies this principle was further extended to achieve GR-deficiency in keratinocytes, macrophages and neutrophils, or T cells[180]. More specifically, the T cell specific GR knockout was generated by breeding $GR^{fl/fl}$ to *Lck*-Cre mice[206], since lymphocyte-specific protein tyrosine kinase (Lck) is involved in the TCR signalling cascade and its expression is restricted to T cells. Making use of such $GR^{fl/fl}$*Lck*-Cre mice it could be established that T cells are the therapeutic targets of glucocorticoids (GC) in EAE[181]. Accordingly, GC treatment efficiently reduced EAE severity in control animals but failed to do so in $GR^{fl/fl}$*Lck*-Cre mice. Moreover, GC-induced apoptosis and down-modulation of migratory molecules was abrogated in T cells derived from knockout mice[181]. In summary, $GR^{fl/fl}$*Lck*-Cre mice represent a powerful tool to study the role of the GR in the T cell population.

After validation of the imported $GR^{fl/fl}$*Lck*-Cre mice and $GR^{fl/fl}$ controls – more extensively described in the results section – the immune cell composition in knockout animals and controls was analysed by flow cytometry to rule out *a priori* differences. Yet, no significant differences in the analysed splenocyte populations including T cells, B cells, neutrophils, macrophages, NK cells, DC, T helper cells, killer T cells and Treg were observed. Next, the capacity of P4 and DEX to enrich Treg was determined in splenocyte cultures from both experimental groups. Strikingly, the Treg enrichment was readily observed in the $GR^{fl/fl}$ controls but completely abolished in $GR^{fl/fl}$*Lck*-Cre mice, thus indicating that GR expression in T cells is indispensable for steroid-driven Treg enrichment. Secondly, since P4 was unable to induce Treg in the absence of GR, P4 clearly appeared to signal via cross-binding to the GR instead of engaging the PR, as previously hypothesised.

Thus, evidence suggested that T cells directly sense both DEX and P4 via their intracellular GR. This GR engagement leads to an increase of Treg frequency in splenocyte cultures and might represent a tolerogenic pathway that is engaged in periods of increased steroid serum levels as present during pregnancy. Hypothesising a possible role of this mechanisms in fetomaternal or CNS tolerance during pregnancy, the influence of T cell specific GR-deficiency was investigated with regards to reproductive efficiency and pregnancy-induced EAE protection.

Admittedly, disturbances in the establishment of fetomaternal tolerance, as observed in CNS1-deficient[43] and galectin1-deficient mice[134] lead to abortions of implanted fetuses, which can be assessed by macroscopic examination of the pregnant uterus at E13.5. Abortions are recognized as scarred or haemorrhagic implantation sites, which can be counted to calculate the fetal loss rate per mother. In order to address the question whether GR in T cells is involved in successful tolerance induction towards the fetus in allogeneic pregnancy, these analyses were conducted comparing $GR^{fl/fl}$*Lck*-Cre mice and $GR^{fl/fl}$ controls. However, both experimental groups presented with similar numbers of implantations and viable fetuses. Moreover, the number of abortions and the fetal loss rate was not significantly different between $GR^{fl/fl}$*Lck*-Cre mice and $GR^{fl/fl}$ controls. Thus, by these experiments a profound alteration of the fetomaternal tolerance could be excluded. However, since multiple partly redundant mechanisms have evolved to prevent fetus-directed immune responses[9,132], the effect size of GR-deficiency in T cells might have been too subtle to be detectable in a quite stable read-out parameter such as the fetal loss rate. Especially since a high evolutionary pressure is exerted on ensuring species propagation by successful reproduction[137].

To further investigate whether pregnancy-associated protection from CNS autoimmunity requires GR expression in T cells for successful tolerance induction, pregnant and non-pregnant $GR^{fl/fl}$*Lck*-Cre mice and $GR^{fl/fl}$ controls were immunised for EAE on E7.5. Expectedly, pregnant control animals were temporarily protected from EAE development as previously observed in C57BL/6 wildtype mice. This protection was reflected in the disease course as well as in the day of onset. Strikingly however, $GR^{fl/fl}$*Lck*-Cre mice failed to establish protection during pregnancy. Accordingly, the course of clinical EAE symptoms and the day of onset were not significantly altered by pregnancy in these animals. Moreover, also the direct comparison between pregnant $GR^{fl/fl}$*Lck*-Cre and pregnant $GR^{fl/fl}$ mice revealed a significant difference in the clinical course. Thus, GR in T cells is required for successfully establishing pregnancy-driven CNS tolerance.

Taken together, Treg enrichment observed by P4 treatment *in vitro* could be demonstrated to depend on P4 cross-signalling via the GR in T cells. *In vivo* analysis by targeted GR-deficiency in T cells revealed that in pregnant animals this mechanism was

indispensable for CNS-directed but dispensable for fetus-directed tolerance induction. Therefore, cross-signalling of pregnancy-related steroid hormones via the GR might represent a novel mechanism by which the Treg population is supported to confer protection from MS disease activity during pregnancy. However, *GR*$^{fl/fl}$*Lck*-Cre mice were reported to present some additional alterations that might potentially interfere with the obtained results. Some of which will be discussed in the following.

First, it has been reported that GR in thymocytes is also involved in moderating the thymic selection process[182]. Using an independently generated *GR*$^{fl/fl}$*Lck*-Cre mouse model, the authors observed an immunocompromised phenotype in these mice with reduced polyclonal T cell proliferative responses to alloantigen, defined peptide antigens, and viral infection. This was not due to an intrinsic proliferation defect, because upon unspecific TCR cross-linking T cell responses were normal[182]. In fact, the authors detected alterations of the TCR repertoire, introduced by increased thymocyte negative selection[182]. However, in this work *GR*$^{fl/fl}$*Lck*-Cre mice did not show impaired EAE responses to the $MOG_{35–55}$ peptide but were rather unable to control the response during pregnancy. Hence, alterations of the TCR repertoire are unlikely to be responsible for the obtained results.

Second, a more recent study showed that GC are induced in the course of acute *Toxoplasma gondii* infection and *GR*$^{fl/fl}$*Lck*-Cre rapidly succumb to this infection without displaying higher parasite burdens. This was caused by an overshooting pathogen-driven immune response that provoked severe collateral tissue damage and consequently compromised host survival[207]. Thus, a general hyper-responsiveness of GR-deficient T cells might have led to their hindered control during pregnancy in this work. However, one argument that speaks against this possibility is that such a difference should have led to increased disease activity also in non-pregnant *GR*$^{fl/fl}$*Lck*-Cre mice. Yet, no differences between non-pregnant *GR*$^{fl/fl}$*Lck*-Cre and non-pregnant *GR*$^{fl/fl}$ mice have been observed.

Nevertheless, it remains difficult to dissect to which extent GR engagement might work via a relative Treg enrichment and to which by direct suppression of effector T cells. To more closely study a possible differential effect of GR engagement in Treg and Tcon, steroid assays under proliferative and non-proliferative conditions were performed.

4.5 Differential steroid sensitivity in T cells

As mentioned earlier, the P4-driven increase of Treg frequencies did not appear to be driven by active Treg proliferation but was rather accompanied by a general reduction of $CD4^+$ cells, indicating a possible passive enrichment of Treg. In such a setting one would assume that Treg would be more resistant to apoptosis mediated by GR engagement.

Consequently, steroid-sensitive Tcon would be more effectively depleted upon steroid challenge, while Treg would be positively selected and would hence accumulate. In order to investigate this hypothesis, two experimental settings were used.

First, Treg and Tcon were isolated by MACS and cultured separately in the presence of anti-CD3, IL-2 and increasing concentrations of DEX. After 48 h, cells were pulsed with [3H]-Thymidine and proliferation was determined by [3H]-Thymidine incorporation 16 h later. Markedly, especially at higher DEX concentrations (10^{-8} M and more), better proliferative responses were observed in Treg as compared to Tcon. Importantly, this was not due to a general proliferation advantage of Treg, because at low DEX concentrations Tcon tended to be even better proliferators. Second, Treg and Tcon were isolated and separately cultured as before, however in the absence of a proliferative stimulus. As read-out, induced cell death was measured by propidium iodide positivity. Again, with increasing DEX concentrations Treg were less affected by GR-driven cell death induction. In conclusion, Treg appeared to be more resistant to steroid challenges than Tcon under both proliferative and non-proliferative conditions. Thus, this differential sensitivity of Treg and Tcon might be a mechanism underlying the enrichment of Treg *in vitro* but also the need for GR expression in T cells to establish protection from CNS autoimmunity during pregnancy *in vivo*.

In principle, the reduced GR effect in Treg could be driven by reduced GR expression, reduced availability of GR engaging ligands or suppression of down-stream signalling pathways. Since GR expression was already determined throughout pregnancy, and no differences between Treg and Tcon were found, the other two possibilities were now addressed. To this end, gene expression of the steroid metabolizing enzymes 11β-HSD-1 and 11β-HSD-2[183,184] and the GR signalling down-stream marker Gilz[185,208] were analysed. Indeed, the GC-activating enzyme 11β-HSD-1 was higher expressed in Tcon than in Treg. Likewise, GR down-stream signalling as assessed by Gilz expression tended to be more active in Tcon. Thus indicating that differences in GC metabolising machinery and GR pathway-activity might be the reason for increased steroid sensitivity of Tcon. Interestingly however, Tcon adaptively down-regulated 11β-HSD-1 and up-regulated GC-inactivating 11β-HSD-2 in late gestation, thus potentially rendering themselves more steroid resistant. Nevertheless, Gilz expression was still higher in these cells in comparison to Treg.

In conclusion, for the first time evidence supporting a differential steroid sensitivity of Treg and Tcon could be obtained. Steroid resistance of Treg was found to most probably mediate their enrichment upon prolonged steroid exposure as present during pregnancy. Moreover, lower expression of GC-activating 11β-HSD-1 in Treg might be the causal mechanism leading to reduced GR pathway activity and better Treg survival. Finally, Tcon might also acquire steroid resistance at late gestational stages indicated by increased

11β-HSD-2 and decreased 11β-HSD-1 expression in E18.5 Tcon. This acquired Tcon resistance could also play a role in the post-partum rebound phenomenon when steroid levels drop to endogenous baseline levels. However, to substantiate this assumption further supporting evidence is needed.

4.6 Pregnancy-regulated genes in Treg

To identify so far unrecognized molecules that might render Treg during pregnancy more potent to compete with Tcon-driven feto- and autoreactive responses, a non-biased whole genome expression analysis was performed.

Since subtle changes were expected, a high purity of Treg preparations was pursued. However, Foxp3$^+$ Treg are naturally not accessible to fluorescence-activated cell sorting, as intracellular staining of Foxp3 involves fixation and permeabilisation, which impedes the extraction of high-quality RNA. To overcome this obstacle, a transgenic mouse line expressing a green fluorescent protein (GFP) under the Foxp3 promoter was used[170] for high purity sorting of Treg from pregnant and non-pregnant female mice. Then, RNA was extracted and subjected to microarray analysis, which was carried out in quadruplicate. After statistical processing, four up- and eleven down-regulated candidates were identified and three of them were additionally validated by real-time PCR from independent Treg samples.

Interestingly, although only a limited number of genes was detected to be differentially regulated, two array-probes targeting the enzyme carnitine palmitoyltransferase 1a (Cpt1a) were significantly enriched in Treg from pregnant mice. Cpt1a is localised at the outer mitochondrial membrane and loads fatty acids onto the carnitine shuttle, thus enabling their transport into the mitochondrial matrix where fatty acids become substrate of energy-producing beta oxidation. More importantly, Cpt1a controls the rate-limiting step to utilize fatty acids as energy source and long-lived memory CD8$^+$ T cells have been recently shown to rely on this specific pathway[209]. The authors show, that by switching from glucose to fatty acid consumption, T cells are becoming independent of glucose supply, increase their mitochondrial spare respiratory capacity and gain a survival advantage over glucose metabolizing T cells[209].

Similarly, the IL-7 receptor (Il7r), which was also found to be up-regulated in Treg from pregnant mice, plays an important role in the generation of long-lived CD4$^+$ and CD8$^+$ memory cells[210-212]. Correspondingly, IL-7$^{-/-}$ mice or mice that had been depleted of IL-7 by antibody treatment are able to mount proper primary T cell responses but fail to translate these responses into long lasting memory[212].

Taken together, induction of Cpt1a and Il7r in Treg during pregnancy might render these cells more stable, long-lived and independent. These adaptational changes might further support fetomaternal and possibly also CNS tolerance during gestation. Cpt1a, Il7r and other differentially expressed candidate genes represent promising starting points for more detailed analysis and are going to be further investigated in future research projects.

5 Summary

Multiple sclerosis (MS) is the most frequent inflammatory disease affecting the central nervous system (CNS). During pregnancy, MS patients show ameliorated disease activity resulting in decreased relapse rates, while post-partum disease activity is increased before returning to the individual pre-pregnancy rates. Foxp3^{+} regulatory T cells (Treg), which are expanding during pregnancy and are crucial for establishing tolerance to the semiallogeneic fetus, are hypothesized to play a pivotal role in mediating this pregnancy-associated control of autoimmunity. However, the precise mechanism by which this occurs is currently unknown. Thus, the goal of this work was to investigate the underlying molecular pathways of pregnancy-induced CNS tolerance in a mouse model of MS with a special focus on Treg.

For this purpose, a mouse model of pregnancy-associated CNS tolerance was established. In this model, pregnant mice are temporarily protected from developing experimental autoimmune encephalomyelitis (EAE) and present with reduced CNS infiltration of immune cells. Similar to MS patients, a rebound phenomenon is observed after delivery. Additionally, Treg frequency, phenotype and function were assessed throughout pregnancy and post-partum. Treg preferentially accumulated in uterus-draining lymph nodes and persisted as long as 30 days post-partum. Moreover, late gestational Treg presented elevated expression of Ki67 and Ctla4 and showed increased suppressive capacity. Accumulation of Treg could be emulated *in vitro* by the pregnancy hormone progesterone (P4). This effect could be attributed to P4 cross-engagement of the glucocorticoid receptor (GR) in T cells. Accordingly, T cell-restricted GR-deficiency in *GR*$^{fl/fl}$*Lck*-Cre mice abrogated Treg accumulation. Furthermore, the relevance of this mechanism was evaluated in pregnancy *in vivo*. While GR in T cells was required for pregnancy-induced protection from EAE, it was dispensable for effective reproduction, as the fetal loss rate was unchanged in comparison to control animals. Treg accumulation by GR engagement could be further attributed to differential steroid resistance of Treg and conventional T cells (Tcon), rendering Treg more steroid resistant. Finally, whole genome expression analysis was utilized to identify Cpt1a, Il7r and other target genes potentially involved in rendering the Treg population more resilient during pregnancy.

In summary, this works proposes a role for differential GR-mediated sensitivity of Treg and Tcon to pregnancy-related steroid hormones being dispensable for fetomaternal tolerance but indispensable for pregnancy-induced amelioration of CNS autoimmunity.

Zusammenfassung

Multiple Sklerose (MS) ist die häufigste entzündliche Erkrankung des zentralen Nervensystems (ZNS). Während der Schwangerschaft von MS-Patientinnen kommt es zu einer Reduktion der Krankheitsaktivität mit Verminderung der Schubrate. Nach der Geburt des Kindes steigt die Schubrate zunächst sprunghaft an, um sich in der Folge wieder auf das Vor-Schwangerschafts-Niveau einzupendeln. Es wird angenommen, dass $Foxp3^+$ regulatorische T-Zellen (Treg), die während der Schwangerschaft eine immunologische Toleranz gegenüber dem semiallogenen Fetus sicherstellen, am Aufbau dieses temporären Schutzes vor Autoimmunität beteiligt sind. Wie genau dieser Schutz jedoch vermittelt wird, ist bisher nicht ausreichend verstanden. Ziel dieser Arbeit war es daher, die zugrundeliegenden zellulären und molekularen Zusammenhänge in einem Mausmodel der MS unter besonderer Berücksichtigung von Treg zu untersuchen.

Zu diesem Zweck wurde ein Mausmodel etabliert, in dem trächtige Mäuse temporär vor der Entwicklung einer experimentellen autoimmunen Enzephalomyelitis (EAE) geschützt sind und eine verminderte ZNS-Infiltration von Immunzellen aufweisen. Wie bei MS-Patientinnen kommt es nach der Geburt zu einem Rebound-Phänomen. Zusätzlich wurden Frequenz, Phänotyp und Funktion von Treg während der Trächtigkeit und im postpartalen Verlauf untersucht. Treg reicherten sich insbesondere in den Uterus-drainierenden Lymphknoten an und blieben bis 30 Tage postpartum erhöht nachweisbar. Weiterhin zeigten Treg in der späten Trächtigkeit eine erhöhte Expression von Ki67 und Ctla4 und hatten eine erhöhte suppressive Kapazität. Die Anreicherung von Treg konnte *in vitro* mit dem Schwangerschaftshormon Progesteron (P4) nachgestellt werden. Dieser Effekt konnte ferner auf eine Kreuz-Reaktivität von P4 am Glukokortikoid-Rezeptor (GR) zurückgeführt werden. Insbesondere da eine auf T-Zellen beschränkte GR-Defizienz in $GR^{fl/fl}$*Lck*-Cre-Mäusen die Treg-Anreicherung aufhob. Daraufhin wurde die Bedeutung dieses Mechanismus während der Trächtigkeit *in vivo* untersucht. Während der GR in T-Zellen unerlässlich für den Trächtigkeits-induzierten Schutz vor EAE war, war er für die Toleranz gegenüber den Feten nicht zwingend notwendig. Die Treg-Anreicherung konnte weiterhin auf eine höhere Steroid-Resistenz von Treg gegenüber konventionellen T-Zellen (Tcon) zurückgeführt werden. Schließlich wurden in eine genomweiten Genexpressionsanalyse Cpt1a, Il7r und weitere Kandidaten identifiziert, die potentiell an einer erhöhten Widerstandkraft von Treg während der Trächtigkeit beteiligt sind.

Zusammenfassend wurde in der vorliegenden Arbeit eine differenzielle GR-vermittelte Sensitivität von Treg und Tcon gegenüber Schwangerschafts-assoziierten Steroidhormonen gezeigt. Dieser Mechanismus war keine zwingende Voraussetzung für die Toleranz gegenüber den Feten, war jedoch andererseits unerlässlich für einen Schwangerschafts-induzierten Schutz vor ZNS-Autoimmunität.

6 References

1. *Atlas of MS 2013*. 1–28 (Multiple Sclerosis International Federation, 2013).
2. Compston, A. & Coles, A. Multiple sclerosis. *Lancet* **372,** 1502–1517 (2008).
3. Goverman, J. Autoimmune T cell responses in the central nervous system. *Nat Rev Immunol* **9,** 393–407 (2009).
4. Confavreux, C., Hutchinson, M., Hours, M. M., Cortinovis-Tourniaire, P. & Moreau, T. Rate of pregnancy-related relapse in multiple sclerosis. Pregnancy in Multiple Sclerosis Group. *N. Engl. J. Med.* **339,** 285–291 (1998).
5. Vukusic, S. *et al.* Pregnancy and multiple sclerosis (the PRIMS study): clinical predictors of post-partum relapse. *Brain* **127,** 1353–1360 (2004).
6. Finkelsztejn, A. *et al.* The Brazilian database on pregnancy in multiple sclerosis. *Clin Neurol Neurosurg* **113,** 277–280 (2011).
7. Patas, K., Engler, J. B., Friese, M. A. & Gold, S. M. Pregnancy and multiple sclerosis: feto-maternal immune cross talk and its implications for disease activity. *Journal of Reproductive Immunology* **97,** 140–146 (2013).
8. Sakaguchi, S. Naturally arising Foxp3-expressing CD25+CD4+ regulatory T cells in immunological tolerance to self and non-self. *Nat Immunol* **6,** 345–352 (2005).
9. Erlebacher, A. Mechanisms of T cell tolerance towards the allogeneic fetus. *Nat Rev Immunol* **13,** 23–33 (2012).
10. Matzinger, P. The danger model: a renewed sense of self. *Science* **296,** 301–305 (2002).
11. Schenten, D. & Medzhitov, R. The control of adaptive immune responses by the innate immune system. *Adv. Immunol.* **109,** 87–124 (2011).
12. Le, Y., Zhou, Y., Iribarren, P. & Wang, J. Chemokines and chemokine receptors: their manifold roles in homeostasis and disease. *Cell. Mol. Immunol.* **1,** 95–104 (2004).
13. Litman, G. W., Cannon, J. P. & Dishaw, L. J. Reconstructing immune phylogeny: new perspectives. *Nat Rev Immunol* **5,** 866–879 (2005).
14. Janeway, C. A., Travers, P., Walport, M. & Shlomchik, M. J. *Immunobiology.* (Garland Science, 2001).
15. Pasare, C. & Medzhitov, R. Toll-like receptors and acquired immunity. *Semin. Immunol.* **16,** 23–26 (2004).
16. Harty, J. T., Tvinnereim, A. R. & White, D. W. CD8+ T cell effector mechanisms in resistance to infection. *Annu. Rev. Immunol.* **18,** 275–308 (2000).
17. Bailey, S. R. *et al.* Th17 Cells in Cancer: The Ultimate Identity Crisis. *Front Immunol* **5,** (2014).
18. Charlton, B. & Lafferty, K. J. The Th1/Th2 balance in autoimmunity. *Current Opinion in Immunology* **7,** 793–798 (1995).
19. Cua, D. J. *et al.* Interleukin-23 rather than interleukin-12 is the critical cytokine for autoimmune inflammation of the brain. *Nature* **421,** 744–748 (2003).

20. Iwakura, Y., Nakae, S., Saijo, S. & Ishigame, H. The roles of IL-17A in inflammatory immune responses and host defense against pathogens. *Immunol. Rev.* **226,** 57–79 (2008).

21. Manel, N., Unutmaz, D. & Littman, D. R. The differentiation of human T(H)-17 cells requires transforming growth factor-beta and induction of the nuclear receptor RORgammat. *Nat Immunol* **9,** 641–649 (2008).

22. Korn, T., Bettelli, E., Oukka, M. & Kuchroo, V. K. IL-17 and Th17 Cells. *Annu. Rev. Immunol.* **27,** 485–517 (2009).

23. Ravetch, J. V. & Bolland, S. IgG Fc receptors. *Annu. Rev. Immunol.* **19,** 275–290 (2001).

24. Daniels, M. A. *et al.* Thymic selection threshold defined by compartmentalization of Ras/MAPK signalling. *Nature* **444,** 724–729 (2006).

25. Singer, A., Adoro, S. & Park, J.-H. Lineage fate and intense debate: myths, models and mechanisms of CD4- versus CD8-lineage choice. *Nat Rev Immunol* **8,** 788–801 (2008).

26. Klein, L., Hinterberger, M., Wirnsberger, G. & Kyewski, B. Antigen presentation in the thymus for positive selection and central tolerance induction. *Nat Rev Immunol* **9,** 833–844 (2009).

27. Klein, L., Kyewski, B., Allen, P. M. & Hogquist, K. A. Positive and negative selection of the T cell repertoire: what thymocytes see (and don't see). *Nat Rev Immunol* (2014). doi:10.1038/nri3667

28. Gershon, R. K., Cohen, P., Hencin, R. & Liebhaber, S. A. Suppressor T cells. *J. Immunol.* **108,** 586–590 (1972).

29. Sakaguchi, S., Sakaguchi, N., Asano, M., Itoh, M. & Toda, M. Immunologic self-tolerance maintained by activated T cells expressing IL-2 receptor alpha-chains (CD25). Breakdown of a single mechanism of self-tolerance causes various autoimmune diseases. *J. Immunol.* **155,** 1151–1164 (1995).

30. Wildin, R. S. *et al.* X-linked neonatal diabetes mellitus, enteropathy and endocrinopathy syndrome is the human equivalent of mouse scurfy. *Nat. Genet.* **27,** 18–20 (2001).

31. Bennett, C. L. *et al.* The immune dysregulation, polyendocrinopathy, enteropathy, X-linked syndrome (IPEX) is caused by mutations of FOXP3. *Nat. Genet.* **27,** 20–21 (2001).

32. Campbell, D. J. & Koch, M. A. Phenotypical and functional specialization of FOXP3+ regulatory T cells. *Nat Rev Immunol* **11,** 119–130 (2011).

33. Yadav, M., Stephan, S. & Bluestone, J. A. Peripherally induced tregs - role in immune homeostasis and autoimmunity. *Front Immunol* **4,** 232 (2013).

34. Vignali, D. A. A., Collison, L. W. & Workman, C. J. How regulatory T cells work. *Nat Rev Immunol* **8,** 523–532 (2008).

35. Ohkura, N., Kitagawa, Y. & Sakaguchi, S. Development and maintenance of regulatory T cells. *Immunity* **38,** 414–423 (2013).

36. Zheng, S. G., Wang, J. H., Gray, J. D., Soucier, H. & Horwitz, D. A. Natural and induced CD4+CD25+ cells educate CD4+CD25- cells to develop suppressive activity: the role of IL-2, TGF-beta, and IL-10. *J. Immunol.* **172,** 5213–5221 (2004).

37. Abbas, A. K. *et al.* Regulatory T cells: recommendations to simplify the nomenclature. *Nat Immunol* **14,** 307–308 (2013).

38. Kim, H.-P. & Leonard, W. J. CREB/ATF-dependent T cell receptor-induced FoxP3 gene expression: a role for DNA methylation. *J. Exp. Med.* **204,** 1543–1551 (2007).

39. Baron, U. *et al.* DNA demethylation in the human FOXP3 locus discriminates regulatory T cells from activated FOXP3(+) conventional T cells. *Eur. J. Immunol.* **37,** 2378–2389 (2007).

40. Floess, S. *et al.* Epigenetic control of the foxp3 locus in regulatory T cells. *PLoS Biol.* **5,** e38 (2007).

41. Bains, I., van Santen, H. M., Seddon, B. & Yates, A. J. Models of self-peptide sampling by developing T cells identify candidate mechanisms of thymic selection. *PLoS Comput. Biol.* **9,** e1003102 (2013).

42. Zheng, Y. *et al.* Role of conserved non-coding DNA elements in the Foxp3 gene in regulatory T-cell fate. *Nature* **463,** 808–812 (2010).

43. Samstein, R. M., Josefowicz, S. Z., Arvey, A., Treuting, P. M. & Rudensky, A. Y. Extrathymic generation of regulatory T cells in placental mammals mitigates maternal-fetal conflict. *Cell* **150,** 29–38 (2012).

44. Fallarino, F. *et al.* Modulation of tryptophan catabolism by regulatory T cells. *Nat Immunol* **4,** 1206–1212 (2003).

45. Liang, B. *et al.* Regulatory T cells inhibit dendritic cells by lymphocyte activation gene-3 engagement of MHC class II. *J. Immunol.* **180,** 5916–5926 (2008).

46. Hawrylowicz, C. M. & O'Garra, A. Potential role of interleukin-10-secreting regulatory T cells in allergy and asthma. *Nat Rev Immunol* **5,** 271–283 (2005).

47. Charcot, J.-M. Histologie de la sclérose en plaques. *Gazette Hôpitaux* **41,** 554–566 (1868).

48. Noseworthy, J. H., Lucchinetti, C., Rodriguez, M. & Weinshenker, B. G. Multiple sclerosis. *N. Engl. J. Med.* **343,** 938–952 (2000).

49. Scalfari, A. *et al.* The natural history of multiple sclerosis: a geographically based study 10: relapses and long-term disability. *Brain* **133,** 1914–1929 (2010).

50. Confavreux, C. & Vukusic, S. Age at disability milestones in multiple sclerosis. *Brain* **129,** 595–605 (2006).

51. Palmer, A. J., Colman, S., O'Leary, B., Taylor, B. V. & Simmons, R. D. The economic impact of multiple sclerosis in Australia in 2010. *Mult. Scler.* **19,** 1640–1646 (2013).

52. Tutuncu, M. *et al.* Onset of progressive phase is an age-dependent clinical milestone in multiple sclerosis. *Mult. Scler.* **19,** 188–198 (2013).

53. Haghikia, A., Hohlfeld, R., Gold, R. & Fugger, L. Therapies for multiple sclerosis: translational achievements and outstanding needs. *Trends Mol Med* **19,** 309–319 (2013).

54. Filippini, G. *et al.* Interferons in relapsing remitting multiple sclerosis: a systematic review. *Lancet* **361,** 545–552 (2003).

55. Munari, L., Lovati, R. & Boiko, A. Therapy with glatiramer acetate for multiple sclerosis. *Cochrane Database Syst Rev* CD004678 (2004). doi:10.1002/14651858.CD004678

56. O'Connor, P. *et al.* Randomized trial of oral teriflunomide for relapsing multiple sclerosis. *N. Engl. J. Med.* **365,** 1293–1303 (2011).

57. Gold, R. *et al.* Placebo-controlled phase 3 study of oral BG-12 for relapsing multiple sclerosis. *N. Engl. J. Med.* **367,** 1098–1107 (2012).

58. Prinz, M. *et al.* Distinct and nonredundant in vivo functions of IFNAR on myeloid cells limit autoimmunity in the central nervous system. *Immunity* **28,** 675–686 (2008).

59. Aharoni, R. The mechanism of action of glatiramer acetate in multiple sclerosis and beyond. *Autoimmunity Reviews* **12,** 543–553 (2013).

60. Rückemann, K. *et al.* Leflunomide inhibits pyrimidine de novo synthesis in mitogen-stimulated T-lymphocytes from healthy humans. *J. Biol. Chem.* **273,** 21682–21691 (1998).

61. Albrecht, P. *et al.* Effects of dimethyl fumarate on neuroprotection and immunomodulation. *J Neuroinflammation* **9,** 163 (2012).

62. Polman, C. H. *et al.* A randomized, placebo-controlled trial of natalizumab for relapsing multiple sclerosis. *N. Engl. J. Med.* **354,** 899–910 (2006).

63. Kappos, L. *et al.* A placebo-controlled trial of oral fingolimod in relapsing multiple sclerosis. *N. Engl. J. Med.* **362,** 387–401 (2010).

64. Martinelli Boneschi, F., Rovaris, M., Capra, R. & Comi, G. Mitoxantrone for multiple sclerosis. *Cochrane Database Syst Rev* CD002127 (2005). doi:10.1002/14651858.CD002127.pub2

65. La Mantia, L., Milanese, C., Mascoli, N., D'Amico, R. & Weinstock-Guttman, B. Cyclophosphamide for multiple sclerosis. *Cochrane Database Syst Rev* CD002819 (2007). doi:10.1002/14651858.CD002819.pub2

66. Yednock, T. A. *et al.* Prevention of experimental autoimmune encephalomyelitis by antibodies against alpha 4 beta 1 integrin. *Nature* **356,** 63–66 (1992).

67. Schwab, S. R. & Cyster, J. G. Finding a way out: lymphocyte egress from lymphoid organs. *Nat Immunol* **8,** 1295–1301 (2007).

68. Willer, C. J. *et al.* Twin concordance and sibling recurrence rates in multiple sclerosis. *Proc. Natl. Acad. Sci. U.S.A.* **100,** 12877–12882 (2003).

69. Mumford, C. J. *et al.* The British Isles survey of multiple sclerosis in twins. *Neurology* **44,** 11–15 (1994).

70. Baranzini, S. E. *et al.* Genome, epigenome and RNA sequences of monozygotic twins discordant for multiple sclerosis. *Nature* **464,** 1351–1356 (2010).

71. Ebers, G. C., Sadovnick, A. D. & Risch, N. J. A genetic basis for familial aggregation in multiple sclerosis. Canadian Collaborative Study Group. *Nature* **377,** 150–151 (1995).

72. Robertson, N. P. *et al.* Age-adjusted recurrence risks for relatives of patients with multiple sclerosis. *Brain* **119 (Pt 2),** 449–455 (1996).

73. International Multiple Sclerosis Genetics Consortium *et al.* Genetic risk and a primary role for cell-mediated immune mechanisms in multiple sclerosis. *Nature* **476,** 214–219 (2011).

74. International Multiple Sclerosis Genetics Consortium *et al.* Risk alleles for multiple sclerosis identified by a genomewide study. *N. Engl. J. Med.* **357,** 851–862 (2007).

75. Ascherio, A. & Munger, K. L. Environmental risk factors for multiple sclerosis. Part II: Noninfectious factors. *Ann Neurol.* **61,** 504–513 (2007).

76. Ascherio, A. & Munger, K. L. Environmental risk factors for multiple sclerosis. Part I: the role of infection. *Ann Neurol.* **61,** 288–299 (2007).

77. Ebers, G. C. Environmental factors and multiple sclerosis. *Lancet Neurol* **7,** 268–277 (2008).

78. Alter, M., Leibowitz, U. & Speer, J. Risk of multiple sclerosis related to age at immigration to Israel. *Arch. Neurol.* **15,** 234–237 (1966).

79. Dean, G. & Kurtzke, J. F. On the risk of multiple sclerosis according to age at immigration to South Africa. *Br Med J* **3,** 725–729 (1971).

80. Elian, M., Nightingale, S. & Dean, G. Multiple sclerosis among United Kingdom-born children of immigrants from the Indian subcontinent, Africa and the West Indies. *J. Neurol. Neurosurg. Psychiatr.* **53,** 906–911 (1990).

81. Hammond, S. R., English, D. R. & McLeod, J. G. The age-range of risk of developing multiple sclerosis: evidence from a migrant population in Australia. *Brain* **123 (Pt 5),** 968–974 (2000).

82. Serafini, B. *et al.* Dysregulated Epstein-Barr virus infection in the multiple sclerosis brain. *J. Exp. Med.* **204,** 2899–2912 (2007).

83. Lünemann, J. D. *et al.* EBNA1-specific T cells from patients with multiple sclerosis cross react with myelin antigens and co-produce IFN-gamma and IL-2. *J. Exp. Med.* **205,** 1763–1773 (2008).

84. Tejada-Simon, M. V., Zang, Y. C. Q., Hong, J., Rivera, V. M. & Zhang, J. Z. Cross-reactivity with myelin basic protein and human herpesvirus-6 in multiple sclerosis. *Ann Neurol.* **53,** 189–197 (2003).

85. Münz, C., Lünemann, J. D., Getts, M. T. & Miller, S. D. Antiviral immune responses: triggers of or triggered by autoimmunity? *Nat Rev Immunol* **9,** 246–258 (2009).

86. Hedström, A. K. *et al.* Smoking and two human leukocyte antigen genes interact to increase the risk for multiple sclerosis. *Brain* **134,** 653–664 (2011).

87. Popescu, B. F. G. & Lucchinetti, C. F. Pathology of demyelinating diseases. *Annu Rev Pathol* **7,** 185–217 (2012).

88. Kutzelnigg, A. *et al.* Cortical demyelination and diffuse white matter injury in multiple sclerosis. *Brain* **128,** 2705–2712 (2005).

89. Frischer, J. M. *et al.* The relation between inflammation and neurodegeneration in multiple sclerosis brains. *Brain* **132,** 1175–1189 (2009).

90. Ota, K. *et al.* T-cell recognition of an immunodominant myelin basic protein epitope in multiple sclerosis. *Nature* **346,** 183–187 (1990).

91. Olsson, T. *et al.* Autoreactive T lymphocytes in multiple sclerosis determined by antigen-induced secretion of interferon-gamma. *J. Clin. Invest.* **86,** 981–985 (1990).

92. Bielekova, B. *et al.* Expansion and functional relevance of high-avidity myelin-specific CD4+ T cells in multiple sclerosis. *J. Immunol.* **172,** 3893–3904 (2004).

93. Bielekova, B. *et al.* Encephalitogenic potential of the myelin basic protein peptide (amino acids 83-99) in multiple sclerosis: results of a phase II clinical trial with an altered peptide ligand. *Nat Med* **6,** 1167–1175 (2000).

94. Oksenberg, J. R. *et al.* Selection for T-cell receptor V beta-D beta-J beta gene rearrangements with specificity for a myelin basic protein peptide in brain lesions of multiple sclerosis. *Nature* **362,** 68–70 (1993).

95. Krogsgaard, M. *et al.* Visualization of myelin basic protein (MBP) T cell epitopes in multiple sclerosis lesions using a monoclonal antibody specific for the human histocompatibility leukocyte antigen (HLA)-DR2-MBP 85-99 complex. *J. Exp. Med.* **191,** 1395–1412 (2000).

96. Friese, M. A. *et al.* The value of animal models for drug development in multiple sclerosis. *Brain* **129,** 1940–1952 (2006).

97. Baxter, A. G. The origin and application of experimental autoimmune encephalomyelitis. *Nat Rev Immunol* **7,** 904–912 (2007).

98. Rivers, T. M., Sprunt, D. H. & Berry, G. P. The neuro-paralytic accidents of anti-rabies treatment. *Ann. Trop. Med.* **22,** (1928).

99. Rivers, T. M., Sprunt, D. H. & Berry, G. P. Observations on attempts to produce acute disseminated encephalomyelitis in monkeys. *J. Exp. Med.* **58,** 39–53 (1933).

100. de Rosbo, N. K. *et al.* The myelin-associated oligodendrocytic basic protein region MOBP15-36 encompasses the immunodominant major encephalitogenic epitope(s) for SJL/J mice and predicted epitope(s) for multiple sclerosis-associated HLA-DRB1*1501. *J. Immunol.* **173,** 1426–1435 (2004).

101. Kuchroo, V. K. *et al.* Experimental allergic encephalomyelitis mediated by cloned T cells specific for a synthetic peptide of myelin proteolipid protein. Fine specificity and T cell receptor V beta usage. *J. Immunol.* **148,** 3776–3782 (1992).

102. Krishnamoorthy, G. & Wekerle, H. EAE: an immunologist's magic eye. *Eur. J. Immunol.* **39,** 2031–2035 (2009).

103. Krishnamoorthy, G., Lassmann, H., Wekerle, H. & Holz, A. Spontaneous opticospinal encephalomyelitis in a double-transgenic mouse model of autoimmune T cell/B cell cooperation. *J. Clin. Invest.* **116,** 2385–2392 (2006).

104. Bettelli, E. *et al.* Myelin oligodendrocyte glycoprotein-specific T cell receptor transgenic mice develop spontaneous autoimmune optic neuritis. *J. Exp. Med.* **197,** 1073–1081 (2003).

105. Madsen, L. S. *et al.* A humanized model for multiple sclerosis using HLA-DR2 and a human T-cell receptor. *Nat. Genet.* **23,** 343–347 (1999).

106. Gregersen, J. W. *et al.* Functional epistasis on a common MHC haplotype associated with multiple sclerosis. *Nature* **443,** 574–577 (2006).

107. Friese, M. A. & Fugger, L. Pathogenic CD8(+) T cells in multiple sclerosis. *Ann Neurol.* **66,** 132–141 (2009).

108. Friese, M. A. *et al.* Opposing effects of HLA class I molecules in tuning autoreactive CD8+ T cells in multiple sclerosis. *Nat Med* **14,** 1227–1235 (2008).

109. Pette, M. *et al.* Myelin basic protein-specific T lymphocyte lines from MS patients and healthy individuals. *Neurology* **40,** 1770–1776 (1990).

110. Burns, J., Rosenzweig, A., Zweiman, B. & Lisak, R. P. Isolation of myelin basic protein-reactive T-cell lines from normal human blood. *Cell. Immunol.* **81,** 435–440 (1983).

111. Ransohoff, R. M., Kivisäkk, P. & Kidd, G. Three or more routes for leukocyte migration into the central nervous system. *Nat Rev Immunol* **3,** 569–581 (2003).

112. Costantino, C. M., Baecher-Allan, C. & Hafler, D. A. Multiple sclerosis and regulatory T cells. *J. Clin. Immunol.* **28,** 697–706 (2008).

113. Kleinewietfeld, M. & Hafler, D. A. Regulatory T cells in autoimmune neuroinflammation. *Immunol. Rev.* **259,** 231–244 (2014).

114. Humrich, J. Y. *et al.* Homeostatic imbalance of regulatory and effector T cells due to IL-2 deprivation amplifies murine lupus. *Proceedings of the National Academy of Sciences* **107,** 204–209 (2010).

115. Engler, J. B. *et al.* Unmasking of autoreactive CD4 T cells by depletion of CD25 regulatory T cells in systemic lupus erythematosus. *Ann. Rheum. Dis.* **70,** 2176–2183 (2011).

116. Nie, H. *et al.* Phosphorylation of FOXP3 controls regulatory T cell function and is inhibited by TNF-α in rheumatoid arthritis. *Nat. Med.* 1–9 (2013). doi:10.1038/nm.3085

117. Munoz-Suano, A., Kallikourdis, M., Sarris, M. & Betz, A. G. Regulatory T cells protect from autoimmune arthritis during pregnancy. *Journal of Autoimmunity* **38,** J103–8 (2012).

118. Kriegel, M. A. *et al.* Defective suppressor function of human CD4+ CD25+ regulatory T cells in autoimmune polyglandular syndrome type II. *J. Exp. Med.* **199,** 1285–1291 (2004).

119. Baca Jones, C. *et al.* Regulatory T cells control diabetes without compromising acute anti-viral defense. *Clin. Immunol.* **153,** 298–307 (2014).

120. Haas, J. *et al.* Reduced suppressive effect of CD4+CD25high regulatory T cells on the T cell immune response against myelin oligodendrocyte glycoprotein in patients with multiple sclerosis. *Eur. J. Immunol.* **35,** 3343–3352 (2005).

121. Viglietta, V., Baecher-Allan, C., Weiner, H. L. & Hafler, D. A. Loss of functional suppression by CD4+CD25+ regulatory T cells in patients with multiple sclerosis. *J. Exp. Med.* **199,** 971–979 (2004).

122. Sellebjerg, F., Krakauer, M., Khademi, M., Olsson, T. & Sørensen, P. S. FOXP3, CBLB and ITCH gene expression and cytotoxic T lymphocyte antigen 4 expression on CD4(+) CD25(high) T cells in multiple sclerosis. *Clin. Exp. Immunol.* **170,** 149–155 (2012).

123. Huan, J. *et al.* Decreased FOXP3 levels in multiple sclerosis patients. *J. Neurosci. Res.* **81,** 45–52 (2005).

124. Venken, K. *et al.* Compromised CD4+ CD25(high) regulatory T-cell function in patients with relapsing-remitting multiple sclerosis is correlated with a reduced frequency of FOXP3-positive cells and reduced FOXP3 expression at the single-cell level. *Immunology* **123,** 79–89 (2008).

125. Olivares-Villagómez, D., Wang, Y. & Lafaille, J. J. Regulatory CD4(+) T cells expressing endogenous T cell receptor chains protect myelin basic protein-specific transgenic mice from spontaneous autoimmune encephalomyelitis. *J. Exp. Med.* **188,** 1883–1894 (1998).

126. Hori, S., Haury, M., Coutinho, A. & Demengeot, J. Specificity requirements for selection and effector functions of CD25+4+ regulatory T cells in anti-myelin basic protein T cell receptor transgenic mice. *Proc. Natl. Acad. Sci. U.S.A.* **99,** 8213–8218 (2002).

127. Kohm, A. P., Carpentier, P. A., Anger, H. A. & Miller, S. D. Cutting edge: CD4+CD25+ regulatory T cells suppress antigen-specific autoreactive immune responses and central nervous system inflammation during active experimental autoimmune encephalomyelitis. *J. Immunol.* **169,** 4712–4716 (2002).

128. Kasagi, S. *et al.* In vivo-generated antigen-specific regulatory T cells treat autoimmunity without compromising antibacterial immune response. *Sci Transl Med* **6,** 241ra78 (2014).

129. Stephens, L. A., Malpass, K. H. & Anderton, S. M. Curing CNS autoimmune disease with myelin-reactive Foxp3+ Treg. *Eur. J. Immunol.* **39,** 1108–1117 (2009).

130. McGeachy, M. J., Stephens, L. A. & Anderton, S. M. Natural recovery and protection from autoimmune encephalomyelitis: contribution of CD4+CD25+ regulatory cells within the central nervous system. *J. Immunol.* **175,** 3025–3032 (2005).

131. Zhang, X. *et al.* IL-10 is involved in the suppression of experimental autoimmune encephalomyelitis by CD25+CD4+ regulatory T cells. *International Immunology* **16,** 249–256 (2004).

132. Arck, P. C. & Hecher, K. Fetomaternal immune cross-talk and its consequences for maternal and offspring's health. *Nat. Med.* **19,** 548–556 (2013).

133. Kopcow, H. D. *et al.* T cell apoptosis at the maternal-fetal interface in early human pregnancy, involvement of galectin-1. *Proceedings of the National Academy of Sciences* **105,** 18472–18477 (2008).

134. Blois, S. M. *et al.* A pivotal role for galectin-1 in fetomaternal tolerance. *Nat. Med.* **13,** 1450–1457 (2007).

135. Collins, M. K., Tay, C.-S. & Erlebacher, A. Dendritic cell entrapment within the pregnant uterus inhibits immune surveillance of the maternal/fetal interface in mice. *J. Clin. Invest.* **119,** 2062–2073 (2009).

136. Nancy, P. *et al.* Chemokine gene silencing in decidual stromal cells limits T cell access to the maternal-fetal interface. *Science* **336,** 1317–1321 (2012).

137. Andersen, K. G., Nissen, J. K. & Betz, A. G. Comparative Genomics Reveals Key Gain-of-Function Events in Foxp3 during Regulatory T Cell Evolution. *Front Immunol* **3,** 113 (2012).

138. Schumacher, A. & Zenclussen, A. C. Regulatory T Cells: Regulators of Life. *Am. J. Reprod. Immunol.* (2014). doi:10.1111/aji.12238

139. Aluvihare, V. R., Kallikourdis, M. & Betz, A. G. Regulatory T cells mediate maternal tolerance to the fetus. *Nat Immunol* **5,** 266–271 (2004).

140. Zenclussen, A. C. *et al.* Regulatory T cells induce a privileged tolerant microenvironment at the fetal-maternal interface. *Eur. J. Immunol.* **36,** 82–94 (2006).

141. Somerset, D. A., Zheng, Y., Kilby, M. D., Sansom, D. M. & Drayson, M. T. Normal human pregnancy is associated with an elevation in the immune suppressive CD25+ CD4+ regulatory T-cell subset. *Immunology* **112,** 38–43 (2004).

142. HEIKKINEN, J., MOTTONEN, M., ALANEN, A. & LASSILA, O. Phenotypic characterization of regulatory T cells in the human decidua. *Clin. Exp. Immunol.* **136,** 373–378 (2004).

143. Sánchez-Ramón, S. *et al.* Pregnancy-induced expansion of regulatory T-lymphocytes may mediate protection to multiple sclerosis activity. *Immunol. Lett.* **96,** 195–201 (2005).

144. Mjösberg, J. *et al.* Systemic reduction of functionally suppressive CD4dimCD25highFoxp3+ Tregs in human second trimester pregnancy is induced by progesterone and 17beta-estradiol. *The Journal of Immunology* **183,** 759–769 (2009).

145. Sasaki, Y. *et al.* Decidual and peripheral blood CD4+CD25+ regulatory T cells in early pregnancy subjects and spontaneous abortion cases. *Mol. Hum. Reprod.* **10,** 347–353 (2004).

146. Yang, H. *et al.* Proportional change of CD4+CD25+ regulatory T cells in decidua and peripheral blood in unexplained recurrent spontaneous abortion patients. *Fertil. Steril.* **89,** 656–661 (2008).

147. Jin, L.-P., Chen, Q.-Y., Zhang, T., Guo, P.-F. & Li, D.-J. The CD4+CD25 bright regulatory T cells and CTLA-4 expression in peripheral and decidual lymphocytes are down-regulated in human miscarriage. *Clin. Immunol.* **133,** 402–410 (2009).

148. Mei, S., Tan, J., Chen, H., Chen, Y. & Zhang, J. Changes of CD4+CD25high regulatory T cells and FOXP3 expression in unexplained recurrent spontaneous abortion patients. *Fertil. Steril.* **94,** 2244–2247 (2010).

149. Winger, E. E. & Reed, J. L. Low circulating CD4(+) CD25(+) Foxp3(+) T regulatory cell levels predict miscarriage risk in newly pregnant women with a history of failure. *Am. J. Reprod. Immunol.* **66,** 320–328 (2011).

150. Rowe, J. H., Ertelt, J. M., Xin, L. & Way, S. S. Pregnancy imprints regulatory memory that sustains anergy to fetal antigen. *Nature* **490,** 102–106 (2013).

151. Kahn, D. A. & Baltimore, D. Pregnancy induces a fetal antigen-specific maternal T regulatory cell response that contributes to tolerance. *Proceedings of the National Academy of Sciences* **107,** 9299–9304 (2010).

152. Rowe, J. H., Ertelt, J. M., Aguilera, M. N., Farrar, M. A. & Way, S. S. Foxp3(+) regulatory T cell expansion required for sustaining pregnancy compromises host defense against prenatal bacterial pathogens. *Cell Host Microbe* **10,** 54–64 (2011).

153. de Man, Y. A., Dolhain, R. J. E. M., van de Geijn, F. E., Willemsen, S. P. & Hazes, J. M. W. Disease activity of rheumatoid arthritis during pregnancy: results from a nationwide prospective study. *Arthritis Rheum.* **59,** 1241–1248 (2008).

154. Förger, F. *et al.* Pregnancy induces numerical and functional changes of CD4+CD25 high regulatory T cells in patients with rheumatoid arthritis. *Ann. Rheum. Dis.* **67,** 984–990 (2008).

155. Buchel, E., Van Steenbergen, W., Nevens, F. & Fevery, J. Improvement of autoimmune hepatitis during pregnancy followed by flare-up after delivery. *Am. J. Gastroenterol.* **97,** 3160–3165 (2002).

156. Langer-Gould, A., Garren, H., Slansky, A., Ruiz, P. J. & Steinman, L. Late pregnancy suppresses relapses in experimental autoimmune encephalomyelitis: evidence for a suppressive pregnancy-related serum factor. *J. Immunol.* **169,** 1084–91 (2002).

157. Gatson, N. N. *et al.* Induction of pregnancy during established EAE halts progression of CNS autoimmune injury via pregnancy-specific serum factors. *J. Neuroimmunol.* **230,** 105–113 (2011).

158. McClain, M. A. *et al.* Pregnancy suppresses experimental autoimmune encephalomyelitis through immunoregulatory cytokine production. *J. Immunol.* **179,** 8146–8152 (2007).

159. Kim, M. R. *et al.* Progesterone-dependent release of transforming growth factor-beta1 from epithelial cells enhances the endometrial decidualization by turning on the Smad signalling in stromal cells. *Mol. Hum. Reprod.* **11,** 801–808 (2005).

160. Holinka, C. F., Tseng, Y. C. & Finch, C. E. Reproductive aging in C57BL/6J mice: plasma progesterone, viable embryos and resorption frequency throughout pregnancy. *Biol. Reprod.* **20,** 1201–1211 (1979).

161. Holinka, C. F., Tseng, Y. C. & Finch, C. E. Impaired preparturitional rise of plasma estradiol in aging C57BL/6J mice. *Biol. Reprod.* **21,** 1009–1013 (1979).

162. Polanczyk, M. *et al.* The protective effect of 17beta-estradiol on experimental autoimmune encephalomyelitis is mediated through estrogen receptor-alpha. *Am. J. Pathol.* **163,** 1599–1605 (2003).

163. Wang, C. *et al.* Oestrogen modulates experimental autoimmune encephalomyelitis and interleukin-17 production via programmed death 1. *Immunology* **126,** 329–335 (2009).

164. Yates, M. A. *et al.* Progesterone treatment reduces disease severity and increases IL-10 in experimental autoimmune encephalomyelitis. *J. Neuroimmunol.* **220,** 136–139 (2010).

165. Tai, P. *et al.* Induction of regulatory T cells by physiological level estrogen. *J. Cell. Physiol.* **214,** 456–464 (2008).

166. Mao, G. *et al.* Progesterone increases systemic and local uterine proportions of CD4+CD25+ Treg cells during midterm pregnancy in mice. *Endocrinology* **151,** 5477–5488 (2010).

167. Subramanian, S., Yates, M., Vandenbark, A. A. & Offner, H. Oestrogen-mediated protection of experimental autoimmune encephalomyelitis in the absence of Foxp3+ regulatory T cells implicates compensatory pathways including regulatory B cells. *Immunology* **132,** 340–347 (2011).

168. Bodhankar, S., Wang, C., Vandenbark, A. A. & Offner, H. Estrogen-induced protection against experimental autoimmune encephalomyelitis is abrogated in the absence of B cells. *Eur. J. Immunol.* **41,** 1165–1175 (2011).

169. Papenfuss, T. L. *et al.* Estriol generates tolerogenic dendritic cells in vivo that protect against autoimmunity. *The Journal of Immunology* **186,** 3346–3355 (2011).

170. Lahl, K. *et al.* Selective depletion of Foxp3+ regulatory T cells induces a scurfy-like disease. *J. Exp. Med.* **204,** 57–63 (2007).

171. Tronche, F. *et al.* Disruption of the glucocorticoid receptor gene in the nervous system results in reduced anxiety. *Nat. Genet.* **23,** 99–103 (1999).

172. Baumann, S. *et al.* Glucocorticoids inhibit activation-induced cell death (AICD) via direct DNA-dependent repression of the CD95 ligand gene by a glucocorticoid receptor dimer. *Blood* **106,** 617–625 (2005).

173. Gerdes, J., Schwab, U., Lemke, H. & Stein, H. Production of a mouse monoclonal antibody reactive with a human nuclear antigen associated with cell proliferation. *Int. J. Cancer* **31,** 13–20 (1983).

174. Scholzen, T. & Gerdes, J. The Ki-67 protein: from the known and the unknown. *J. Cell. Physiol.* **182,** 311–322 (2000).

175. Walunas, T. L. *et al.* CTLA-4 can function as a negative regulator of T cell activation. *Immunity* **1,** 405–413 (1994).

176. Sather, B. D. *et al.* Altering the distribution of Foxp3(+) regulatory T cells results in tissue-specific inflammatory disease. *J. Exp. Med.* **204,** 1335–1347 (2007).

177. Huehn, J. *et al.* Developmental stage, phenotype, and migration distinguish naive- and effector/memory-like CD4+ regulatory T cells. *J. Exp. Med.* **199,** 303–313 (2004).

178. Heng, T. S. P., Painter, M. W.Immunological Genome Project Consortium. The Immunological Genome Project: networks of gene expression in immune cells. *Nat Immunol* **9,** 1091–1094 (2008).

179. Ojasoo, T., Doré, J. C., Gilbert, J. & Raynaud, J. P. Binding of steroids to the progestin and glucocorticoid receptors analyzed by correspondence analysis. *J. Med. Chem.* **31,** 1160–1169 (1988).

180. Tuckermann, J. P. *et al.* Macrophages and neutrophils are the targets for immune suppression by glucocorticoids in contact allergy. *J. Clin. Invest.* **117,** 1381–1390 (2007).

181. Wüst, S. *et al.* Peripheral T cells are the therapeutic targets of glucocorticoids in experimental autoimmune encephalomyelitis. *J. Immunol.* **180,** 8434–8443 (2008).

182. Mittelstadt, P. R., Monteiro, J. P. & Ashwell, J. D. Thymocyte responsiveness to endogenous glucocorticoids is required for immunological fitness. *J. Clin. Invest.* **122,** 2384–2394 (2012).

183. Holmes, M. C., Kotelevtsev, Y., Mullins, J. J. & Seckl, J. R. Phenotypic analysis of mice bearing targeted deletions of 11beta-hydroxysteroid dehydrogenases 1 and 2 genes. *Mol. Cell. Endocrinol.* **171,** 15–20 (2001).

184. Ferrari, P. The role of 11β-hydroxysteroid dehydrogenase type 2 in human hypertension. *Biochim. Biophys. Acta* **1802,** 1178–1187 (2010).

185. Ayroldi, E. *et al.* GILZ mediates the antiproliferative activity of glucocorticoids by negative regulation of Ras signaling. *J. Clin. Invest.* **117,** 1605–1615 (2007).

186. Birk, K. & Rudick, R. Pregnancy and multiple sclerosis. *Arch. Neurol.* **43,** 719–726 (1986).

187. Sweeney, W. J. Pregnancy and multiple sclerosis. *Am. J. Obstet. Gynecol.* **66,** 124–130 (1953).

188. Douglass, L. H. & Jorgensen, C. L. Pregnancy and multiple sclerosis. *Am. J. Obstet. Gynecol.* **55,** 332–336 (1948).

189. Zhao, J.-X., Zeng, Y.-Y. & Liu, Y. Fetal alloantigen is responsible for the expansion of the CD4(+)CD25(+) regulatory T cell pool during pregnancy. *Journal of Reproductive Immunology* **75,** 71–81 (2007).

190. Robertson, S. A. *et al.* Seminal fluid drives expansion of the CD4+CD25+ T regulatory cell pool and induces tolerance to paternal alloantigens in mice. *Biol. Reprod.* **80,** 1036–1045 (2009).

191. Moldenhauer, L. M. *et al.* Cross-presentation of male seminal fluid antigens elicits T cell activation to initiate the female immune response to pregnancy. *The Journal of Immunology* **182,** 8080–8093 (2009).

192. Erlebacher, A., Vencato, D., Price, K. A., Zhang, D. & Glimcher, L. H. Constraints in antigen presentation severely restrict T cell recognition of the allogeneic fetus. *J. Clin. Invest.* **117,** 1399–1411 (2007).

193. Kontula, K., Paavonen, T., Luukkainen, T. & Andersson, L. C. Binding of progestins to the glucocorticoid receptor. Correlation to their glucocorticoid-like effects on in vitro functions of human mononuclear leukocytes. *Biochem. Pharmacol.* **32,** 1511–1518 (1983).

194. Polanczyk, M. J., Hopke, C., Huan, J., Vandenbark, A. A. & Offner, H. Enhanced FoxP3 expression and Treg cell function in pregnant and estrogen-treated mice. *J. Neuroimmunol.* **170,** 85–92 (2005).

195. Bodhankar, S., Vandenbark, A. A. & Offner, H. Oestrogen treatment of experimental autoimmune encephalomyelitis requires 17β-oestradiol-receptor-positive B cells that up-regulate PD-1 on CD4 + Foxp3 +regulatory T cells. *Immunology* **137,** 282–293 (2012).

196. Kim, S., Liva, S. M., Dalal, M. A., Verity, M. A. & Voskuhl, R. R. Estriol ameliorates autoimmune demyelinating disease: implications for multiple sclerosis. *Neurology* **52,** 1230–1238 (1999).

197. Voskuhl, R. R. & Palaszynski, K. Sex hormones in experimental autoimmune encephalomyelitis: implications for multiple sclerosis. *Neuroscientist* **7,** 258–270 (2001).

198. Palaszynski, K. M., Liu, H., Loo, K. K. & Voskuhl, R. R. Estriol treatment ameliorates disease in males with experimental autoimmune encephalomyelitis: implications for multiple sclerosis. *J. Neuroimmunol.* **149,** 84–89 (2004).

199. Head, K. A. Estriol: safety and efficacy. *Altern Med Rev* **3,** 101–113 (1998).

200. Gold, S. M. & Voskuhl, R. R. Estrogen treatment in multiple sclerosis. *Journal of the Neurological Sciences* **286,** 99–103 (2009).

201. Sicotte, N. L. *et al.* Treatment of multiple sclerosis with the pregnancy hormone estriol. *Ann Neurol.* **52,** 421–428 (2002).

202. Soldan, S. S., Alvarez Retuerto, A. I., Sicotte, N. L. & Voskuhl, R. R. Immune modulation in multiple sclerosis patients treated with the pregnancy hormone estriol. *J. Immunol.* **171,** 6267–6274 (2003).

203. Gold, S. M. *et al.* Estrogen treatment decreases matrix metalloproteinase (MMP)-9 in autoimmune demyelinating disease through estrogen receptor alpha (ERalpha). *Lab. Invest.* **89,** 1076–1083 (2009).

204. Lee, J. H., Ulrich, B., Cho, J., Park, J. & Kim, C. H. Progesterone promotes differentiation of human cord blood fetal T cells into T regulatory cells but suppresses their differentiation into Th17 cells. *The Journal of Immunology* **187,** 1778–1787 (2011).

205. Cole, T. J. *et al.* Targeted disruption of the glucocorticoid receptor gene blocks adrenergic chromaffin cell development and severely retards lung maturation. *Genes Dev.* **9,** 1608–1621 (1995).

206. Orban, P. C., Chui, D. & Marth, J. D. Tissue- and site-specific DNA recombination in transgenic mice. *Proc. Natl. Acad. Sci. U.S.A.* **89,** 6861–6865 (1992).

207. Kugler, D. G., Mittelstadt, P. R., Ashwell, J. D., Sher, A. & Jankovic, D. CD4+ T cells are trigger and target of the glucocorticoid response that prevents lethal immunopathology in toxoplasma infection. *J. Exp. Med.* (2013). doi:10.1084/jem.20122300

208. Riccardi, C., Cifone, M. G. & Migliorati, G. Glucocorticoid hormone-induced modulation of gene expression and regulation of T-cell death: role of GITR and GILZ, two dexamethasone-induced genes. *Cell Death Differ.* **6,** 1182–1189 (1999).

209. van der Windt, G. J. W. *et al.* Mitochondrial respiratory capacity is a critical regulator of CD8+ T cell memory development. *Immunity* **36,** 68–78 (2012).

210. Mazzucchelli, R. & Durum, S. K. Interleukin-7 receptor expression: intelligent design. *Nat Rev Immunol* **7,** 144–154 (2007).

211. Schluns, K. S., Kieper, W. C., Jameson, S. C. & Lefrançois, L. Interleukin-7 mediates the homeostasis of naïve and memory CD8 T cells in vivo. *Nat Immunol* **1,** 426–432 (2000).

212. Kondrack, R. M. *et al.* Interleukin 7 regulates the survival and generation of memory CD4 cells. *J. Exp. Med.* **198,** 1797–1806 (2003).

Abbreviations

11β-HSD	11-beta hydroxysteroid dehydrogenase
ANOVA	Analysis of variance
APC	Allophycocyanin; Antigen presenting cell
BCA	Bicinchoninic acid
BSA	Bovine serum albumin
CCL	CC chemokine ligand
CD	Cluster of differentiation
cDNA	Complementary DNA
CFA	Complete Freund's adjuvant
CNS	Central nervous system
CNS1	Conserved non-coding DNA sequence 1
cpm	Counts per minute
cTEC	Cortical thymic epithelial cell
Ctla4	Cytotoxic T lymphocyte antigen 4
CXCL	Chemokine (C-X-C motif) ligand
Cy	Cyanine
DC	Dendritic cell
DEX	Dexamethasone
DNA	Deoxyribonucleic acid
dNK	Decidual NK cell
dNTP	Deoxyribonucleotide
DSC	Decidual stromal cells
E	Embryonic day
E2	Estradiol
E3	Estriol
EAE	Experimental autoimmune encephalomyelitis
EBV	Epstein–Barr virus
EDTA	Ethylenediaminetetraacetic acid
ER	Estrogen receptor
EtOH	Ethanol
FACS	Fluorescence-activated cell sorting
FCS	Fetal calf serum

FITC	Fluorescein isothiocyanate
Foxp3	Forkhead box protein 3
GA	Glatiramer acetate
GC	Glucocorticoids
GFP	Green fluorescent protein
Gilz	Glucocorticoid-induced leucine zipper
GR	Glucocorticoid receptor
GWAS	Genome-wide association study
HBSS	Hank's Balanced Salt Solution
HHV6	Human herpes virus 6
HRP	Horseradish peroxidase
IDO	Indoleamine 2,3-dioxygenase
IFN	Interferon
IL	Interleukin
IPEX	Immunodysregulation polyendocrinopathy enteropathy X-linked syndrome
Lag3	Lymphocyte-activation gene 3
Lck	Lymphocyte-specific protein tyrosine kinase
LDS	Lithium dodecyl sulfate
LN	Lymph node
MACS	Magnetic-activated cell sorting
MBP	Myelin basic protein
MHC	Major histocompatibility complex
MIC-1	Macrophage inhibitory cytokine-1
MOG	Myelin oligodendrocyte glycoprotein
MOPS	3-(N-morpholino)propanesulfonic acid
mOVA	Membrane-bound ovalbumin
mRNA	Messenger RNA
MS	Multiple sclerosis
mTEC	Medullary thymic epithelial cell
NK	Natural killer
NOR	Norgestrel
P4	Progesterone
PAMP	Pathogen-associated molecular pattern
PBS	Phosphate buffered saline
PCR	Polymerase chain reaction
PE	Phycoerythrin

PerCP	Peridinin chlorophyll
PLP	Proteolipid protein
PP	Post-partum day
PPMS	Primary progressive multiple sclerosis
PR	Progesterone receptor
PRR	Pattern recognition receptors
pTreg	Peripherally induced regulatory T cell
PTX	Pertussis toxin
RAG-1	Recombination-activating gene 1
RBC	Red blood cell
RIPA buffer	Radioimmunoprecipitation assay buffer
RNA	Ribonucleic acid
RPMI	Roswell park memorial institute
RRMS	Relapsing-remitting multiple sclerosis
RT	Room temperature
RU486	Mifepristone
SDS	Sodium dodecyl sulphate
SNP	Single nucleotide polymorphism
SPMS	Secondary progressive multiple scleros
STAT	Signal transducer and activator of transcription,
TBS	Tris-buffered saline
TBST	TBS-Tween
Tcon	Conventional T cell
TCR	T cell receptor
tDC	Tolerogenic DC
TGF	Tumour growth factor
T_H	T helper cell
TNF	Tumour necrosis factor
Treg	Regulatory T cell
Tris	Tris(hydroxymethyl)aminomethane
TSDR	Treg-specific demethylated region
tTreg	Thymus-derived regulatory T cell
VCAM-1	Vascular cell adhesion molecule 1
VLA-4	Very late antigen 4

Acknowledgement

I would like to thank my supervisor Prof. Dr. Manuel A. Friese for the opportunity to work on this exciting topic, for the great support and for his constant encouragement to take part in international scientific congresses and to extend my scientific skills.

I thank Prof. Dr. Petra C. Arck and Prof. Dr. Christian Gerloff for following this work as part of my thesis committee and for their valuable advises and kind support. In particular, I am grateful to Prof. Dr. Petra C. Arck for giving me the opportunity to join the Feto-Maternal Immune Cross Talk Community, to continuously present my work in internal seminars and benefit from their experience and critical questions.

I would like to thank Prof. Dr. Holger Reichardt (Göttingen University Medical School) and Prof. Dr. Ulf Panzer (UKE) for generously providing us with decisive mouse models and Dr. Gabriela Salinas-Riester (Göttingen University Medical School) for the microarray analyses.

I thank the whole Friese lab, especially Dr. Melanie Piedavent, Dr. Benjamin Schattling, Dr. Friederike Ufer and Dr. Anne Willing for teaching me the basic immunological and experimental tools and for creating a cooperative and inspiring atmosphere. Special thanks also goes to Sabine Wehrmann, Nina Kursawe and Birgit Schiller for their invaluable support with experimental procedures and to the animal caretakers for their dedicated work.

I also would like to thank Dr. Stefan M. Gold, Dr. Konstantinos Patas, Dr. Ole Pless, PD Dr. Eva Tolosa and Dr. Emilia Solano for inspiring joint discussions and Michael Moles for proofreading the manuscript.

Finally, I am extremely grateful to my partner, my family and my friends for their love and unconditional support.

Curriculum vitae

Entfällt aus datenschutzrechtlichen Gründen.

Eidesstattliche Versicherung

Ich versichere ausdrücklich, dass ich die Arbeit selbständig und ohne fremde Hilfe verfasst, andere als die von mir angegebenen Quellen und Hilfsmittel nicht benutzt und die aus den benutzten Werken wörtlich oder inhaltlich entnommenen Stellen einzeln nach Ausgabe (Auflage und Jahr des Erscheinens), Band und Seite des benutzten Werkes kenntlich gemacht habe.

Ferner versichere ich, dass ich die Dissertation bisher nicht einem Fachvertreter an einer anderen Hochschule zur Überprüfung vorgelegt oder mich anderweitig um Zulassung zur Promotion beworben habe.

Ich erkläre mich einverstanden, dass meine Dissertation vom Dekanat der Medizinischen Fakultät mit einer gängigen Software zur Erkennung von Plagiaten überprüft werden kann.

Unterschrift: .....

Jan Broder Engler